SLOPE STABILITY ANALYSIS ALONG SELECTED STEEP SECTIONS OF DIBIBISA RIDGE OF ADAMA TOWN USING LIMIT EQUILIBRIUM AND FINITE ELEMENT METHODS, CENTRAL ETHIOPIA

By:

Firew Feyissa Fasiko

A Thesis Submitted to the Department of Applied Geology

School of Applied Natural Science

Presented in Partial Fulfillment of the Requirement for the Degree of Master of Science in Applied Geology

Office of Graduate Studies

Adama Science and Technology University

June, 2022

Adama, Ethiopia

Slope Stability Analysis Along Selected Steep Sections of Dibibisa Ridge of Adama Town Using Limit Equilibrium and Finite Element Methods, Central Ethiopia

By:

Firew Feyissa Fasiko

Major Advisor: Mohammed Haji (Ph.D.)

Co-Advisor: Tola Garo (MSc)

A Thesis Submitted to the Department of Applied Geology

School of Applied Natural Science

Presented in Partial Fulfillment of the Requirement for the Degree of Master of Science in Applied Geology

Office of Graduate Studies

Adama Science and Technology University

June, 2022

Adama, Ethiopia

DECLARATION

I hereby declare that this MSc thesis entitled **"Slope Stability Analysis Along Selected Steep Sections of Dibibisa Ridge of Adama Town Using Limit Equilibrium and Finite Element Methods, Central Ethiopia"** is my original work. That is it has not been submitted for the award of any academic degree, diploma, or certificate in any other university. All sources of material that are used for this thesis have been duly acknowledged through citation.

Name of student	Signature	Date

RECOMMENDATION

We, the advisors of this thesis, hereby certify that we have read the revised version of the thesis entitled **"Slope Stability Analysis Along Selected Steep Sections of Dibibisa Ridge of Adama Town Using Limit Equilibrium and Finite Element Methods, Central Ethiopia"** prepared under our guidance by Firew Feyissa submitted in partial fulfillment of the requirements for the degree of Masters of Science in Applied geology. Therefore, we recommend the submission of the revised version of the thesis to the department following the applicable procedures.

Main Advisor	Signature	Date
Co-Advisor	Signature	Date

APPROVAL SHEET

We, the advisors of the thesis entitled **"Slope Stability Analysis Along Selected Steep Sections of Dibibisa Ridge of Adama Town Using Limit Equilibrium and Finite Element Methods, Central Ethiopia"** developed by Firew Feyissa, hereby certify that the recommendation and suggestions made by the board of examiners are appropriately incorporated into the final version of the thesis.

______________________	______________________	________________
Major Advisor	Signature	Date
______________________	______________________	________________
Co-advisor	Signature	Date

We, the undersigned, members of the Board of Examiners of the thesis by Firew Feyissa have read and evaluated the thesis entitled **"Slope Stability Analysis Along Selected Steep Sections of Dibibisa Ridge of Adama Town Using Limit Equilibrium and Finite Element Methods, Central Ethiopia"** and examined the candidate during open defense. This is, therefore, to certify that the thesis is accepted for partial fulfillment of the requirement of the degree of Master of Science in Applied geology.

________________________	____________________	____________________
Chairperson	Signature	Date
________________________	____________________	____________________
Internal Examiner	Signature	Date
________________________	____________________	____________________
Eternal Examiner	Signature	Date

Final approval and acceptance of the thesis is contingent upon the submission of its final copy to the Office of Postgraduate Studies (OPGS) through the Department Graduate Council (DGC) and School Graduate Committee (SGC).

______________________	_________________	________________
Department Head	Signature	Date
____________________________	__________________	________________
School Dean	Signature	Date
_____________________________	__________________	________________
Office of Postgraduate Studies, Dean	Signature	Date

ACKNOWLEDGMENT

First of all, I offer my deeply felt thanks to Almighty God for being with me from the very beginning, through progress to the end of my work, and for his countless protection on me. My deepest gratitude also goes to my family for their help in a different way, particularly to my father Feyissa for his unlimited encouragement and support during my study.

Dr. Mohammed Haji, my advisor, and co-advisor Mr. Tola Garo deserve special credit for all-around cooperation during the entire period of this project. I highly appreciate the commitment that Mr. Tola had to enhance my knowledge of the subject matter by closely following my activities and strictly checking my progress.

I would extend my acknowledgment to the Addis Ababa Science and Technology University Department of Civil Engineering Geotechnical laboratory & Geology Department for their commitment during laboratory work & field instrument assistance.

Lastly, I offer a great thanks to Adama Science and Technology University for their financial help and the Department of Geology for providing different materials like field equipment.

TABLE OF CONTENTS

Contents

LIST OF TABLES

LIST OF FIGURES

LIST OF ABBREVIATIONS AND ACRONYMS

ASTM	American Society for Testing Materials Standard
D	Disturbance factor
DEM	Digital Elevation Model
E	Modulus of Elasticity
EBCS	Ethiopian Building Code of Standard
EGS	Ethiopian Geological Survey
FEM	Finite Element Method
FOS	Factor of Safety
GSI	Geological Strength Index
ISRM	International Society for Rock Mechanics
JCS	Joint wall compressive strength
JV	Joint volume
LEM	Limit Equilibrium Method
MC	Mohr-Coulomb
mi	Material constant for intact rock
NMER	Northern Main Ethiopian Rift
RQD	Rock Quality Designation
R	Rebound number
RMR	Rock Mass Rating
SRF	Strength Reduction Factor
SSR	Shear Strength Reduction
STP N	Standard Penetration Test Number
UCS	Unconfined compressive strength
V	Poisson Ratio
WFB	Wonji Fault Belt

ABSTRACT

Adama town is one of the rapidly growing towns in the country, and its population is growing at a staggering rate as well. The town is bounded by the two ridges (one of whom is Dibibisa ridge) and are both striking nearly in the NNE-SSW direction. Moreover, urbanization and population growth of the town is leading to the construction of infrastructures such as roads and residential buildings near this relatively steeply sloped ridges. However, these ridges in particular, the Dibibisa Ridge regularly have slope instability issues that endanger surrounding infrastructure projects and human life. As a result, the goal of this study is to examine slope instability issues along selected sections of the Dibibisa ridge in Adama town. Detailed fieldwork which includes discontinuity surveying, in-situ strength test, mapping, sampling, and laboratory testing was carried out to achieve the intended objective. Based on a detailed field work a total of five critical slope sections (i.e. two structural controlled rock slopes and three soil slope sections) were identified during field work and analyzed using kinematic(dips), finite element (Phase), and limit equilibrium (Slide2D,rocplane & swedge) methods of stability analysis. The rock mass rating showed that the rock of the study area ranges from fair to good quality. Under kinematic analysis, the two rock slope sections are admissible to two planar and one wedge mode of failure. All three critical soil slope sections are unstable at all anticipated conditions under both limit equilibrium and finite element method of slope stability analysis. From the results of slope modification analysis the factor of safety increases as the width of benches as well as number of benches increases and in the slope section (D1S4) the factor of safety was increased to 1.222 as two benches of 5m wide used under slide 2D on which was initially unstable with the factor of safety 0.267, Similarly as 3 benches of the same width used under slide 2D the factor of safety of the slope section reaches 1.219. At the slope section (D1S2) flattening of slope angle from initial 45^o to 35^o, 28^o, 25^o and 18^o *increases the factor of safety of the slope from initial 0.284 to 0.77, 0.89, 1.022 and 1.151 respectively under slide 2D analysis. At slope section (D2S1) flattening of slope angle from initial 46^o to 35^o, 25^o, 23^o, and 20^o increases the factor of safety from initial 0.412 to 0.684, 0.920, 1.02, and 1.315 respectively. As indicated from the analysis of the results, the identified slope sections are susceptible to failure under actual field scenario under different projected conditions. Hence, this study recommended Benching method to be adopted as economical mitigating measure for soil slope sections.*

Key words: *Benching, Critical section, Rock slope, Slope stability, Soil slope,*

CHAPTER ONE

1. INTRODUCTION

1.1 Background

Slope stability refers to the condition that an inclined slope can withstand its own weight and external forces without experiencing displacement and it is the potential of a naturally occurring or engineered soil and rock slope to withstand ground movement. Throughout the world, slope instabilities are challenging problems mainly to the civil engineering structure such as roads, tunnels, dams, open-pit mines, and the nature of the earth (Lamessa and Meten, 2021). In Ethiopia, most areas of the north, south, and western regions of the Ethiopian plateau have a history of slope instability in both superficial materials and bedrocks (Ayalew, 1999).

However, slope instability problems take place due to human and nature disturbs the delicate nature of the soil and rock slope (Abramson *et al.*, 2001). Mountain slope failure, like landslides and rock falls, are natural activities, often seen in hill slope roads, hill stations, open cast mining areas, and underground/tunnel areas. Slope instabilities also occur by human activities like; cutting the slope in an unplanned manner, steepening the slope gradient, inappropriate excavation on the slope's toe, and adding an extra load are the most common human actions that might cause the slope to fail (Hamza and Raghuvanshi, 2017).

Slope stability is governed by both external and internal factors. External forces such as heavy rain and earthquakes frequently cause slope failure and landslides, which result in massive economic losses and human deaths around the world (Pantelidis, 2009). Between 1850 and 1992, 395 rock slope failures were recorded in Nevada, the majority of which were caused by rainfall (Pantelidis, 2009). Wherever there is high rainfall, agricultural activities, abnormal erosion and seismic activities along the hill slope gradient, it induces instability of hill slope. The main internal governing factors are; the geometry of the slope, potential failure plane characteristics, surface drainage, and groundwater condition (Wang and Niu, 2009). The main driving force acting on the slope is the gravitational force which is directly proportional to the slope inclination. Slope instability may occur in the form of rotational, translational and wedge modes of failure, causing a different impact on properties, lives, and blocking traffic (Hoek and Bray, 1981).

To mitigate slope instability problems detailed study of the stability of slope should be carried out. To assess and analyze the stability of the slope, some the methods such as Kinematic, Deterministic, Probabilistic, and Numerical methods (Hoek and Bray, 1981; Abramson *et al.*, 2001; Wyllie and Mah, 2004) were used frequently.

The present study is aimed to analyze the slope stability situation of the Dibibisa ridge of Adama town and this study intended to analyze the stability of slope at critical slope sections of rock and soil slopes of the ridge by using the slope stability analysis methods such as kinematic analysis, limit equilibrium method and finite element method. Kinematic analysis methods are mainly based on the body motion without taking into account forces action and geotechnical parameters (Wu and Kulatilake, 2012). Limit equilibrium methods are used to assess the stability of the slope regardless of slope conditions (Eberhardt *et al.*, 2004). The finite element method is a potential alternative to the traditional approach for slope stability analysis because it is accurate, adaptable, and requires fewer a priori assumptions, particularly for the failure mechanism. After the compilation of the study, appropriate remedial measures will be suggested based on the result of the analysis.

1.2 Description of the Study Area

1.2.1. Location of the study area

The study area for this research work is located in the Eastern Showa zone of Oromia regional state, Central Ethiopia (Figure 1.1). It is incorporated in the Northern Main Ethiopian Rift (NMER) with the Wonji Fault Belt (WFB) and it is situated around 100 Km from the capital, Addis Ababa, in the Southeastern direction. It is bounded by geographic coordinates of 39^{o} 12' 0" to 39^{o} 21' 0" E and 8^{o} 27' 0" to 8^{o} 36 ' 0" N in the UTM Zone of 37. Topographically, it is characterized by flat to rugged topography.

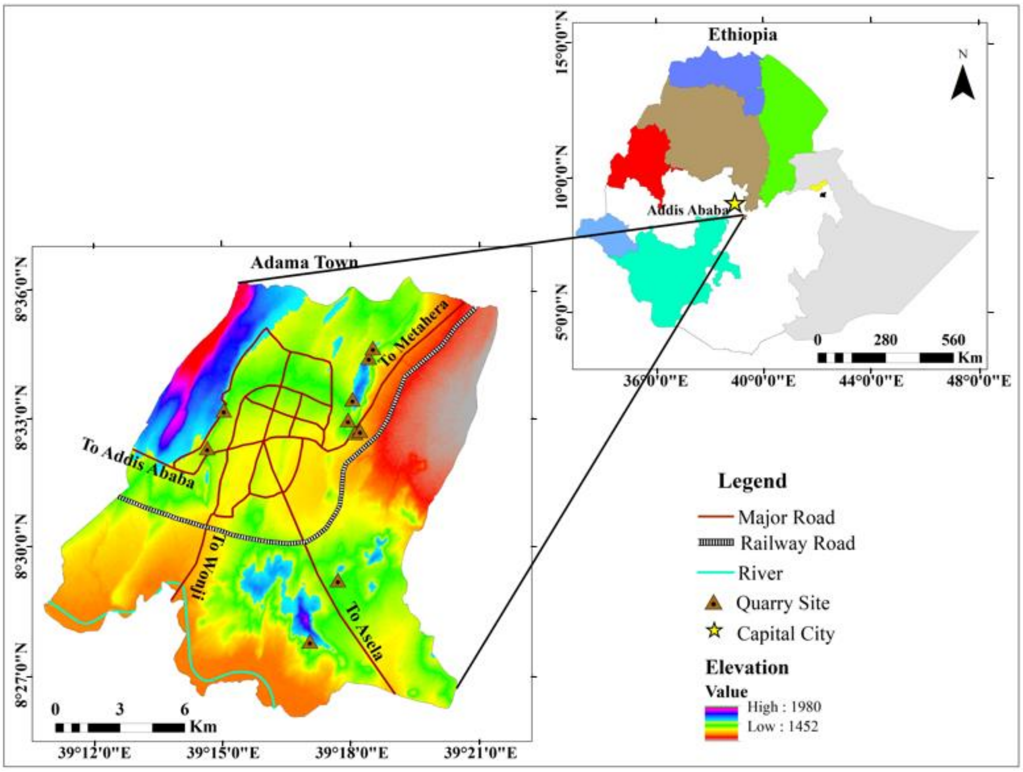

Fig 1.1: Location map of the study area.

1.2.2. Physiography of study area

Adama town is situated within the Main Ethiopian Rift on a regional scale and locally the town is bordered by elongated ridges. Topographically the town area is situated in graben which is bounded by fault escarpments in western eastern directions (Chemeda, 2020). The physiography of the study area is highly controlled by the tectonic process that occurred in the area in the past. See fig 1.2 below.

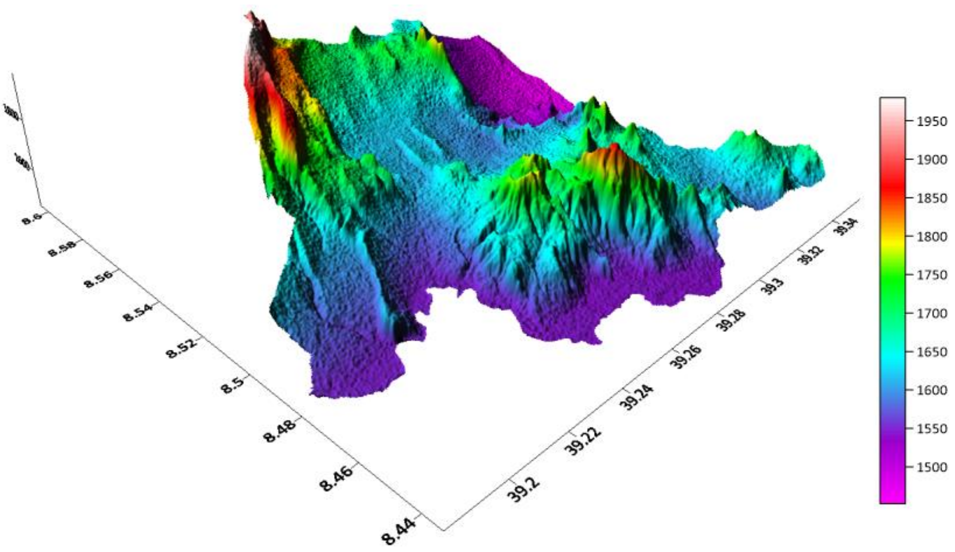

Fig 1.2: physiographic map of the study area.

1.2.3. Climatic condition of the study area

The records of the national meteorological service agency from the Adama observatory substation show that the mean annual rainfall for the past eleven years (2011-2021) is 910.6mm at an altitude of 1622m above mean sea level. High rainfall occurs in July and August covering around 50% of the annual rainfall. In the other months, it is less than or equal to the evaporation rate of the area. According to (Abera *et al.*, 2016), the groundwater recharge from rainfall is negligible in this area because much of the rainfall is changed into run-off. Hence deep slope failure due to commutative infiltration will not be a problem in the area. However, rainfall may cause erosion and shallow slides of the ridge slope. From previous case studies ground water table is located at depth at a depth of 80 to 100 m from the ground surface (Abera *et al.*, 2016). The average monthly rainfall for eleven consecutive years (2011-2021) of the study area has been summarized as follows in (fig 1.3).

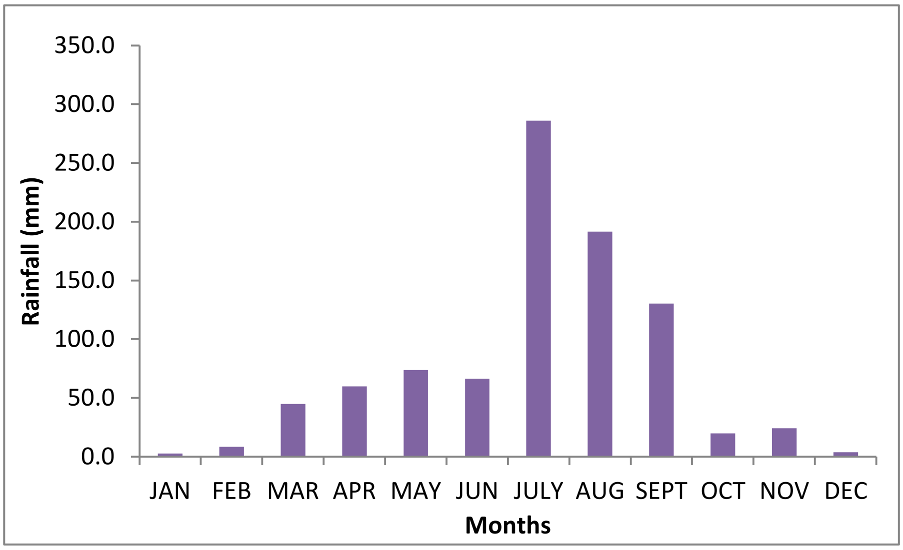

Fig1.3: Mean monthly rainfall distribution of study area.

The mean minimum, mean maximum, and mean average monthly temperatures of the study area are 14.3, 28.1, and 21.2°C respectively. The highest temperature occurs during March, April, May, and June whereas November, December, and January have low temperatures. The Mean monthly average temperature ranges from 19.33°c to 23.54°c which shows almost the same variation throughout the year.

1.3 Statement of Problem

Adama town is one of the rapidly growing towns in the country, and its population is growing at a staggering rate as well. The town is bounded by two ridges that are striking nearly in the NNE-SSW direction. Among the ridges, one is the Dibibisa ridge. The urbanization and population growth of the town is leading to the construction of infrastructures such as roads and residential buildings near this relatively steeply sloped ridge of Dibibisa. With the expansion of the construction industry, parts of this ridge of the town are also currently being used for quarry sites for the extraction of construction materials. However, parts of this relatively steeply sloped ridge of the town are affected by slope instability problems as shown (fig 1.4) that pose a danger to human lives infrastructures constructed in nearby areas. Furthermore, the study area is located in a seismically active region of the Main Ethiopian Rift (MER), which further exaggerates this instability problem. Therefore, it is extremely important to identify, locate and analyze slope instability problems along this relatively steeply sloped ridge to ensure safe territorial expansion and extraction of construction materials in these parts of the town. Hence, in this research work, an attempt will be made to determine the geotechnical properties of rocks and soils along critical slope sections and analyze their stability using LEM and FEMs.

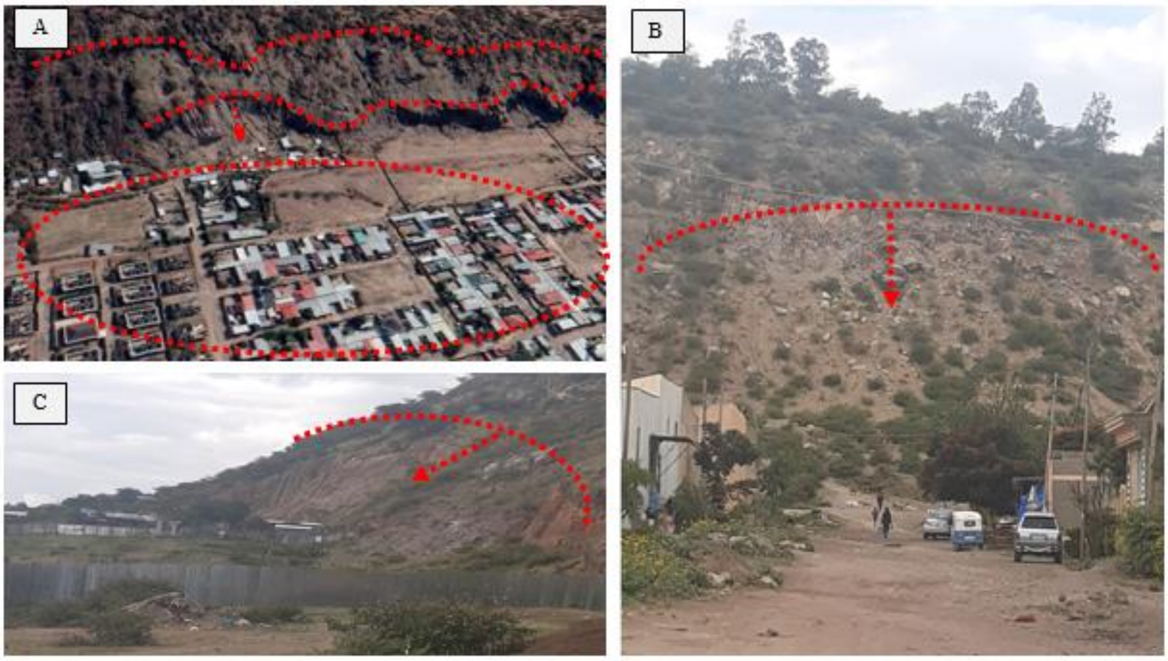

Fig1.4: A) Google Earth image of part of the study area showing slope instability problem toward residential buildings, and B & C) Field photograph illustrating similar problem.

1.4 Objective of the study

1.4.1 General objective

The main objective of this study is to analyze the stability of the slope along selected steep sections of the Dibibisa ridge of Adama town.

1.4.2 Specific objective

- To identify and locate the potential slope instability problems along steep sections of the Dibibisa ridge of Adama town.
- To determine the engineering geological properties of soils and geotechnical properties of rock at the critical slope sections.
- To determine the factor of safety/or Stress Reduction Factor of the critical slope sections.
- To suggest effective remedial measures for the identified problems.

1.5 Significance of the Study

The result of this study will be essential to provide detailed information about the slope stability situation of an area. The findings of this study will be used to design appropriate remedial measures that will be used in stabilizing critical slope sections that are on the verge of failure. In general, the results of this study will be crucial in the risk or loss of either material or human life which may be caused by this instability problem.

1.6 Expected outcome of the study

An expected outcome of this study will be:-

- Detailed information about the geological properties of soils and geotechnical properties of rock at the critical slope sections.
- Determination of factor of safety of the critical slope sections.
- Suggesting appropriate remedial measures, which help in minimization or avoidance of slope failure risk of an area.

CHAPTER TWO

2. LITERATURE REVIEW

2.1. Introduction

Slope instabilities are one of the most common and difficult problems in mining and the construction of civil engineering infrastructures like roads, tunnels, and dams all over the world. Slope collapse is a worldwide issue that has resulted in damage to infrastructure, human lives, and natural resources. Slope failure can take the form of rotational, translational, or wedge failure, all of which have different effects on property, life, traffic flow (Hoek and Bray, 1981). Slope instability concerns, on the other h, occur when humans nature interfere with the sensitive nature of the soil rock slope (Abramson *et al.*, 2001), it is a global issue. Because of the cutting of hills road-sides in Ethiopia, most areas of the north, south, western regions of the Ethiopian plateau have a history of slope instability, both in superficial materials at bedrocks (Ayalew, 1999). Conducting a rigorous investigation and analysis is critical to reducing the loss caused by this slope stability problem. Limit equilibrium and finite element approaches are among the methods used for slope stability analysis. The most frequent and oldest method for studying slope stability is the limit equilibrium method, which identifies potential failure processes and determines factors of safety for a specific geotechnical scenario. The finite element method is a powerful alternative approach for slope stability analysis that is accurate, versatile, requires fewer a priori assumptions, particularly in terms of failure mechanism (Griffiths and Lane, 1999).

2.2. Slope Stability Studies in Ethiopia

Slope stability issues are frequent widespread in most portions of the Ethiopian plateau's north, south, west, the regions have a history of slope instability. Many scholars conducted investigations at different times utilizing different slope stability analysis methods to explore, analyze, and suggest different stabilization strategies for these slope stability concerns.

(Tsige *et al.*, 2017) used the limit equilibrium method of slope stability analyses to undertake geotechnical conditions and stability analyses of landslide-prone areas near Bonga Town. According to the findings, many slides and related ground subsidence occurred in Bonga Town, causing considerable cracks in the walls and floors of several private and governmental buildings. Water pipelines along the road were disturbed by the sliding and the main highway that connects Bonga-Tepi- Masha via Alamo and Gatiba has been disrupted at four locations. The study identified that the problem becomes higher during the rainy season.

(Bushira *et al.*, 2018) conducted slope stability analysis on Wozeka–Gidole road and this road experiences frequent slope failure initially and also triggered during road construction. The study identified the failed slope to verify numerical results of both the limit equilibrium method (LEM) and finite element method (FEM) with the failed slope. Numerical results of both FEM and LEM verify the instability of the slope.

Modified landslide hazard zonation techniques were adopted to investigate landslide hazards in Mersa and Wurgessa areas. The results of the analysis revealed that a combination of 9 inherent causative triggering elements, such as slope morphometry, incompetent slope material, structural discontinuities, extended intensive rainfall, construction activities, might cause slope instability landslide activity (Raghuvanshi *et al.*, 2014).

(Ayele *et al.*, 2014) investigated the slope stability of the road from Gohatsion to Dejen town using a deterministic technique. The slope was found to be unstable under all expected conditions, except for static dry conditions.

2.3. Slope Stability Governing Factors

When material moves due to gravity and shear pressures exceeding the shear strength, slope instability can arise at a specific location. There are a lot of elements that influence the slope's stability, some of which operate as driving forces and others as resistive forces. Internal elements such as slope geometry, probable failure planes, surface drainage, groundwater conditions, and shear strength parameters of the materials that make up the slope are separated into two categories (Anbalagan, 1992; Turrini and Visintainer, 1998; Ayalew *et al.*, 2004). Seismicity, rainfall, and human activity are external elements that influence slope stability (Hoek and Bray, 1981; Dahal *et al.*, 2008; Raghuvanshi *et al.*, 2014; Kumar and Anbalagan, 2016; Sorbi and Farrokhnia, 2018). The regulating variables are described in-depth further down.

2.3.1 Internal Factors

2.3.1.1 Geometry of the Slope

For rock slopes, slope geometry includes parameters such as slope dip and dip direction, failure plane, slope height, upper slope dip, tension crack (Hoek and Bray, 1981;

Raghuvanshi, 2019). The gravitational force, which is directly proportional to the slope inclination, is the principal driving force operating on the slope. Instability will be more likely on a steeper slope (Raghuvanshi *et al.*, 2014; Hamza and Raghuvanshi, 2017). As an inclination of the upper slope rises, more rock mass is added to the weight component, increasing shearing stresses causing slope instability (Stead *et al.*, 2006). Shear stresses will grow as the slope's height rises (Anbalagan, 1992; Kroy *et al.*, 2002; Raghuvanshi *et al.*, 2014).

2.3.1.2 Potential Failure Planes

Internal factors that control the stability of soil and rock slopes include the potential failing plane and its characteristics. The shear strength parameters cohesion (c) and angle of friction (u) define the major resistive stress along the possible failure surface (Fig. 2.1). The engineering geological properties of the discontinuity surface determine the shear strength along the possible failure plane. These include the failure plane's direction, the failure surface's continuity, the surface's roughness, the aperture, among others (Mulatu *et al.*, 2010). The possible failure plane's dip should be smaller than the slope face's dip but more than the friction angle along the failure plane for a specific mode of rock slope failure to occur (Hoek and Bray, 1981; Cravero *et al.*, 2010).

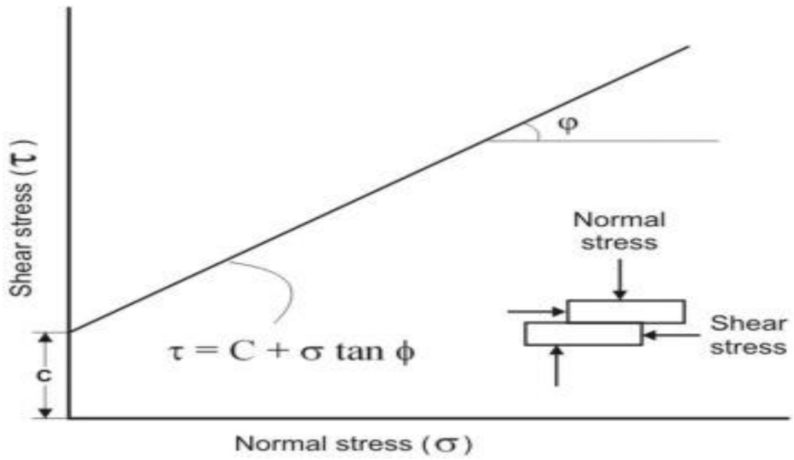

Fig 2.1: Relation between normal and shear stress along the potential failure plane

(Raghuvanshi, T. K. (2019).

2.3.1.3 Surface Water Drainage and Groundwater Conditions

The upper slope's surface water flow will easily pass through the tension crack, recharging the possible failure surface. As a result of the inflowing water in the tension crack, a water force (V) and an uplift water force (U) would emerge along the probable failure surface, reducing the slope's stability (Hoek and Bray, 1981; Kim *et al.*, 2004; Ahmadi and Eslami, 2011; Shukla and Hossain, 2011). (Fig. 2.2) As groundwater levels near the failure plane, it reduces shear strength and increases the shear stress applied to the failure plane, destabilizing the slope. Water on the probable failure surface reduces shear strength lubricates the surface, which may aid in the sliding process (Raghuvanshi, 2019).

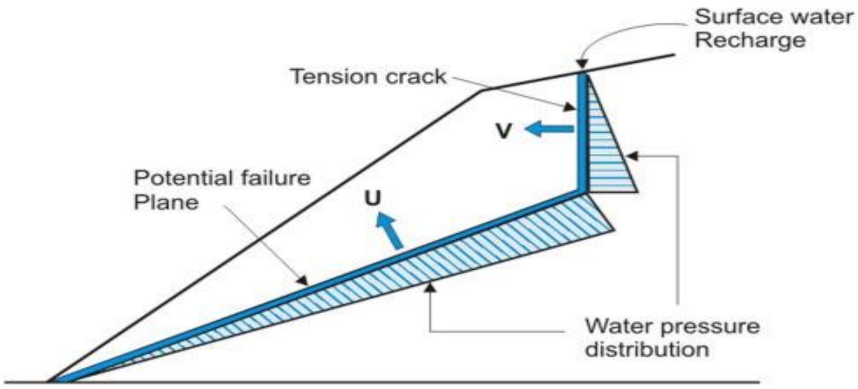

Fig2.2: Water force and pressure distribution in slope having potential plane mode of failure (Raghuvanshi, T. K. (2019).

2.3.1.4 Shear Strength Parameter of Materials Composing the Slope

Shear strength parameters of materials that compose the slope are the main factors that define resisting force acting normal to the failure plane (Barton and Bandis, 1990). The shear strength parameters in turn depend on the conditions of discontinuities such as roughness, continuity, aperture, filling (Leulalem *et al.*, 2016).

(Barton, 2016) specifically determine shear strength along failure plane or natural joints using empirical law of basic friction angle first proposed by (Barton, 1973) non-linear equation written as follow.

$$\tau = \sigma n \tan\left[JRC \log 10\left({JCS}/{\sigma n}\right) + \phi b\right] \qquad (2.1)$$

Where τ = is peak shear strength (kPa),

σn = is effective normal stress (kPa),

JRC = is joint roughness coefficient,

JCS = is joint wall compressive strength (kPa)

ϕb = is basic friction angle.

Joint wall compressive strength (JCS) is the strength of a layer of rock adjacent to a joint it controls the strength deformation properties of the rock mass (Barton, 1973). The appropriate value of uniaxial compressive strength (σc) determined from Schmidt rebound value (R) applied on an un-weathered rock surface with unit weight (γ) will represent the joint wall compressive strength of the rock (JCS). However, for the weathered rock surface or in the absence of Schmidt hammer reading, JCS will become a fraction of the uniaxial compressive strength of the rock approximately (1/4σc) (Barton, 1976). The joint roughness coefficient (JRC) is the coefficient of joint surface roughness having a value ranging from 0 to 20 (smoothest to roughest) as described by (Barton and Choubey, 1977). A basic friction angle ($\emptyset b$) is an angle with a flat, planar, un-weathered rock surface in which its value ranges from 25º-35º (Barton, 1973). It can be determined from a tilt test on smooth, planar un-weathered joints cut from rock surface by a saw or adopted from a basic friction angle determined by (Barton and Choubey, 1977; Mishra, 2016). For variably weathered joints, basic friction angle can be correlated with residual friction angle (ϕr) as stated by (Barton and Choubey, 1977) below.

$$\phi r = (\phi b - 20) + 20\left(r/R\right) \tag{2.2}$$

Where r is the Schmidt rebound number of wet and weathered fracture surfaces and *R* is the Schmidt rebound number on dry un-weathered sawn surfaces.

Cohesion and friction angle can be determined by Rocdata software by importing slope height and unit weight of the rock into the rocdata software.

2.3.2 External Factors

2.3.2.1 Rainfall

Rainfall is one of the external and triggering causes of slope instability, and most of the time, rainfall is the primary cause of slope failure (Ayalew *et al.*, 2004; Pantelidis, 2009; Woldearegay, 2013). Rainfall has the effect of raising the elevation of groundwater levels. Groundwater, in turn, has an impact on the rock slope's stability for the following reasons: (Wyllie and Mah, 2004). Rainfall infiltrating the slope reduces shear strength, increasing the instability of the probable collapse plane (Pantelidis, 2009; Raghuvanshi, 2019). Water impacts slope stability by lowering the resistive force along the failure plane, changing the moisture content of the rock, and lowering the shear strength of the rock by speeding up the weathering and freezing of groundwater.

2.3.2.2 Seismicity

Seismic activity is also a triggering factor of slope instability, especially in an active seismic zone (Hoek and Bray, 1981). The vibration released during earthquakes can cause the failure of slopes that were previously stable through the influence of increased vertical acceleration. According to (Muthu and Petrou, 2007) the possibility of an earthquake triggering a landslide event depends on the shaking of the ground rather than on the actual magnitude of the earthquake. The minimum magnitude of an earthquake to cause slope failure is approximately 4-5MM (Pantelidis, 2009). From a safety point of view, it is recommended that seismicity is taken into consideration for critical structures like steep slopes (Nilsen, 2000).

2.3.2.3 Human Activities

Cutting the slope in an unplanned manner, steepening the slope gradient, inappropriate excavation on the slope's toe, adding an extra load is the most common human actions that might cause the slope to fail (Raghuvanshi *et al.*, 2014). This is caused by human activities such as incorrect slope changes and excavations. Undercutting slope modification during road construction, as well as slope overloading during mining quarrying operations, are examples of human activities that affect slope stability. Overloading may raise the risk of slope failure, changing the hydrology could have a significant impact on slope stability (Boylan *et al.*, 2008). Another example is Deforestation caused by human intervention promotes soil slope failure by increasing erosion, as well as lowering evapotranspiration raising water levels (Cruden and Varnes, 1996). Vibrations resulting from artificial causes such as; machine activities and underground explosions may also cause slope instability.

2.4. Type of slope failure

(Kliche, 1999) states that there are four general modes of slope failure: planar failure, rotational failure, wedge failure, and toppling failure. (Hoek and Bray, 1981) (Wyllie and Mah, 2004) also classify rock slope failure into planar, wedge, toppling, and circular types.

Each type of slope failure discussed below; -

2.4.1. Planar failure

When rock blocks lie on an inclined failure like a junction that lets daylight into free space, planar rock slope failure occurs (Sharma *et al.*, 1999). Surface weakness, such as faults, joints, bedding planes, changes in shear strength between layers of bedded deposits, or the contact between firm bedrock overlaying weathered rock, are widely used to control movement structurally see (fig 2.3). There are conditions for the occurrence of planar failure these are; -

- The strike of the slope doesn´t differs more than ± 20° from the strike of the weakness plane.
- The toe of the failure plane has to cross the slope between toe and crest.
- The dip of the failure plane must be less than the dip of the slope face, the internal angle of friction for the discontinuity must be less than the dip of the discontinuity (Hoek and Bray, 1981).

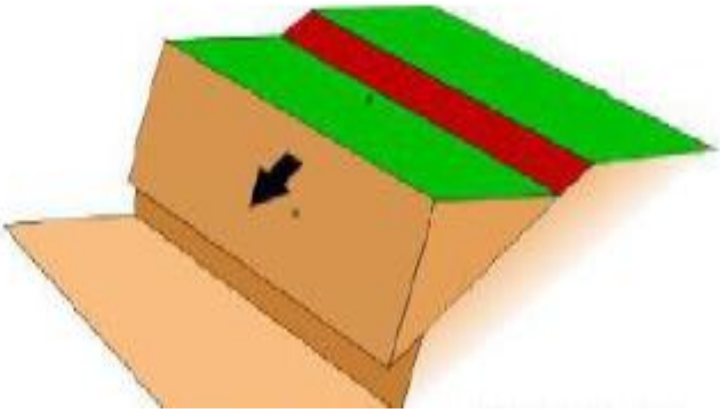

Fig 2.3: Simplified illustrations of planar failure *(Source:(Hoek and Marinos, 2009))*

2.4.2 Wedge Failure

Wedge failure occurs when two discontinuities strike obliquely across the slope face and their line of intersection daylights in the slope face. The wedge mode of rock slope failures occurs over a wider range of geologic geometric conditions than the planar mode of failure (Goodman and Kieffer, 2000; Wyllie and Mah, 2004).

2.4.3. Circular Failure

Circular failure occurs in slopes with homogeneous materials, primarily soil slopes, in heavily fragmented rock on occasion (Abramson *et al.*, 2001). This sort of failure is most common in soils, although it can also occur in weak rock masses that are highly jointed or fractured. The failure will be marked by a single discontinuity surface in this case, but it will most likely follow a circular failure route.

2.4.4. Toppling Failure

A toppling is the overturning of a rock block about a pivot point located below its center of gravity (Hunt and Lipo, 2009). Toppling mode of rock slope occurs due to overturning of rock layers or discontinuities that are dipping steeply into the slope face (Goodman and Kieffer, 2000) as shown in fig 2.4 below it involves rotation of columns or blocks of rocks about a fixed base (Wyllie and Mah, 2004).

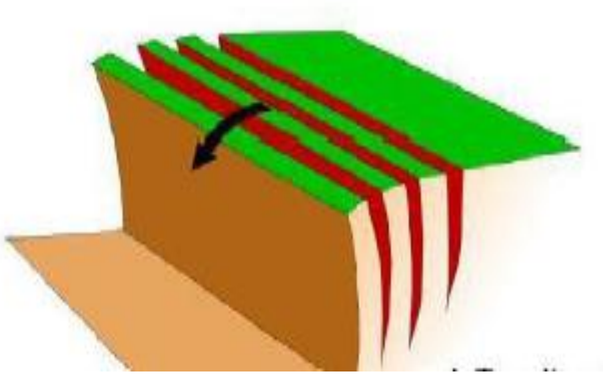

Fig 2.4: Simplified illustrations of toppling failure *(Source: (Hoek and Marinos, 2009)).*

2.5. Slope Stability Analyses Approaches

There are a variety of approaches for determining the slope stability of a particular slope. Different methodologies, such as Rock mass rating, slope mass rating, kinematic, deterministic, probabilistic, numerical methods, can be used to assess slope stability (Abramson *et al.*, 2001; Raghuvanshi, 2019). The stability assessments can be carried out in two steps if the specified slope is a rock slope (Park and West, 2001). To identify the mode and types of rock slope failure, the first step is to undertake a kinematic analysis of rock discontinuities. The second phase involves doing additional stability analyses for the kind and mode of rock slope failure indicated by the kinematic technique using the limit equilibrium method. Slope stability analysis methods in the past were mostly based on calculations that were done by h, which simplified the process. Now a day, more and more powerful computer software becoming commonly available, and experts have developed complicated but more accurate methods. The most common slope stability analysis methods discussed are as follows; -

2.5.1. Rock Mass Rating

Rock Mass Classification is one of the empirical methods for determining the quality and performance of rock based on intrinsic and structural parameters. It is mostly used to determine the possible failure of rock-cut slopes (Pantelidis, 2009). It was first proposed for use in tunnel design, dam design, mine design, excavation design; later, it was used to determine slope stability (Bieniawski and Bernede, 1979).

According to (Bieniawski, 1989), to identify the quality of rock examine the stability of the important rock slope, five fundamental rock mass rating factors can be used to classify the quality of the rock mass into different classes. Classifications of Rock Masses are a system for classifying organizing rock masses into classes based on predetermined relationships most important identifying the most significant parameters that influence the behavior of a rock mass having information on composition, strength, deformation properties (Bieniawski, 1989). The five basic rock mass rating parameters used to classify the quality of the rock mass are, intact rock strength, rock quality designation index (RQD), spacing of discontinuity, condition of discontinuity, groundwater conditions (Bieniawski, 1989).

Intact rock strength is mostly defined as the strength of the rock material between the discontinuities. Strength values used are often from laboratory unconfined compressive strength (UCS) tests. Intact rock strength can be determined either from the uniaxial compressive strength of rock or point load strength index which is measured by the rebound value in a Schmidt hammer test and by its response to a blow from an ordinary hammer. Uniaxial compressive strength of rock (UCS) can be determined from the point load strength index using (Broch and Franklin, 1972) empirical relation stated as follow:

$$UCS = 24 * Is(50) \tag{2.3}$$

Where Is(50) is size corrected point load strength.

Rock Quality Designation (RQD) is a measure of the quality of rock core taken from a borehole. It signifies the degree of jointing or fracture in a rock mass measured in percentage, where RQD of 75% or more shows good quality hard rock less than 50% showed low quality weathered rocks. The rock quality designation index (RQD) is determined from the summation of intact rock greater than 10cm per total core run equation (Deere and Deere, 1989). However, in the area where there was no rock core data occur, the rock quality designation (RQD) index was determined by the volumetric joint count method (Palmstrom, 2005) which is the total number of discontinuities (Jv) greater than 10cm present in one square meter of rock as shown below.

$$RQD = \frac{\sum \text{int}\ act\ rock > 10\ cm}{total\ core\ run} \tag{2.4}$$

$$RQD = 115 - 3.3 * JV \tag{2.5}$$

Where JV is the total number of discontinuity per square meter (1mx1m) of rock mass exposure.

Discontinuity spacing is a basic measurement of the distance between one discontinuity and another. It is a critical characteristic for describing the quality of a rock mass and has numerous applications in rock engineering. In the field, discontinuity spacing was measured by measuring the distance between neighboring discontinuities and taking an average measurement result. In the field, the sub-parameters under conditions of discontinuities, such as persistence, aperture, roughness, infilling, and weathering condition of the wall rock or plane of discontinuity can also be estimated.

The visual observation of either water flowing out of the slope or the presence of water stains on the slope face is also used to determine the state of groundwater (Pantelidis, 2009).

This parameter can be visually determined in the field as dry, damp, and wet. Finally, the rating for five basic rock mass rating parameters will be added together to classify the rock of the study area based on the Rock Mass Rating system.

2.5.2. Kinematic Analyses

The kinematic analysis describes body motion without taking into account the factors that drive them to move (Shi and Goodman, 1989; Goodman and Kieffer, 2000). Kinematic studies are a method for identifying kinds of rock slope failure (plane, wedge, toppling failures) that might occur for existing or projected rock slopes are caused by unfavorably oriented discontinuities along the road, natural steep slope, pit slopes (Hoek and Bray, 1981; Wyllie and Mah, 2004).

By evaluating the strike angle, dip angle, dip direction of the slope discontinuity surface in the kinematic analysis, stereographic projections are utilized to identify the likely mechanism of rock slope failure (planer, wedge, toppling) (Lamessa and Meten, 2021). Importing the friction angle (friction cone), dip, and dip directions can be used to do the analysis. Then, the software undergoes the kinematic analyses by identifying the main joint, daylight envelope, lateral limits, and mode of rock slope failure (Shi and Goodman, 1989; Harrison *et al.*, 2002; Wyllie and Mah, 2004). For kinematic checks, stereographic projection can be also used (ZainAlabideen and Helal, 2016). On a stereo-net, the representative great circles for all preferred discontinuity planes, present on the given slope, are plotted. Also, the great circle for slope face and friction circle, corresponding to the friction angle of the discontinuity plane, are plotted. The zone is demarcated by the friction circle and the slope face is designated as sliding.

According to (Hoek and Bray, 1981; Goodman and Kieffer, 2000; Wyllie and Mah, 2004) to consider the kinematic admissibility of the planar mode of failure the following criteria must be satisfied.

- The plane on which sliding occurs must strike near parallel to the slope face (within approx. ±20°).
- Release surfaces (that provide negligible resistance to sliding) must be present to define the lateral slide boundaries.
- The sliding plane must be "daylight" on the slope face.
- The dip of the sliding plane must be greater than the angle of friction.
- The upper end of the sliding surface either intersects the upper slope or terminates in a tension crack.

Also for wedge failure, there are several conditions relating to the line of intersection that must be met for the failure to be kinematically admissible these are:

- The dip of the slope must exceed the dip of the line of intersection of the two wedge forming discontinuity planes.
- The line of intersection must be daylight on the slope face.
- The upper end of the line of intersection either intersects the upper slope or terminates in a tension crack.

Several favorable conditions can be considered as pre-request for the kinematic admissibility for the occurrence of toppling failure are:

- The presence of jointed rock mass closely spaced and steeply dipping discontinuity sets that dip away from the slope surface.
- The strikes of the sliding plane and the slope face lie parallel (± 10º) to each other.

Another type of slope failure is Circular mode slope failure which occurs in weak materials such as highly weathered or closely fractured rock soils where failure occurs along surfaces having an approximately circular shape (Wyllie and Mah, 2004).

2.5.3. Limit Equilibrium Method (LEM)

The limit equilibrium method is the most common approach for analyzing slope stability and it identifies potential failure mechanisms and derives factors of safety for a particular geotechnical situation. As (Tang *et al.*, 2019) when compared to the numerical methods limit equilibrium methods are relatively simple in their application.

The stability of slopes using limit equilibrium utilizes the Mohr-Coulomb expression to determine the shear strength (τf) along the sliding surface (Aryal, 2006). A state of limit equilibrium is obtained by expressing the mobilized shear stress (τ) as a fraction of the shear strength (τf). The available shear strength depends on the type of soil and the effective normal stress, whereas the mobilized shear stress depends on the external and internal forces acting on the soil mass. Hence, limit equilibrium analysis defines FS as a ratio of shear strength (τf) to mobilized shear stress (τ) (Das *et al.*, 2010).

Shear strength available $$(\tau f) = c' + \sigma' \tan\theta' \tag{2.6}$$

Mobilized shear stress $$(\tau) = \frac{\tau f}{FS} = \frac{c' + \sigma' \tan\theta'}{FS} \tag{2.7}$$

The critical slip surface is defined as the slip surface with the lowest FS, and the slope stability analysis in LEM usually comprises an iterative process until the critical slip surface is determined. The mass process and the method of slices can be used to analyze slope stability in limit equilibrium. When the soil that forms the slope is assumed to be homogeneous, the mass of the soil above the sliding surface is considered as a unit, the mass procedure is utilized (Das *et al.*, 2010). The soil above the sliding surface is divided into numerous vertical parallel slices in the slices method, and the stability of each slice is computed independently. This is a versatile technique as the non-homogeneity of the soils, pore water pressure, and the variation of the normal stress along the potential failure surface can be taken into consideration. The limit equilibrium method provides only an estimate of the stability of a slope but doesn’t provide any information about the magnitude of movement of the slope (Wright and Duncan, 1991).

2.5.4. Finite Element Method

The finite element method is a potent alternative to the traditional approach for slope stability analysis because it is accurate, adaptable, and requires fewer a priori assumptions, particularly for the failure mechanism. In the finite element model, slope failure happens 'naturally' in zones where the soil's shear strength is insufficient to resist the shear stresses. FEM is a new powerful engineering computational method that may replicate a problem's physical characteristics using modern computational tools without the need to simplify it (Kramer *et al.*, 2013).

The ability to analyze any geometry of slope in two three-dimension, the ability to analyze both linear nonlinear problems, the ability to give FOS without having assumptions about the shape position of the sliding plane, the ability to employ various soil material models its ability to consider the stress-strain relationship of the material makes the FEM preferable analysis over conventional limit equilibrium method (Kumar *et al.*, 2021). Furthermore, FEM gives information about the deformations at working stress levels can monitor progressive failure including overall shear failure so, the results obtained from this analysis are considered to be more realistic compared to the limit equilibrium method (Griffiths and Lane, 1999).

In the last two decades, several methods were presented for slope stability analysis by 'FEM'. Through this method, the gravity increase method 'strength reduction method' have been widely used (Nurjanah *et al.*, 2017). In the gravity increase method, the gravity forces, such as; weight, increase gradually until the slope becomes unstable. Then factor of safety defines the ratio between gravitational acceleration in failure time and actual gravitational acceleration. In the 'strength reduction method', the strength parameters of the slope are decreased until the slope becomes unstable (Nurjanah *et al.*, 2017). Hence, the safety of the factor determines the ratio between actual strength parameters and critical strength parameters. The gravity increase method is well suited for analyses of the stability of embankments (Swan and Seo, 1999).

2.6. Shear Strength Parameters

In slope stability analyses, shear strength is the most crucial aspect. Determining shear strength is a difficult task, and understanding the theory is required to complete the study correctly. Limit equilibrium and Finite element approaches for determining slope stability require an accurate and reliable estimation of the slope materials' in-situ shear strength. However, several complicated factors, including the in-situ state of stress, drainage, loading rates, soil or rock composition, have a significant impact on shear strength characteristics (Abramson *et al.*, 2001).

The following sections discuss the shear strength characteristics that have been utilized as input data for slope stability analysis; -

2.6.1. Cohesion and Friction angle

Cohesion is the force that holds together molecules or likes particles within the soil and it is the component of the shear strength of a rock or soil that is independent of interparticle friction. Friction angle is the angle of an inclination concerning the horizontal axis of the

Mohr-Coulomb shear resistance line. Cohesion *'C'* and angle of friction `φ` are usually determined in the laboratory from the direct shear test.

2.6.2 Unit weight

Unit weight of a soil mass is the ratio of the total weight of the soil to the total volume of the soil. Unit weight, γ, is usually determined in the laboratory by measuring the weight and volume of a relatively undisturbed soil sample obtained from the field.

2.7. Shear strength criteria of soil and rock

2.7.1. Mohr-Coulomb Failure Criterion for Soil

Mohr-coulomb provides a failure criterion of soil material based on the critical combination of normal shear stress (Das *et al.*, 2010). The Mohr-Coulomb criterion relates the shear strength of the material on the failure plane to the cohesion, normal stress, and angle of internal friction of the material (Eq.2.8). As shown in (Fig 2.5) any combination of normal shear stress along with the MC failure envelop (B) leads to slope failure, any combination of normal shear stress below the MC envelope (A) is safe no combination of normal shear stress can exist above the failure envelope (C).

$$\tau f = c' + \sigma n \tan \theta' \qquad (2.8)$$

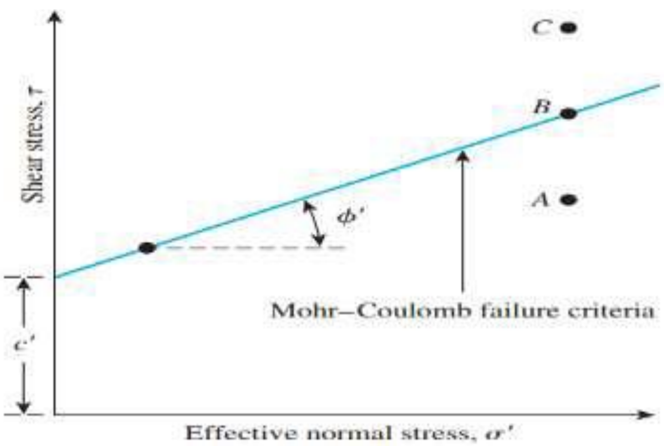

Fig 2.5: Mohr-Coulomb failure criterion (Das *et al.*, 2010).

2.7.2. Shear strength of rocks

Rock slope collapses can occur at discontinuity surfaces or through the rock mass, depending on scale effects geological conditions (Wyllie and Mah, 2004). As illustrated in Figure 2.6, the relative scale between the sliding surface and structural geology influences the selection of adequate rock shear strength criteria for slope stability.

The failure will occur through the jointed rock mass if the total slope dimensions are substantially bigger than the discontinuity length, and the rock mass strength is considered for slope stability calculations. Slope failures, on the other h, occur along the discontinuities of a single joint if the joint length is almost equal to the slope height, and stability analysis is based on discontinuity rock strength.

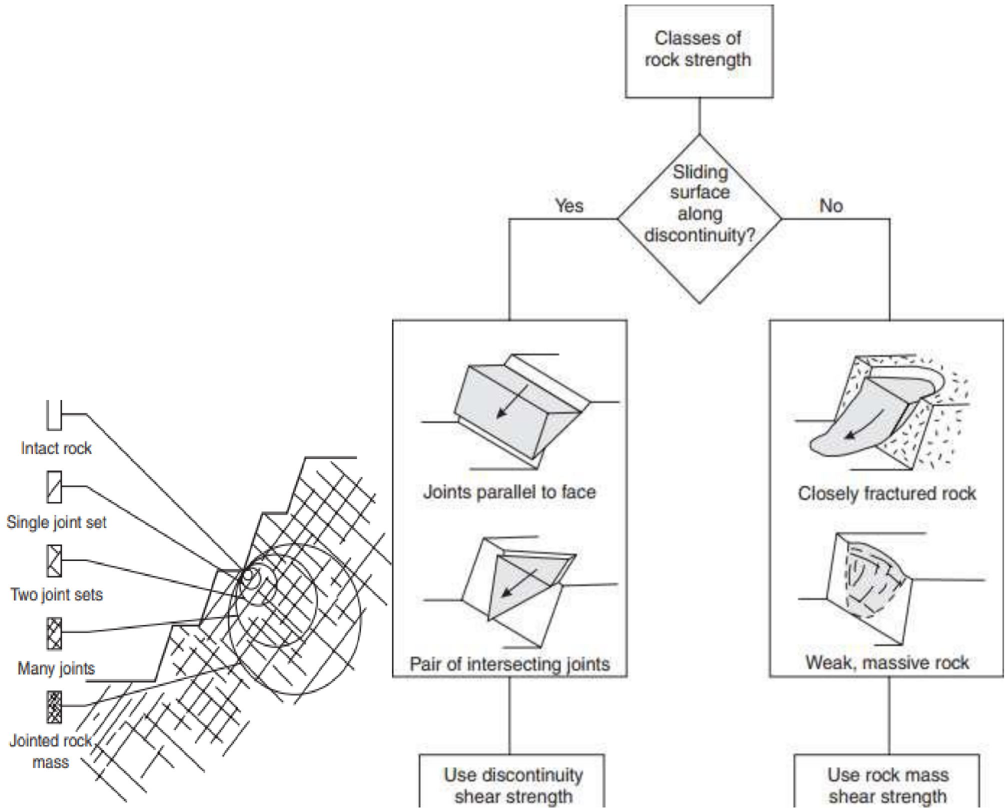

Fig 2.6: The shear strength changes between intact rock, discontinuities, rock mass with increasing sample size (Wyllie and Mah, 2004).

2.7.3. Shear Strength Criterion for discontinuities

To determine the shear strength of discontinuities, (Barton, 1973) developed an empirical low of basic friction angle. The combined effects of surface roughness, rock strength at the surface, applied normal stress, the amount of shear displacement determine the shear strength of discontinuity surfaces in rock slopes (Wyllie and Mah, 2004). Shear tests (Figure 2.7) or correlations with discontinuity characteristics can be used to determine shear strength values.

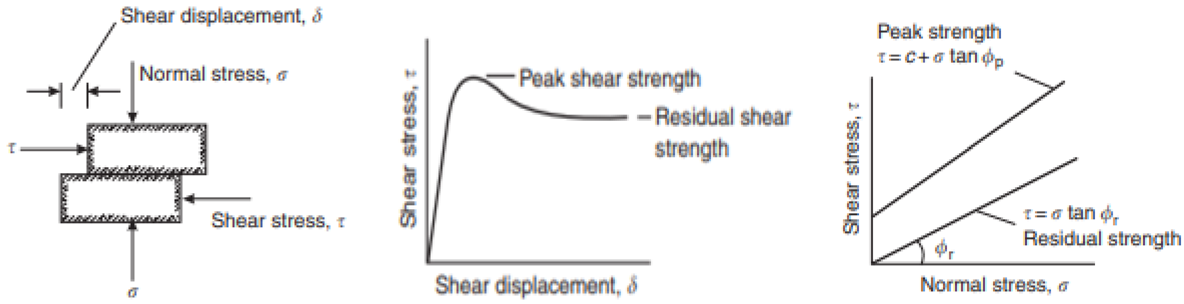

Fig 2.7: Shear test its Mohr coulomb shear strength envelope (Wyllie and Mah, 2004).

$$\tau = \sigma_n \tan \phi_r + c \qquad \text{(Mohr-Coulomb, 1773)} \qquad (2.9)$$

$$\tau = \sigma_n \tan(\phi_r + i) \qquad \text{(Patton and Gardner, 1963)} \qquad (2.10)$$

$$\tau = \sigma_n \tan\left\{\theta_b + JRC * \log_{10}\left(\frac{JCS}{\sigma_n}\right)\right\} \qquad \text{(Barton, 1973)} \qquad (2.11)$$

Joint wall compressive strength (JCS) is the strength of a layer of rock adjacent to the joint it controls the strength deformation properties of the rock mass (Barton, 1973). It is taken as a uniaxial compressive strength (UCS) of un-weathered rock about 25% of the UCS on the weathered rock (Barton and Choubey, 1977). The joint roughness coefficient (JRC) is the

coefficient of joint surface roughness having a value ranging from 0 to 20 (smoothest to roughest) as described by (Barton and Choubey, 1977). A basic friction angle ($\emptyset b$) is an angle with flat, planar, un-weathered rock surface in which its value ranges from 25º-35º (Barton, 1973). For variably weathered joints, basic friction angle can be correlated with residual friction angle (ϕr) using Schmidt rebound number of wet weathered (r) dry weathered surfaces (Eqn. 2.12) as stated by (Barton and Choubey, 1977).

$$\theta_r = (\theta b - 20) + 20\left(r/R\right) \qquad (2.12)$$

2.7.4. Shear strength criterion for rock mass

The shear strength of rock mass can be determined from the generalized Hoek-Brown strength criterion which expresses the shear strength in terms of the major and minor principal stresses.

2.7.4.1. Hoek-Brown Strength criterion for rock Mass

Since 1983, the Hoek-Brown failure criterion for rock mass has been revised numerous times. Correlations between the criterion and rock mass rating factors were introduced to explain the attributes of the rock mass. (Chala and Rao, 2021) summarized the Hoek-Brown rock mass strength criteria presented them as follows: The RMR-system was employed in the original, updated, modified versions, however, Hoek et al. suggested the Geological Strength Index (GSI) for the generalized Hoek-Brown criterion (Merifield *et al.*, 2006). The original Hoek-Brown failure criterion for intact rock and rock mass was developed in 1980. Hoek and Brown (Merifield *et al.*, 2006) found that the peak triaxial strength of a wide range of rock materials could reasonably be represented by the Eq. (2.13).

$$\left(\frac{\sigma_1-\sigma_3}{\sigma_c}\right)^2=\left(\frac{m\sigma_3}{\sigma_c}\right)+s \tag{2.13}$$

This results in a linear graph (y=mx+s) with slope m and intercepts. Where m and s are constants that depend on the properties of the rock and on the extent to which it has been broken before being subjected to the stresses. The unconfined compressive strength of rock mass is expressed as Eq. (2.14).

$$\sigma_{cm}=\sigma_3 * s^{1/2} \tag{2.14}$$

In the 2002 edition of the Hoek-Brown failure criterion, the generalized expression is used (see Eq. 2.15), but with the following modifications of the (mb), (s), and (a) values as follows:

$$\sigma_1'=\sigma_3'+\sigma_{ci}\left(m_b\frac{\sigma_3}{\sigma_{ci}}+s\right)^a \tag{2.15}$$

$$a=\frac{1}{2}+\frac{1}{6}\left(e^{\frac{-GSI}{15}}-e^{\frac{-20}{3}}\right) \tag{2.16}$$

$$s=e^{\left(\frac{GSI-100}{9-3D}\right)} \tag{2.17}$$

$$m_b = m_i e^{\left(\frac{GSI-100}{28-14D}\right)} \tag{2.18}$$

where σci is the uniaxial compressive strength of intact rock, mb is a value depending upon the characteristics of rock mass determined from equation 2.11 mi is for intact rock determined from a triaxial test or the tabulated data proposed by (Hoek and Karzulovic, 2000) for different types of rock, s, α are constants depending upon the GSI value of rock mass. Geological strength index (GSI) an estimate of the reduction in rock mass strength for different geological conditions. Its value is obtained by considering the weathering condition of discontinuity surface, rock mass structure, interlocking of rock blocks proposed by (Wyllie and Mah, 2004). D is a disturbance factor that depends upon the degree of disturbance for rock mass subjected to blasting and mechanical excavation (it varies from 0 for undisturbed to 1 for very disturbed rock masses).

2.7.4.2. Equivalent linear Mohr-Coulomb failure criteria for rock mass

Mohr-Coulomb also provides an equivalent failure criterion which gives a straight-line plot between $\tau - \sigma'n$ plane in rock mass compared to the curved Hoek - Brown failure envelope (Figure 2.8). Equation 2.19 and 2.20 is used to determine the Hoek - brown equivalent Mohr-Coulomb parameters for practical applications.

$$\sin\theta' = \frac{6\alpha m_b\left(s+m_b\sigma' 3n\right)^{(\alpha-1)}}{2(1+\alpha)(2+\alpha)+6\alpha m_b\left(s+m_b\sigma 3n\right)^{(\alpha-1)}} \tag{2.19}$$

$$c' = \frac{\sigma_{ci}\left[(1+2\alpha)s+(1-\alpha)m_b\sigma' 3n\right]\left(s+m_b\sigma' 3n\right)^{\alpha-1}}{(1+\alpha)(2+\alpha)\sqrt{1+\frac{6\alpha m_b\left(s+m_b\sigma' 3n\right)^{\alpha-1}}{(1+\alpha)(2+\alpha)}}} \tag{2.20}$$

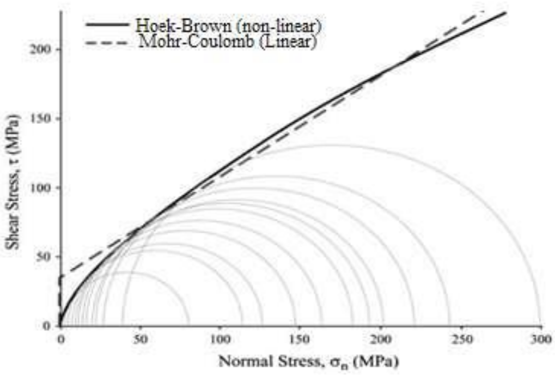

Fig 2.8: Non-linear Hoek–Brown and equivalent linear Mohr-Coulomb failure criteria

2.8. Software Applications

2.8.1. Slide 2D Software

Slide 2D software is a 2D-limit equilibrium-based computer program used to evaluate the safety factor of soil and rock slopes with circular, non-circular, and composite failure surfaces. The software is initially proposed by Rocscience Inc Toronto Canada and used for slope stability analysis of both soil and rock slopes. It analyzes the stability of slopes by vertical slice using different limit equilibrium analysis methods (i.e. Bishop, Janbu's, Spencer, GLE, and Fellenius). The software also has various features including searching for critical surfaces, modeling multiple, anisotropic, non-linear Mohr-Coulomb materials, defining analyzing groundwater problems, viewing detailed analysis results.

2.8.2 RocPlane Software

RocPlane is an interactive program created for performing planar rock slope stability analysis and design. It is simple to use and it also allows users to estimate the support capacity required to achieve a specified factor of safety. RocPlane makes it easy to quickly create planar models, visualize them in both 2D and 3D, and evaluate analysis results. RocPlane also contains many helpful features that allow users to rapidly build modify and run models and it analyzes a slice of unit thickness taken perpendicular to the strike of the slope face.

2.8.3. Swedge Software

Swedge software is quick, interactive, and simple to use and it is an analysis tool for evaluating the geometry and stability of surface wedges in rock slopes. Wedges are defined by two intersecting discontinuity planes, the slope surface, and an optional tension crack. Swedge provides an integrated graphical environment for fast, easy data entry 2D and 3D model visualization. Destabilizing forces due to water pressure, seismic loads, or external forces can also be easily modeled. Joint shear strength options include Mohr-Coulomb, Barton-Bandis, or Power Curve models, and a joint waviness angle can be defined.

2.8.4. Phase 2D Software

Phase2 mining software is a dynamic software program designed for analyzing and modeling soil and rock slopes. It is used in designing underground and surface excavations for geotechnical, civil, and mining applications. Phase2 mining software enables its users to perform various functions, including slope stability analysis and excavation designing to name a few.

CHAPTER THREE

3. METHODOLOGY

This chapter incorporates the general procedures, approaches, or methodologies followed during desk study, detailed field survey, laboratory test, data processing, and analyzing stages to achieve the intended objectives of this research work successfully.

3.1. Desk Study

In chapter two a literature review concerning the cause and impact of slope stability that occur in the world, Ethiopia, and as well as in the study area was done. Similarly, a review of unpublished and published journals, books, and different methods used to analyze slope stability along road sections, open pits of mining, and steep slope areas or ridges was done. To acquire the general conditions of the slope stability in the study area, information was gathered and field reconnaissance survey was undertaken and the condition of slope stability was inferred based on the field manifestations.

3.2. Data Collection

In this stage, the secondary data which are essential to analyze the stability of the slope was collected from different organizations and institutions like the National Metrological Service Agency (Temperature data, Rain fall data, Ground water depth data) Geological Survey of Ethiopia (geological and topographic map, report on regional geology of the area). Finally, the graph of the mean monthly rain fall in the study area was plotted using Microsoft Excel from the data taken from Ethiopia National Metrological Service Agency that was collected at Adama station.

3.3. Detailed Field Survey

After the literature review and reconnaissance survey, a detailed field survey was conducted mainly which focused on a detailed investigation of slope stability in the study area. During this detailed investigation, information on geological structures, types of lithology, the strength of the rocks, and groundwater conditions of the slopes were identified. In addition to this, critical slope failure was identified located based on the field manifestation such as; removal of slope toe, development of tension crack, tilting of slope face, orientation of discontinuity which favor rock slope failures. Surface mapping of structures like the joint set was undertaken by measuring their orientations (dip and dip directions) of slope and discontinuities using the Brunton compass. Conditions of discontinuity such as; joint roughness, aperture, infilling material, and weathering conditions were visually estimated and measured by using a meter on the field. In addition to that, visual classification of soil was done based on physical properties of soil like color, grain size, origin according to (Energy, 2002). To determine shear strength parameters of failing soil mass to determine the unit weight of rock found on the critical sections of the ridge, Both samples of rock soil (undisturbed) were taken kept in plastic immediately after sampling to keep their natural moisture content then brought to the laboratory. In this study uniaxial compressive strength (UCS) of representative, fresh, and weathered exposed rock surface was determined in the field using a portable instrument called an N-type Schmidt hammer as shown in fig 3.1 below. The test was conducted according to the standard suggested by ASTM (2001), (American Society for Testing and Materials).

Later, uniaxial compressive strength (UCS) of the rock which composes critical rock slope along the critical section of the ridge was determined using (Barton and Choubey, 1977) relation as shown below:

$$\log 10(UCS) = 0.00088 * \gamma * R + 1.01 \tag{3.1}$$

Where; ‘UCS’ is the uniaxial compressive strength in Mpa, γ is the dry rock densities in KN/m3 and R and averages Schmidt hammer rebound value.

Fig 3.1: Measuring of In-situ strength of intact rock using Schmidt hammer rebound test for the estimation of uniaxial compressive strength (UCS) (above) and field photos of unstable slope sections (below).

In this study, the input parameter that was used to determine shear strength parameter along the failure plane or discontinuities based on (Barton, 2014) non-linear failure criteria was estimated as follows;

- ✓ Basic friction angle was adopted from Coulson (1972) which was already built-in Rocdata software.
- ✓ Joint roughness was determined by comparing joint roughness visually estimated on the field with (Barton and Choubey, 1977) standard roughness profile which was also built in Rocdata software.
- ✓ Then, joint wall compressive strength was determined from uniaxial compressive strength determined on the field using Schmidt hammer rebound value conducted on representative un-weathered and weathered rock surfaces.
- ✓ Slope height and unit weight of the rocks were determined in the field and laboratory respectively.

Finally, the equivalent Mohr-Coulomb shear strength parameter (c and ϕ) along discontinuities or failure plane was determined by Rocdata software which performs based on (Bandis, 1990) non-linear failure criteria.

3.4. Laboratory Test

In this study, the following test was conducted on different soil and rock samples were taken from the field.

3.4.1. Laboratory Test on Rock Sample

3.4.1.1. Unit Weight Test

In addition to the Schmidt hammer test of rock strength in the field, the unit weight of the rock samples collected from the study area was determined at the laboratory by undergoing buoyancy techniques on irregular rock samples according to the standard suggested by ISRM (1978) as shown in (Fig 3.2). In this study, the unit weight test of rock was conducted on three samples of rocks and the result is summarized in (Table 5.6).

Fig 3. 2 Measuring the saturated volume of a rock sample in a Beaker filled with water.

3.4.2. Laboratory Test on soil Sample

To undergo the stability analyses of the soil slope, to determine the shear strength parameters and unit weight, the unit weight and direct shear strength tests were conducted on representative soil samples taken from the test pit with a minimum depth from 1m to 2m as shown in (Fig 3.3) below.

Fig 3.3: a collection of an undisturbed soil sample from depth.

3.4.2.1. Direct Shear Test

In the present study, the direct shear test is used to determine the shear strength of soil samples taken from critical sections of ridges according to ASTM D 3080 (1998) by using direct shear apparatus, as shown in fig (3.4) below.

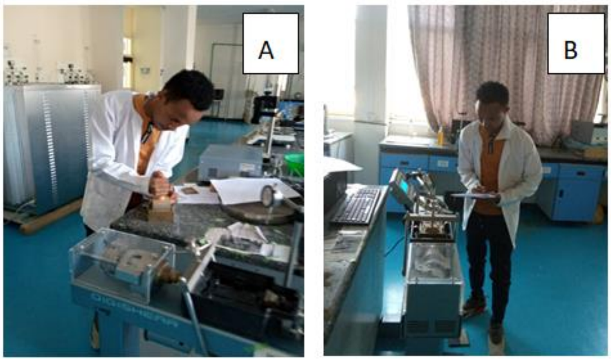

Fig 3.4: preparation of soil sample for direct shear test (A) Taking of readings from Direct Shear test Apparatus (B).

3.4.2.2. Unit Weight Test

In this study, the unit weight test of soil was conducted on representative samples collected during a detailed field survey, and finally, both bulk unit weight and dry unit weight was determined. Dry unit weight was derived or calculated from bulk unit weight. In general, laboratory test on soils and rocks in this study was summarized below in table (3.1).

Table 3.1: summary of laboratory tests on rock and soil samples.

Laboratory test	Type of Material	No of sample	No of trial
Unit weight test	Rock	3	2 for each
	Soil	2	2 for each
Direct shear test	soil	2	3 for each

3.5. Soil Stiffness

The elasticity modulus (E) and Poisson's ratio (v) are soil stiffness parameters and important input parameters used for soil and rock deformation analysis in numerical modeling. When laboratory tests are unavailable for determining the elasticity modulus, they can be determined from empirical correlations (Duncan and Bursey, 2013). The values of the elasticity modulus determined from correlations are more useful effective than direct measurements (Duncan and Bursey, 2013). For this study, the value of Poisson's ratio and Young's modulus ratio of soil parameters were obtained from numerical correlations and different existing literature. The drained poisons ratio of the soils was determined from equation (Eq. 3.6) as suggested by (Kulhawy and Mayne, 1990), (Das *et al.*, 2010). For this study, the corrected standard penetration test SPT N value to an average energy ratio of 60% was determined using equation (Eq.3.7) as recommended by (Wolff and Wang, 1992). The modulus of elasticity of the soil was calculated from the SPT N value as proposed by (Somasundaram *et al.*, 2019) (Das *et al.*, 2010).

$$Vd = 0.1 + 0.3\left(\frac{\phi - 25}{20}\right) \qquad \text{For N < 15} \qquad (3.2)$$

$$\phi(\deg) = 27.1 + 0.3N_{60} - 0.00054N^2{}_{60} \qquad (3.3)$$

$$E = 1200(N + 6)\frac{KN}{m^2} \qquad \text{For N < 15} \qquad (3.4)$$

$$E = 4000 + 1200(N - 6)\frac{KN}{m^2} \qquad \text{For N > 15} \qquad (3.5)$$

The dilatancy parameter describes the ability of soils to change in volume under shearing stresses. For simplicity, this can be interpreted as the ability of grains to slide upward (positive) or downward (negative) over each other during shear. For this study angle of dilation in degree for clay soils considered as zero and for sand and gravel soil it found by subtracting the 30° from the friction angle of the material if it is greater than 30°. For negative value we take it as zero.

3.6. Data Processing and Analyses

The collected data from secondary and primary sources through desk study, reconnaissance and detailed field survey, laboratory test, and literature review were organized and processed in a way that they can be accessed easily during further stability analyses. After the whole data needed for stability analyses was collected and processed, the stability of the slope was analyzed by determining:

- Quality of the rock which composes the critical rock slope section.
- Kinematic analyses of geological structure or discontinuities are oriented along with the critical slope face and favor failure of the slope.
- The factor of safety was determined based on limit equilibrium and finite element methods for identifying critical rock and soil slopes.

3.6.1. Rock Mass Quality

In this study, the five basic parameters that are used to classify determine the quality of rock mass like the spacing of discontinuities, uniaxial compressive strength, rock quality designation index, condition of discontinuity (infill material, persistence, aperture, roughness, weathering conditions) saturation conditions was estimated measured at the field as discussed under detailed field survey. Similarly, since there is no rock core data to determine rock quality designation index (RQD) (Deere and Deere, 1989), the volumetric joint count method developed by (Palmstrom, 2005) was followed. After the five basic parameters were determined, the rock mass quality of the rock at two selected critical rock slope sections was evaluated by adding the rating value for the five basic parameters adopted from the standard table proposed by (Bieniawski, 1989).

3.6.2. Kinematic Analysis

Failure of rock slope mostly takes place along structural discontinuities or weakness planes such as joint, fault, etc. In this study, orientations of slope and structural discontinuities exposed over selected critical rock slope faces were measured on the field using a Brunton compass. The friction angle along the failure plane was used as a basic friction angle or friction cone it was determined by Rocdata software which uses (Barton, 2014) non-linear failure criteria. Kinematic checks or Markland conditions of kinematic admissibility (Wyllie and Mah, 2004) were undertaken along with kinematic analyses. Later, the kinematic analyses for major planes or persistent joints were performed by using dips software (Dips 6.0 Rocscience, 2004) to determine the possible mode of failure under equal-area lower hemisphere projection which is the default projection for dips software and the result is presented in chapter five.

3.6.3. Limit Equilibrium Method

The limit equilibrium method is the most common approach for analyzing slope stability in both two and three dimensions. This method identifies potential failure mechanisms and derives factors of safety for a particular geotechnical situation. In this study, the factor of safety was determined for critical rock slope sections by using Swedge and Rocplane software and for critical soil slope sections by using slide software under the Spenser method among Limit Equilibrium Methods (LEM). Here spencer method is used because the value of the factor of safety under it is smaller as compared with the others.

3.6.4. Finite Element Method

Now a day with the recent advancement in computer technology, the finite element method has become a preferable alternative to traditional methods in geotechnical engineering. Slope stability analyses finite element method is depending on the shear strength reduction (SSR) technique which is helpful to determine the factor of safety the improvement after strengthening (Dawson *et al.*, 1999; Griffiths and Lane, 1999). In this study Phase, 2D software was used to determine the factor of safety under the Finite Element Method (FEM) of slope stability analysis. By using phase 2D, the factor of safety of the three soil slopes was determined at all anticipated conditions (i.e. static dry, dynamic dry, static wet, dynamic wet) under Mohr–Coulombs model.

3.7 Materials

Materials that have been used for this study were the base map of 1: 40000 scales prepared for the collection of geological field data. The material and equipment that were used for this research work include both laboratory and field equipment. The field equipments that were used for field data collection, measurement, and testing included GPS, compass, geological hammer, and Schmidt hammer for the in-situ test of rock strength. Soil mechanics laboratory equipment like direct shear test apparatus, balance, beakers, and cylinders were used for lab works of shear strength tests and unit weight tests. The data processing interpretation were done with the help of different software such as Arc GIS 10.4.1, Surfer 10, Swedge4.0, Dip6.00, Slide6.00, Phase8.0, Rockplane2.00, Rocdata software were used for slope stability analysis. The general flow chart of this study is shown below in figure 3.5.

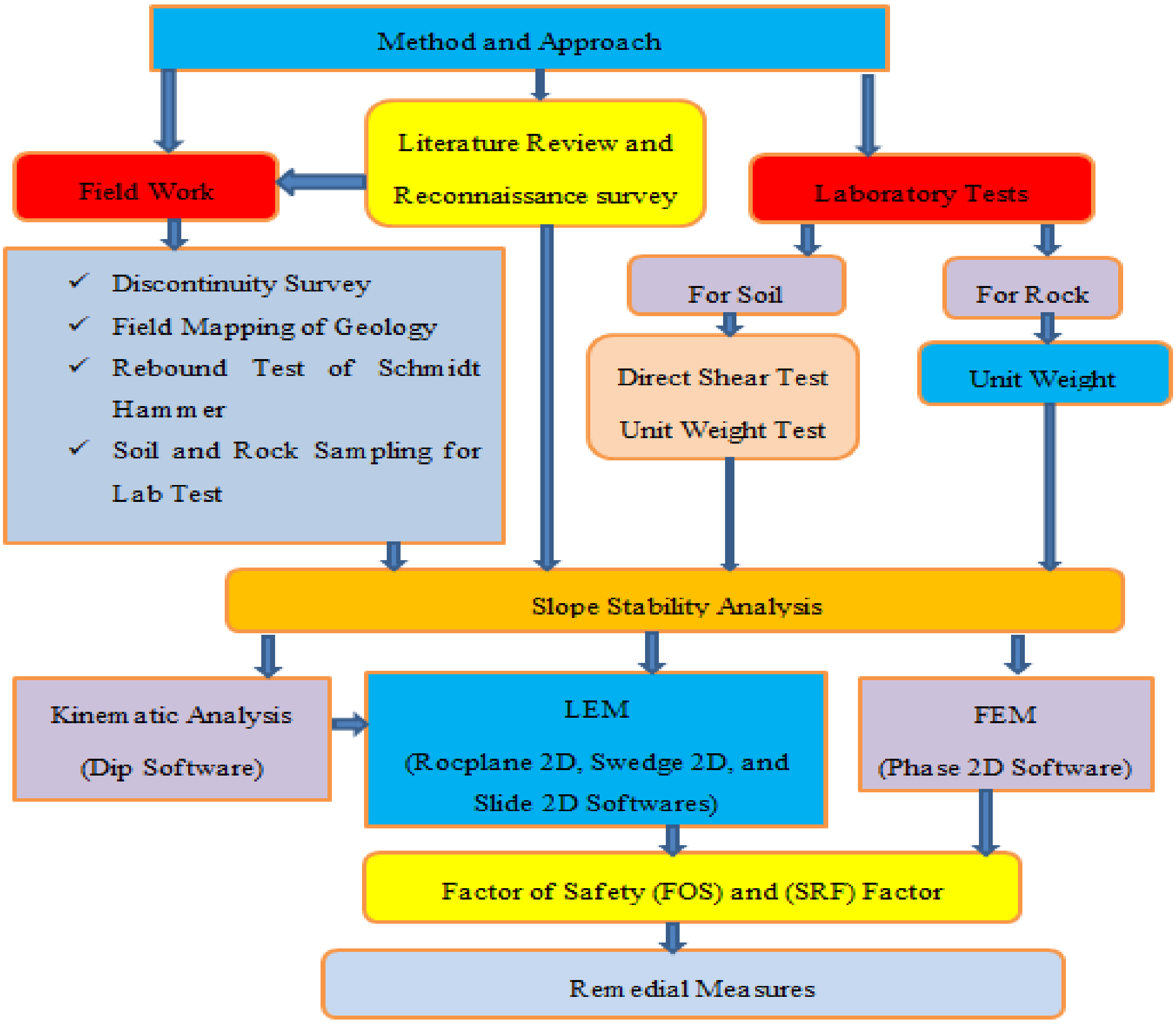

Fig 3.5: General methodology flow chart.

CHAPTER FOUR

4. GEOLOGY OF STUDY AREA

4.1. Regional Geology

In Ethiopia, the major geological units include Precambrian rock, Paleozoic, Mesozoic sedimentary rock, and Cenozoic rocks which include tertiary to quaternary volcanic and quaternary sediments (Mengesha *et al.*, 1996). Since the present study area is situated within Main Ethiopian Rift, most of its lithology is related to the volcanic product. The dominant rocks in the region include basalt tuffs, agglomerates of Paleocene Miocene age, ignimbrites of Miocene to Pleistocene age, rhyolites, trachyte, pumice as described in (Abera *et al.*, 2016) as shown in (fig 4.1). The lithology of an area comprises alaji basalt groups; ignimbrite unit corresponds to Nazreth series, Boku-tede unit which is the product of the collapse of the huge caldera of Boku, Bofa unit of fissural origin, boset unit of lava flows outpoured by the jinjimma trachyte cone (Bosetti-Gudda volcano). In addition to that, an area consists of andosols, fluvisols, lithosols as the major types of soils found in the region (Furi *et al.*, 2011). The physiographic conditions of an area are mainly the result of volcano-tectonic activities that occurred in the past also partly the result of the deposition of sediments, which are considered largely of fluvial lacustrine origin (Furi *et al.*, 2011).

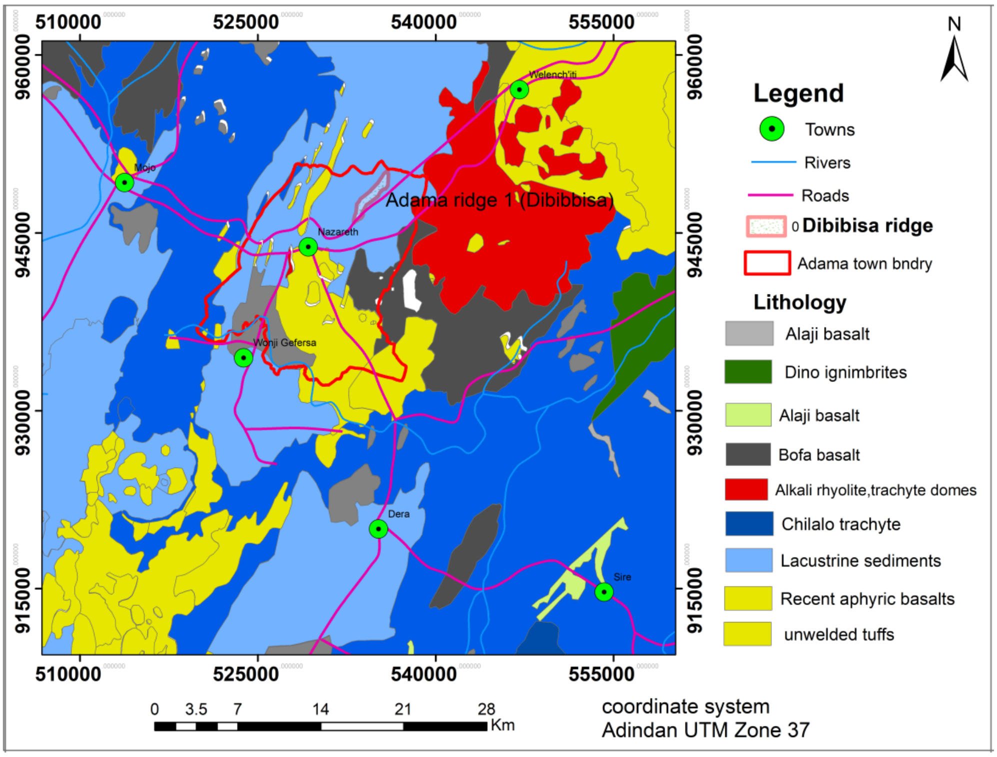

Fig 4.1: Regional geological map of Adama area modified after (GSE).

4.2. Local Geology

The study area is in the Wonji Fault Belt, the main structural system in central Rift Valley which is dominated by escarpments bordering. Specifically, the present study area, locally known as Dibibisa ridge is dominated by ignimbrite rocks. Ignimbrite rocks found in this area are characterized by different degrees of weathering (slightly weathered to highly weathered) and fracturing as well as leaching. In addition to ignimbrite rocks, this study area comprises colluvial, residual and pumice soils. Each of the lithological units are discussed one by one below:

4.2.1. Ignimbrite Rock

Ignimbrite is the one among igneous rocks and it is made from a variety of hardened tuff. Ignimbrites may be white, grey, or pink depending on their composition and density. In the present study area (the Dibibisa ridge) ignimbrite rocks are dominant lithology and there are slightly weathered to highly weathered and fractured ignimbrites as shown in (fig 4.2) which covers the major part of the study area.

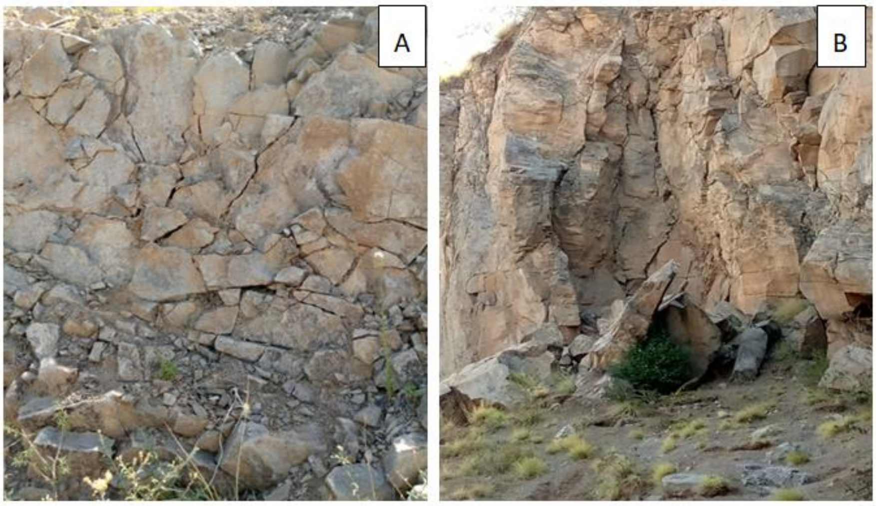

Fig 4.2: Field photo of weathered and fractured ignimbrites (A) and failed slope of Ignimbrite rock (B).

4.2.2. Colluvial Soil

Colluvial soils consist of locally transported detritus materials of soil horizons and parent materials of sloping terrains from the upper sections of the slopes through water erosion or landslides. In the present study area, this soil type was deposited at the toe of the ridge as shown in (fig 4.3) below.

Fig 4.3: Colluvial soil deposit of the study area.

4.2.3. Residual Soil

Residual soil can be defined as a soil material that is the result of weathering and decomposition of rocks that have not been transported or moved a little from their original place. The residual soils found in the present study area are originated from parent material ignimbrite rocks and it found above the colluvial soils as shown in (fig 4.4).

Fig 4.4: Residual soil (originated from parent material Ignimbrite rock) of the study area.

4.2.4. Pumice

Pumice is a fine-grained volcanic rock. It is very light grey to medium grey. It contains a lot of empty gas bubbles, so it is very light and looks rather like a sponge. Sometimes pumice is so light that it will float on water. The present study area consists of pumice that has been already converted into the soil due to its high weathering degree as shown below in fig 4.5. This type of soil is deposited in the southern part of the study area and its deposition extends to the middle height of the ridge.

Fig 4.5: Pumice of study area.

4.3. Local geological structures

The present study area is located within a seismically most active region which is affected by a series of parallel normal faults on the regional scale. Another geological structure that is common in the specific study area (the Dibibisa ridge) was joints. Joints are common at in local level and it is one of the causes of the instability of the ridges around Adama town. Some of the structures are shown below in figure 4.6.

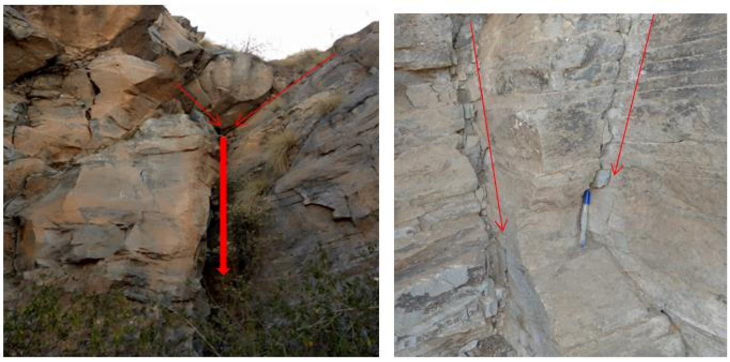

Fig 4.6: Field photos of Joints (wedge failure forming joints at left).

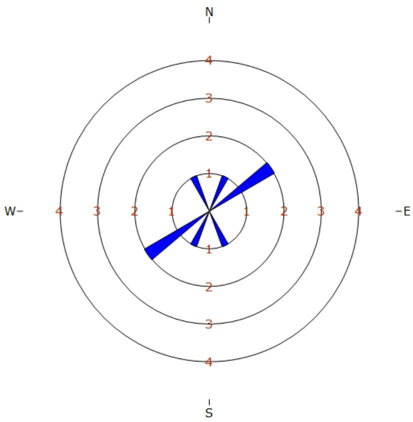

Fig 4.7: Rosset diagram of discontinuity strikes plotted by dip.6.00

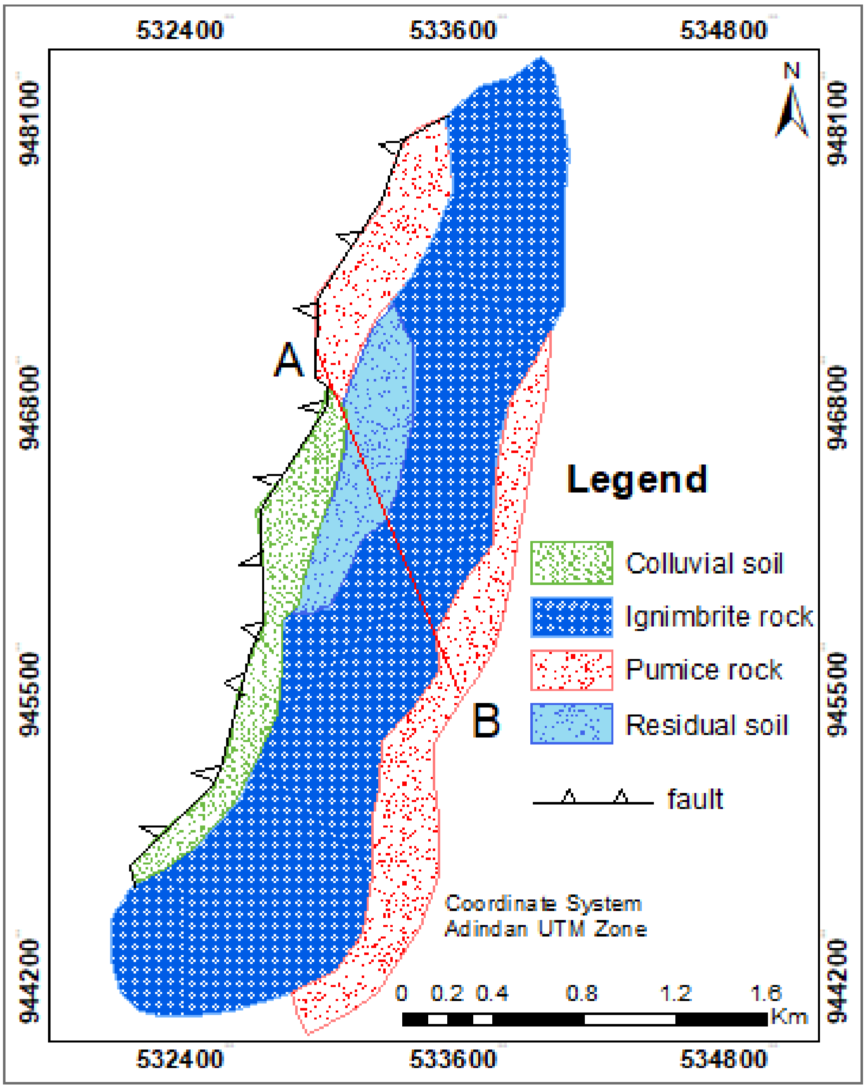

Fig 4.8: local geological map of study area of scale 1:7000

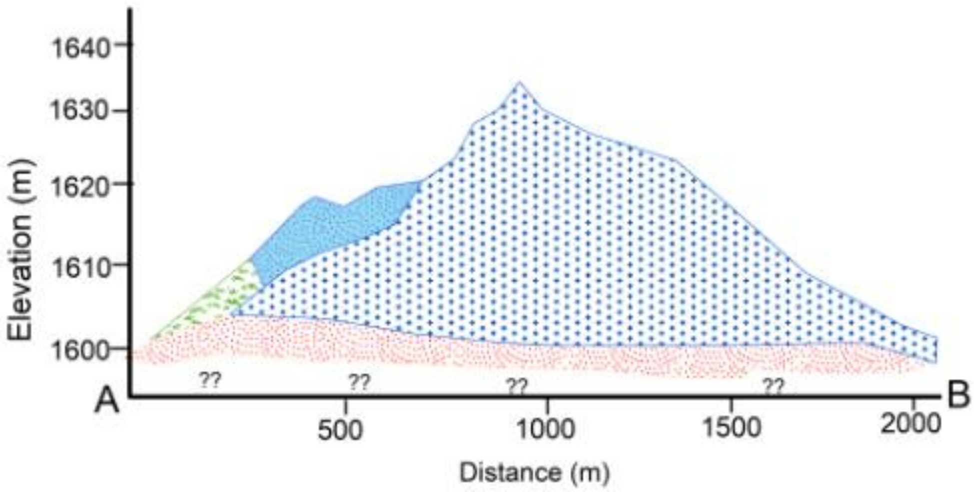

Fig 4.9: Geological cross-section of the study along the lines A-B

4.4 Seismicity of the study area

Ethiopian Building Code of Standard (EBCS- 1995) divides the country into five major earthquake zones which range from the no-risk zone (zone 0) to zones of major damages (zone3 4). The present study area is in the rift valley region and from the seismic hazard map in figure 4.10. The site falls in a high-risk earthquake zone with Modified Mercalli (MM) intensity of VI to IX. The area experiences an earthquake of magnitude 5 in 1993 resulting collapse of several buildings (Ayele *et al.*, 2021). The seismic loading should be considered to minimize the impacts of earthquake shaking on the safety of structures during stability analyses of the slope (Wieland, 2014). Therefore, horizontal seismic acceleration of a minimum of 0.1g can be potentially considered during the initial design stage as per seismic hazard zones of Ethiopia. This map is based on the amplitude of ground acceleration to be expected during 100 years return period.

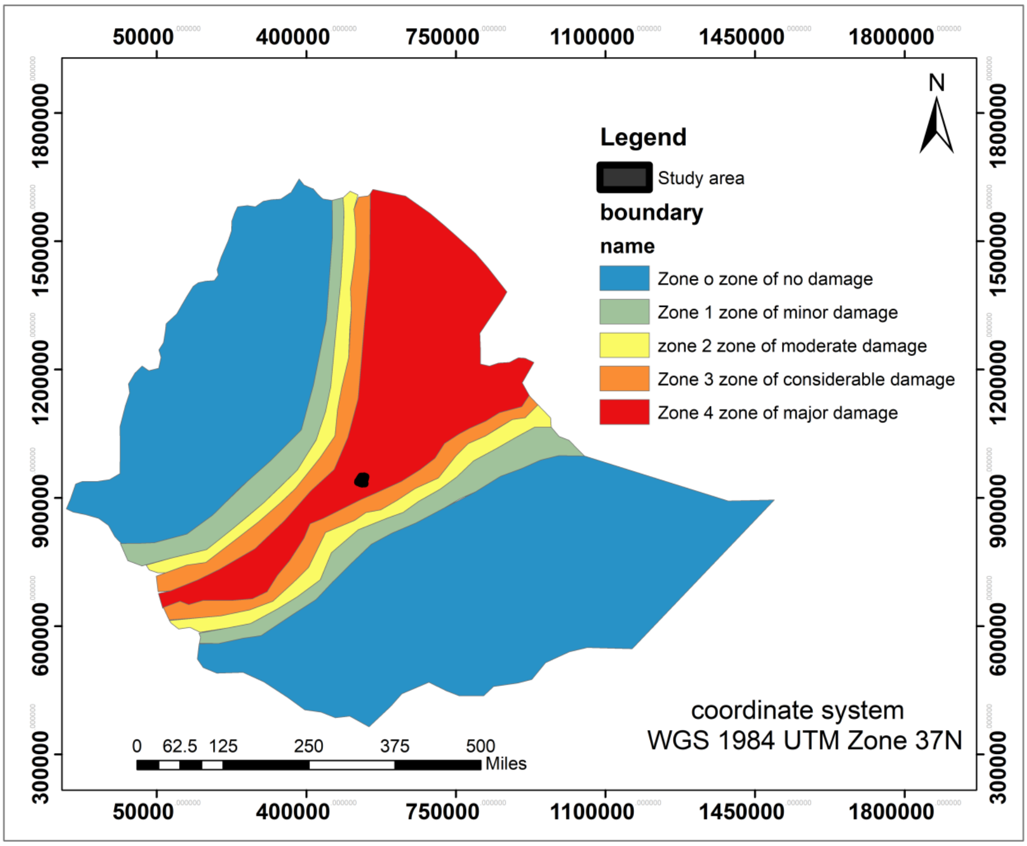

Fig 4.10: Seismic hazard map of Ethiopia for 100 years return period modified after (EBCS, 1995).

CHAPTER FIVE

5. RESULTS DISCUSSION

5.1. Detailed Field Investigation of Geological Materials

A detailed field survey was undertaken to locate critical sections of slope on the steep sections of the ridge on both sides and to identify geological materials like soils and rocks of critical sections of the slope. From field manifestations, three critical soil slope (non-structural controlled) two critical structural controlled rock slope failures were identified based on the occurrence of scarp faces, already failed rocks, failed soil masses, orientations of major rock discontinuities. Saturation conditions of the slope were also visually identified as damp. There was no spring or other water bodies that emanate from or were found around critical sections of the slope the ground water is also far deep around 80-100 meters according to Ethiopian Meteorological Agency data. So ground water cannot be considered as the main destabilizing factor for this specific area but rainfall can be taken into account as a destabilizing factor. The types of soils and rocks found around the study area were identified as follows:

- There were top soils which are reddish in a color that covered the top part of an area it deeps down up to half a meter or less, below that there are ignimbrite rocks which are white to grey there are slightly weathered, highly weathered fractured ignimbrites that covered major part of the study area.
- There are also colluvial soils which consist of locally transported detritus materials of soil horizons and parent materials of sloping terrains from the upper sections of the slopes through water erosion or landslides.
- In addition to the above, there were also residual soils that formed as the result of weathering and decomposition of rocks that has not been transported from their original place. In this study area, there is a residual soil of ignimbrite rock (reddish to brown) and pumice rock (light grey to medium gray).

Table 5.1: Location and descriptions of critical slope sections identified during detailed field survey:

Slope sections	Northing	Easting	Characteristics of the slope sections are based on the field manifestations.
D1S1 (Rock)	945566	533000	Critical rock slope which was found within jointed and slightly fractured as well as steeply dipping ignimbrite rock.
D1S3 (Rock)	945521	533082	Critical rock slope that found within moderately jointed and steeply dipping ignimbrite rock.
D1S2 (Soil)	945727	532997	Critical soil slope with larger scarp face, nearly circular and composed of colluvial soil.
D2S1 (Soil)	945248	532862	Critical soil slope with larger scarp face of residual soil.
D4S1 (Soil)	946395	533109	Critical soil slope with moderately steep-sloped sandy soil that originated from parent material pumice rocks (light grey to medium gray).
D = Day S = Station			

5.2. Engineering Characterization of Rocks

The critical rock slope section was found on cliff-forming ignimbrite rock which has relatively weak to medium strength. Moreover, the soil of the study area was visually classified on the field according to ASTMD 2488 (2002).

5.2.1 Discontinuity Survey Result

Orientation of discontinuities that are persistent concerning slope was measured using the Brunton compass the dip amount of the slope discontinuities measured at several places around critical sections of the ridge were nearly steep (Table.5.2). This indicated that dip of the slope and failure plane or discontinuities may have their role in destabilizing the slope. In addition, conditions of discontinuities determined on a field that, joint roughness varies from smooth to slightly rough, its persistence its aperture were also open which enhance the destabilization of slope as sown in Table 5.3.

Table 5.2: Dip and dip direction of the slope and persistent discontinuities at critical rock slopes:

Slope section	Joint set dip direction/dip			Dip direction/dip of the slope
	J1(degree)	J2(degree)	J3(degree)	
D1S1 (Rock)	320/46	130/58	248/76	265/88
D1S3 (Rock)	118/64	-	-	115/85
Upper slope dip amount	= 20°			

Table 5.3: Condition of discontinuities at critical sections of rock slope of the study area.

Location		D1S1			D1S3
		JS 1	JS 2	JS 3	JS 1
Condition of discontinuity	Spacing (m)	3	3	1	20 cm
	Persistence (m)	>50	>50	>50	>50
	Aperture (mm or cm)	17 cm	5 cm	5mm	16.5 mm
	Filling	Coarse Soil	Partially Open	Open	Partially field with soil
	Wall weathering	Moderately weathered	Moderately weathered	Moderately weathered	Moderately weathered
	Roughness	Slightly rough	Slightly rough	Slightly rough	Slightly rough
	Estimated Field GSI	45 - 55	45 - 55	45 - 55	45 – 55
Ground Water Condition (GWC)		Damp	Damp	Damp	Damp

5.2.2 Rock Quality Designation (RQD)

In this study, since there is no core sample of rock, the rock quality designation index was determined at the field based on the joint volumetric count method. Finally, the results revealed that the minimum and maximum RQD was 69 and 79 respectively as shown below in the table

Table 5.4: Rock quality designation index as determined from joint count method by counting a number of joints that are >10 cm in length or persistence.

Slope sections	Rock type	Joint volume (Jv) (average)/1mx1m	RQD (%) = (115-3.3 Jv)	Deer and Deere(1988)
D1S1	Ignimbrite	11	79	Good
D1S3	Ignimbrite	15	66	Fair

5.2.3 Uniaxial Compressive Strength (UCS)

In addition, in-situ measurement of Schmidt hammer rebound value on representative rocks surface at critical slope sections was conducted by using a portable instrument called N-type Schmidt hammer. The test was conducted according to the standard suggested by (Barton and Choubey, 1977) ASTM C805-08, (American Society for Testing Materials) the resulting Schmidt hammer rebound number was recorded later the average value was converted to the uniaxial compressive strength of rock by using (Eq 3.1).

Table 5.5: Average Schmidt hammer rebound value (R) at critical sections of rock slope

Slope sections	Joint sets	Average Schmidt hammer rebound value (R) according to ASTM C805-08.	Unit Weight (KN/M^3)	UCS, (MPa)
D1S1	Joint set 1	52	26.4	151.34
	Joint set 2	49.3	26.4	141.25
	Joint set 3	50	26.4	147.91
D1S3	Joint set 1	50.5	25.03	131.82

5.2.4 Unit Weight

The unit weight test of rock was conducted at the laboratory on the representative rock samples that were collected from different critical rock slope sections. The dry and saturated unit weight of rock that was determined in the laboratory is presented in table (5.6) below.

Table 5.6: Unit weight of rock taken from the study area.

Rock type	Sample No:	Dry mass (g)	Wet Mass (g)	(V1), cm^3	(V2), cm^3	V2-V1 cm^3	ρdry=M/V (g/ cm^3)	γsat=ρ.g KN/M^3	γdry=ρ.g KN/M^3
Ignimbrite	1.	105.7	107.3	150	192	42	2.52	25.55	25.2
	2.	86.4	88.5	150	186	36	2.4	24.63	24
	3.	92.6	95.1	150	187	37	2.503	25.57	25.03
		Average (γ):						25.25	24.74
(γ; Unit weight, V1& V2; Initial and Final volume respectively, ρ; density, M= mass, V; volume).									

5.3. Stability Analyses of Rock Slopes

5.3.1. Rock Mass Rating

The quality of the rock which composes the critical rock slope in the study area was determined according to the (Bieniawski, 1989) basic rock mass rating system. The five basic parameters such as uniaxial compressive strength, rock quality designation index, spacing of discontinuity, condition of discontinuity, and groundwater condition were determined and used as input parameters for RMR determination (Table.5.7) below. According to ISRM (1978), the determined spacing of the discontinuities ranges from 0.2m to 3m which is classified as moderately spacing to wide spacing.

Table 5.7: Input parameter used to classify rock at critical slope section.

parameter		Location of critical rock slope section	
		D1S1	D1S3
UCS (Mpa)		146.8	131.82
RQD (%)		79	69
Joint spacing		2.5 m	20 cm
Condition of discontinuity	Persistence(m)	>50	>50
	Aperture(mm/cm)	7.5 cm	16.5 mm
	Filling	Partially Open	Partially field with soil
	Roughness	Slightly rough	Slightly rough
	Degree of weathering	Moderately weathered	Moderately weathered
Ground water condition		Damp	Damp

To classify the rocks of critical slope sections according to (Bieniawski, 1989) rating value given for each parameter was added together to calculate RMR describe the rocks based on the value. According to (Bieniawski, 1989) in this study area, the quality of rock at the critical slope section (D1S1) was described as Good rock the rock at the critical slope section (D1S3) was described as Fair rock.

Table 5.8: classification of rock of critical slope sections based on Rock Mass Rating Method.

Slope sections	Rock type	The five basic RMR parameters rating value					RMR	Class	Description
		UCS	RQD	J. SPC	C. DSC	GWC			
D1S1	IGN	12	17	20	6	10	65	II	Good rock
D1S3	IGN	12	13	10	6	10	51	III	Fair rock
UCS = uniaxial compressive strength, RQD = Rock quality designation index, J. SPC=Spacing of discontinuity, C. DSC = Conditions of discontinuity, GWC = Groundwater conditions, IGN = Ignimbrite.									

5.3.2. Kinematic Analyses

Kinematic analysis has been conducted to verify the mode of rock failure identified on the field manifestations, it was done through pole data stereographic projections by considering both slope major joint set dip and dip directions friction cone based on the procedure outlined in (Hoek and Bray, 1981; Wyllie and Mah, 2004). The kinematic analyses were done using dips software from the input parameter listed in (Table.5.9) and the result is shown in fig 5.1 & 5.2 below. The friction cone was determined using Rocdata software.

Table 5.9: Input parameters for kinematic analyses

Slope sections	Input parameters				
	J1(⁰) DD/D	J2(⁰) DD/D	J3(⁰) DD/D	Slope (⁰) DD/D	Friction angle (⁰)
D1S1	320/46	130/58	248/76	265/88	37.2
D1S3	118/64	-	-	115/85	28.62

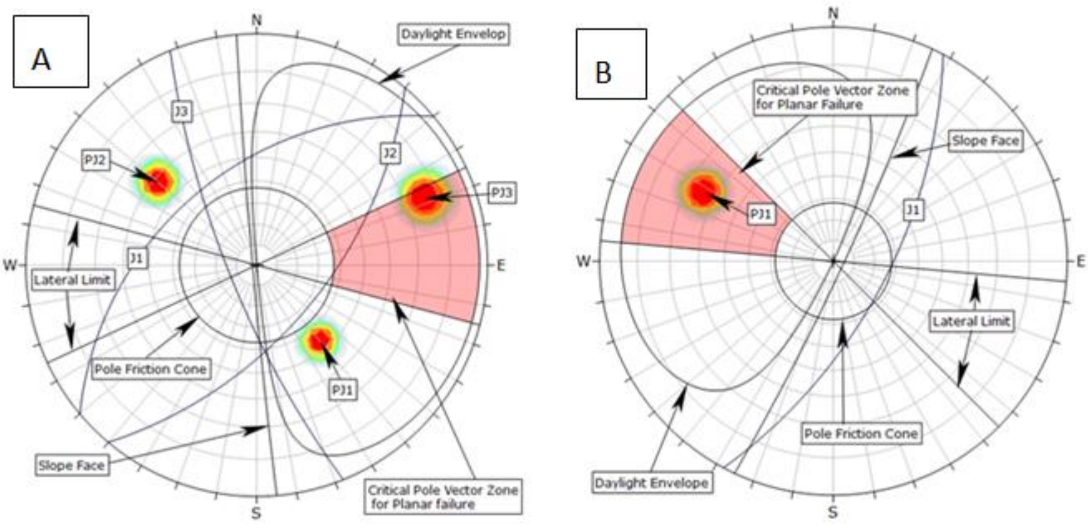

Fig 5.1: Kinematic slope stability analysis results of a planar mode of failure in the rock slope section. A) For the planar mode of failure at the D1S1 rock slope section and B) for a planar mode of failure at the D1S3 rock slope section.

The result from the kinematic analysis of the planar mode of failure by dips 6.0 software shows that there is one critical planar failure zone that is admissible to failure along with joint 3 (D1S1) (A) one critical planar failure zone which is also admissible to failure along with joint 1 (D1S3) (B).

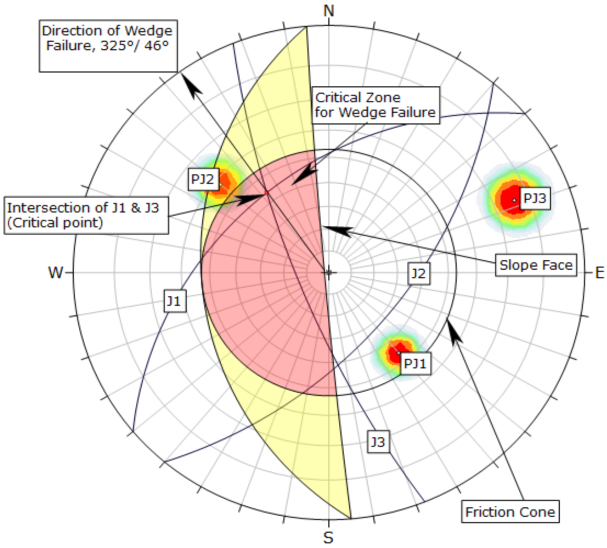

Fig 5.2: Kinematic slope stability analysis results of wedge mode of failure in rock slope section D1S1.

According to the result from kinematic analysis by dips software, there is one critical wedge failure that is kinematically admissible to fail along the intersection of J3 and J1 at (D1S1).

5.3.3. Limit Equilibrium Methods of Slope Stability Analysis

In this study limit equilibrium slope stability analysis was conducted on both structural controlled rock slope sections and soil slope sections by different softwares. For structural controlled rock slope Rocplane 2.0 and Swedge 4.0 were used. For the soil slope analysis Slide, 6.0 software was utilized. The Input parameters used in this software are material properties such as cohesion, angle of internal friction, and unit weight of the soil and rocks. For this study Shear strength parameters(c and ϕ) of rock mass for the selected slope section were obtained from Hoek-Brown Failure criteria using Rockdata software. In addition unit weight of rock was determined using the buoyancy technique in the laboratory. During analysis using the above input parameters factor of safety (FOS) and slip surface was computed and interpreted for both static and dynamic loading conditions using the Spenser method (Slide 6.0) among limit equilibrium methods since it gives a smaller value of factor of safety.

__5.3.3.1. Limit Equilibrium Slope Stability Analysis of Rock Slope__

Table 5.10: Input parameters for Rocplane software

Rock slope sections	Slope DD/D $(^{o})$	Failure plane $(^{o})$	Slope height (m)	Unit weight KN/M^3 dry/wet	Seismic Coeffi.	Cohesion KN/M^2	waviness	Friction angle $(^{o})$
D1S1	265/88	76	30	23.74/25.3	0.1	18.54	14	37.2
D1S3	115/85	64	30	23.74/25.3	0.1	5.12	0	28.62

By using the above input parameters factor of safety was determined under Rocplane 2.0 software as follows (fig 5.3) and (5.4).

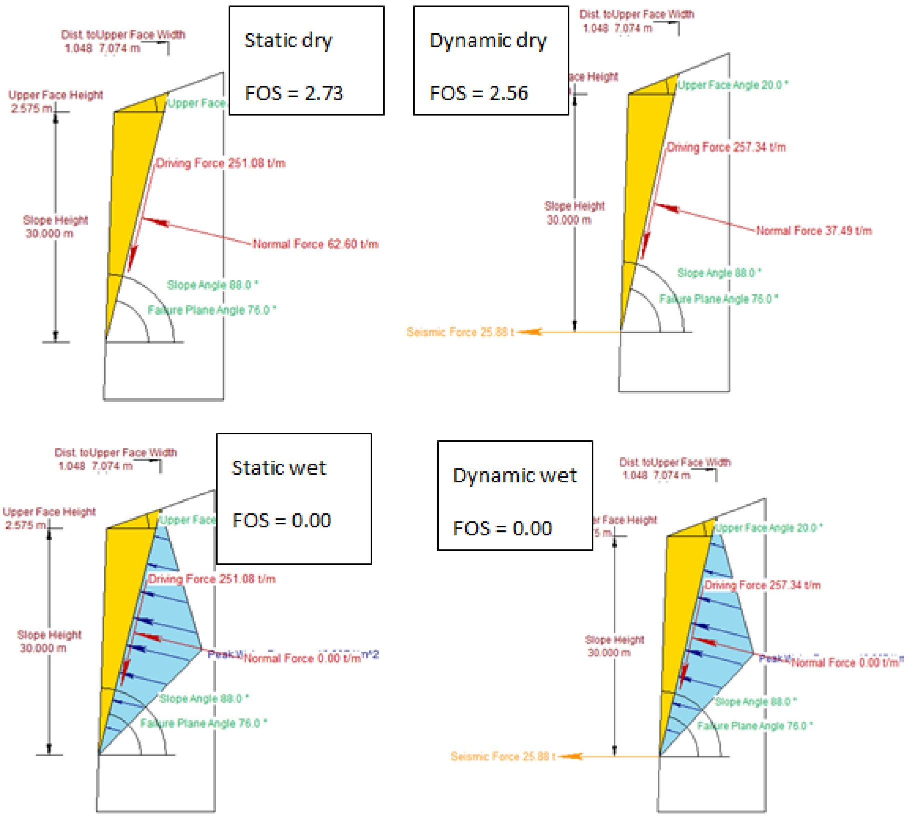

Fig 5.3: Result from rocplane 2D of Limit equilibrium rock slope stability analysis of D1S1 planar failure at all four anticipated conditions its factor of safety accordingly.

According to the above results of analysis, which was conducted to determine the factor of safety of planar failure using Rocplane 2.0 software, the value of the factor of safety in dry conditions is greater than one but in saturated conditions, it became zero in both static and dynamic saturation as fully saturated condition. The rock slope section of D1S1 is stable during dry conditions but it was unstable as water (fully saturated). This shows that an introduction of water could be the main cause of instability of this slope section and also the variation of a factor of safety become large due to the presence of water. In this rock slope section when the percentage of saturation made 50%, the factor of safety became (1.6) at static wet condition but as it increased to a fully saturated level the factor of safety reduces to zero.

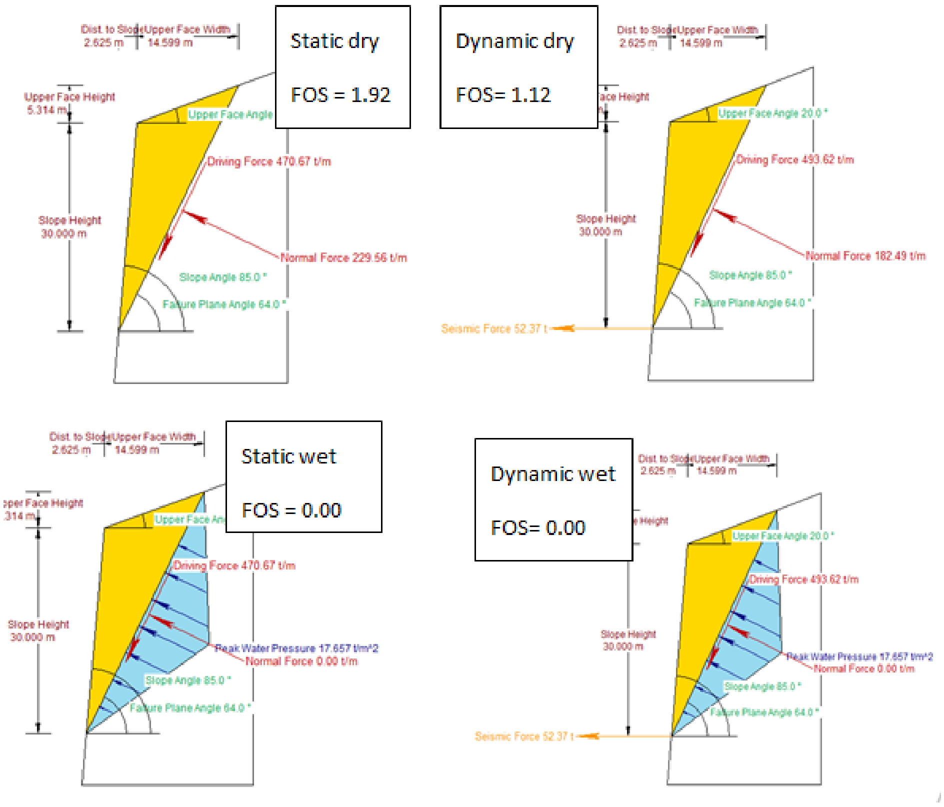

Fig 5.4 Result from rocplane 2D of Limit equilibrium rock slope stability analysis of D1S3 planar failure at all four anticipated conditions its factor of safety accordingly.

At rock slope section D1S3 according to the result of analysis using Rocplane 2.0 software, the value of factor of safety at dry static dry dynamic condition is greater than one as the section get saturated the factor of safety diminishes to zero. So the rock slope section of D1S3 is unstable under static wet and dynamic wet conditions. In this slope section at the fully saturated condition, the factor of safety is zero (i.e. totally unstable) so, the introduction of water plays an important role in the variability of the number of a factor of safety and it takes a major part in the instability of slope. This slope section is also unstable at 50%, of saturation.

In the rock slope section D1S1, wedge failure was also checked and the results were summarized in (fig 5.5).

Table 5.11: Input parameters for Swedge 4.0 software.

Joint sets	DD/D (^{0})	Cohesion (kpa)	Friction cone (^{0})	Upper face (^{0}) DD/D	Slope face (^{0}) DD/D	Slope height (m)	Unit weight (KN/M^3) Dry/wet	Seismic Coeffi.
Js1	320/46	18.54	37.2	141/20	265/88	30	23.74/25.3	0.1
Js 3	248/76	18.54	36					

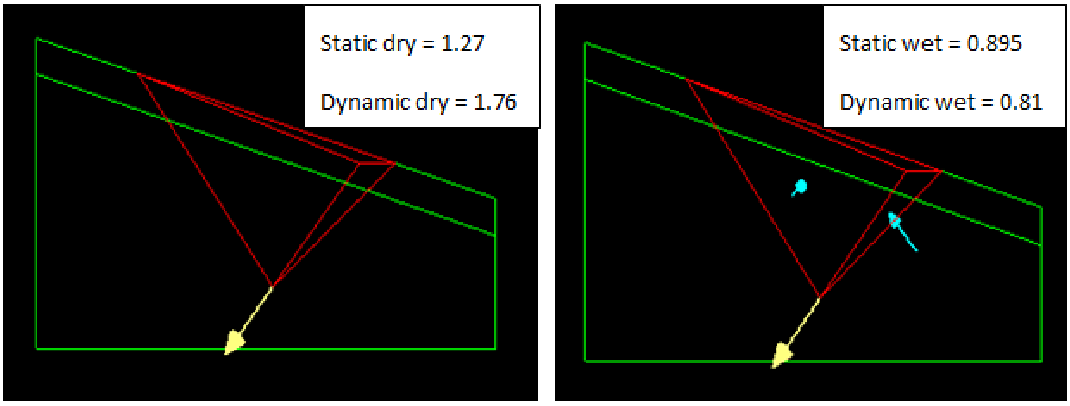

Fig 5.5: Result from swedge software along with J1and J3 intersection at slope section (D1S1).

In addition to planar failure evaluation, rock slope section D1S1 was also analyzed under Swedge 4.0 software to evaluate the existence of wedge failure at the slope. According to the result from Swedge 4.0, at dry static and dry dynamic conditions the value of the factor of safety is greater than one and the slope section is stable in these conditions. At static wet and dynamic wet conditions, the value of the factor of safety is below one. So the slope section is stable in only dry conditions while it is unstable in saturated conditions due to the effect of pore water pressure.

Table 5.12: Summary of the factor of safety value determined under Limit Equilibrium Method.

Slope sections	Software used	Loading conditions			
		static	Factor of safety	dynamic	Factor of safety
Rock slope section (D1S1)	Rocplane 2D	Dry	2.73	Dry	2.56
		Wet	0.00	Wet	0.00
Rock slope section (D1S1)	Swedge 2D	Dry	1.267	Dry	1.12
		Wet	0.895	Wet	0.8
Rock slope section (D1S3)	Rocplane 2D	Dry	1.92	Dry	1.76
		Wet	0.00	Wet	0.00

5.4. Laboratory Tests of Soils

In this study, some soil tests have been conducted to characterize engineering properties like shear strength which is the maximum resistance to shear stresses just before failure of the soil. Since the shear strength of the soil is the principal engineering property that controls: the stability of the soil under loads, stability of the soil slope, and earth pressure against the retaining structure. Shear failure of a soil mass occurs when stress induced due to the applied compressive loads exceeds the shear strength of the soils (Arora *et al.*, 1999). The soil tests that have been conducted for this study are the followings:

5.4.1. Direct Shear Test

The direct shear test is the one among different shear strength tests of soil and it determines the maximum resistance of soil to shear stresses just before failure of soil. In this study, a direct shear test was conducted according to ASTM D 3080 (2002) respectively, on two soil samples (D1S2 and D1S4) taken from test pits with the depth from 1m to 2m. The test was conducted in three trials each the normal stress used were 50 kpa, 100 kpa, 200 kpa in ascending order as the trial progressed from first to third. The result of the test is organized in a table and graph below. The shear stress was calculated from the following formula the shear force and area utilized in the test.

Shear stress (kpa) = Shear force/area*1000

Then by using maximum shear stress (kpa) and normal stress (kpa) from the test of soil samples of different trials, the graph of shear stress vs normal stress was plotted to determine cohesion and friction angle.

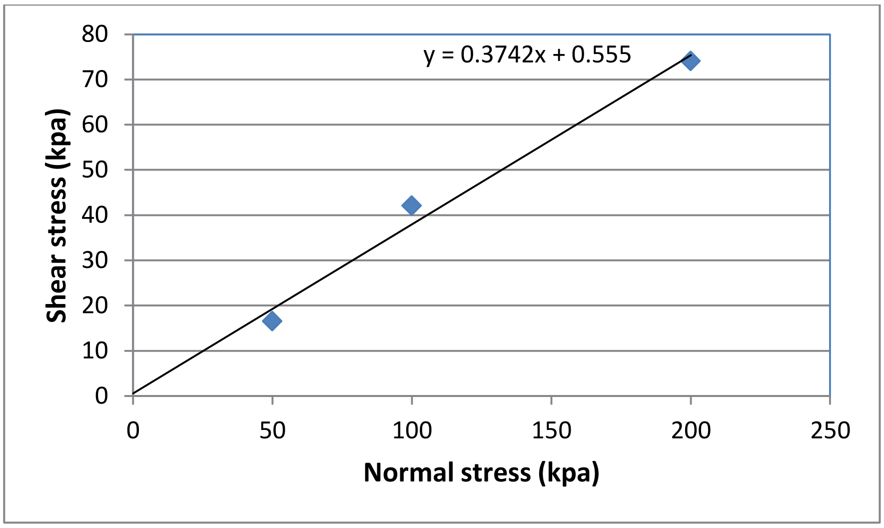

Fig 5.6: Normal vs Shear stress graph of direct shear test of soil sample (D1S4).

The value of cohesion and friction angle of soil slope section D1S4 were 0.6 kpa and 20.516 ^{0} respectively.

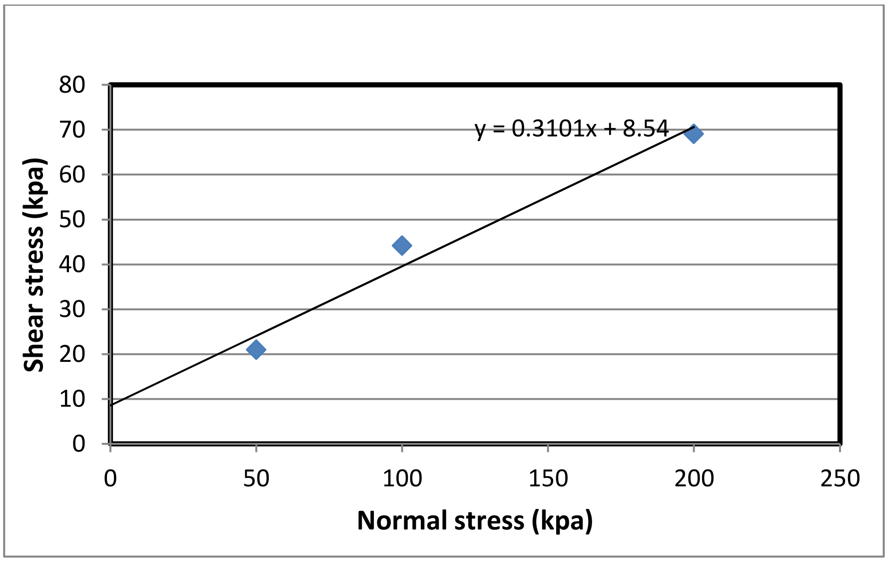

Fig 5.7: Normal vs Shear stress graph of direct shear test of soil sample (D1S2).

The value of cohesion and friction angle of soil slope section D1S2 were 8.54 kpa and 17.224 ^{0} respectively.

The results obtained from the direct shear test of soil were the cohesion value and friction angle which in turn were used as input parameters for the further stability analysis of soil.

5.4.2 Unit weight test

The unit weight test of soil was conducted at the laboratory on the representative soil samples that were collected from two different critical soil slope sections.

Table 5.13: Summary of unit weight test of soil sample collected from two critical sections.

Soil type	Sample no	Ms total (g)	Ms dry (g)	Vs (cm^3)	ρ=M/V g/cm^3	γsat=ρ.g, KN/M^3	γdry=ρ.gs, KN/M^3
pumice	1.	29.33	29.28	22.21	1.32	13.2	13.2
residual	2.	24.27	22.61	12.1	2.006	19.66	18.7

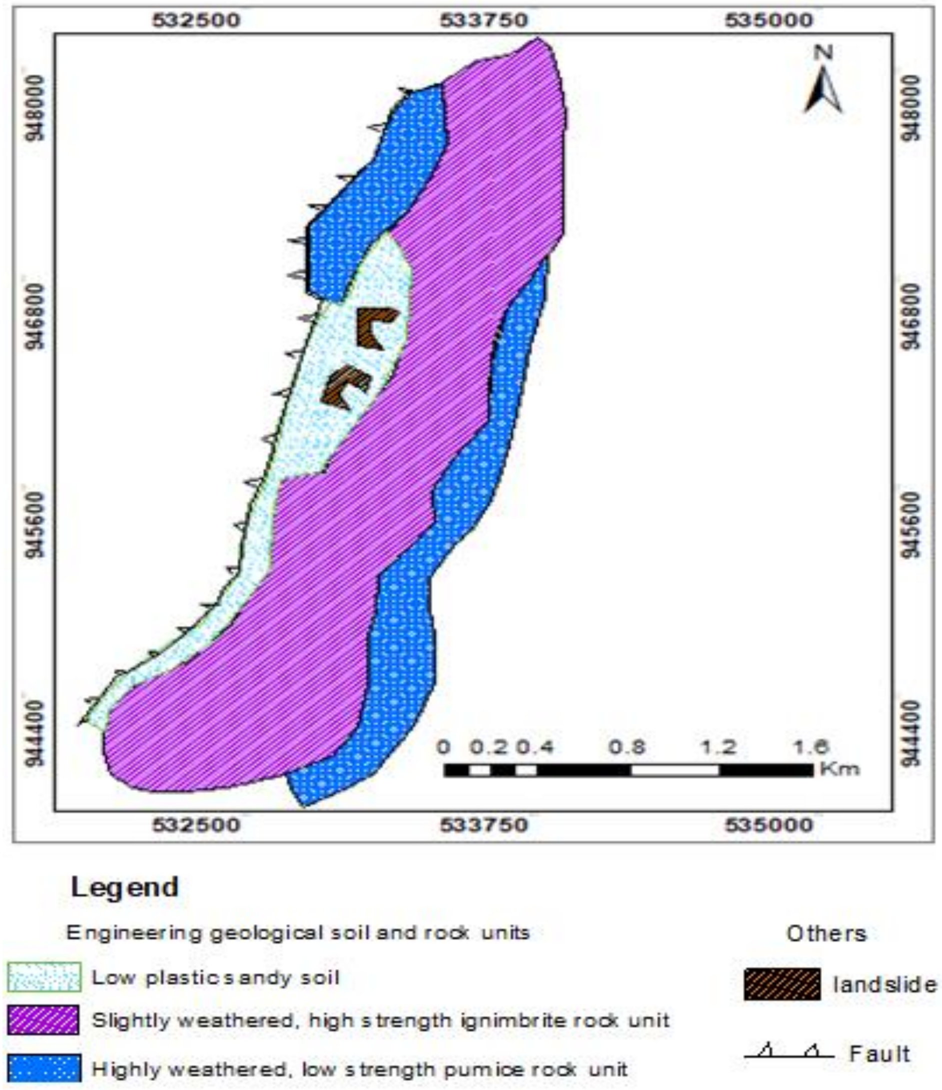

Fig 5. 8 Multi-purpose engineering geological map of Dibibisa ridge of scale (1: 7,000).

5.5 slope stability analysis of soil slope

5.5.1. Limit equilibrium Slope stability analysis of Soil slope

In this study, the analysis of soil slope stability, and the dimensions of lithology at critical soil slope sections measured in the field were introduced to Slide 2D software in the form of a polygon. In slide 2D software, the stability of the slope section was evaluated for the static and dynamic loading conditions, and the analysis was made under both saturated and dry conditions using the spencer method of LEM. The results modeled by slide 2D and the value of factor of safety are presented below in fig 5.8, 5.9, and 5.10.

Table 5.14: Input parameters for soil slope used in slide 2D.

Soil slope sections	Unit weight (KN/M^3)		Cohesion in (kpa)	Friction angle (⁰)	Seismic coefficient	Slope angle in (⁰)	
	γsat	γdry					
D1S2	19.66	18.7	8.54	17.22	0.1	Top	20
						Bottom	45
D1S4	12.9	12	0.6	20.516	0.1	Top	65
						Bottom	40
D2S1	19.66	18.7	8.54	17.22	0.1	Top	75
						Bottom	46

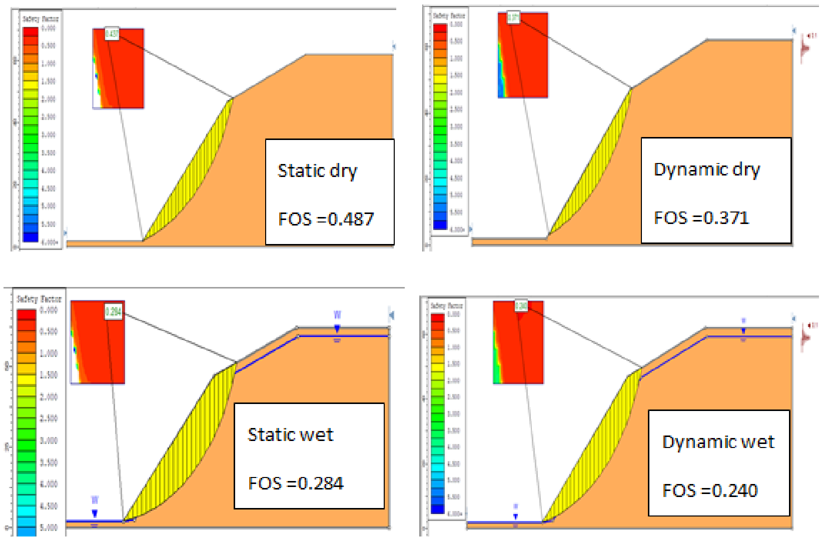

Fig 5.9: The model and value of factor of safety for soil slope section D1S2 determined using slide 2D software.

The results of the analysis show that the soil slope section (D1S2) is unstable for all anticipated conditions. As the result of analysis under slide 2D software indicates that the soil slope is highly susceptible to failure even if under dry static conditions without an effect of external factors or loadings like seismic loading and groundwater effect. In addition to this, since an area is situated in a seismically active zone, the effect would be serious as an earthquake happened suddenly and a heavy rainfall occurs.

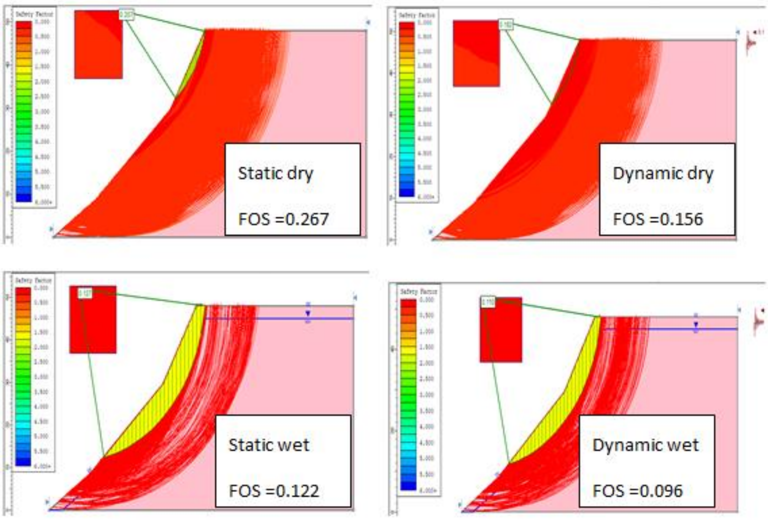

Fig 5.10: The model and value of factor of safety for soil slope section D1S4 determined using slide 2D software.

The soil slope section (D1S4) is also unstable according to the result of the Limit Equilibrium analysis under Slide 2D. The value of the factor of safety is less than one in all anticipated conditions. When compared with the rest unstable slope sections, this soil slope section is seriously susceptible to slope instability as well as its factor of safety is very small (i.e. 0.267, 0.156, 0.122, 0.096) at dry static, dry dynamic, static wet dynamic wet conditions respectively according to slide 2D slope stability analysis. This makes the slope section D1S4 highly vulnerable to slope failure.

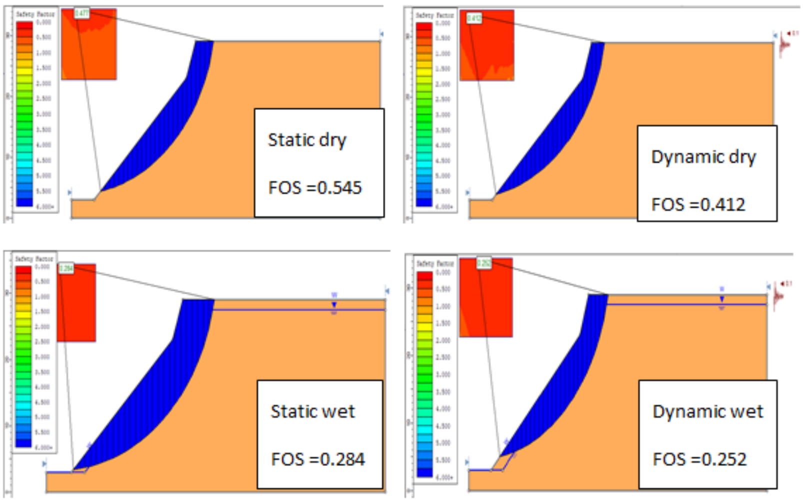

Fig 5.11: The model and value of factor of safety for soil slope section D2S1determined using slide 2D software.

Similarly, the slope section of soil (D2S1) is also unstable that its factor of safety is less than one at all anticipated condition. In these soil slope sections, an introduction of water to the slope section highly influences the stability of the slope. As shown in the above figure 5.10, the factor of safety decreases from 0.545 in static dry condition to 0.284 in static wet condition, this shows that the slope stability of this soil slope would be affected by the pore pressure which could be exerted by water. The detailed summary of a factor of safety calculated under Slide software using the spencer method is presented in (Table 5.15) below.

Table 5.15: Summary of the factor of safety value determined to limit equilibrium method of soil slope sections.

Slope sections	Loading conditions			
	Static	Strength Reduction Factor	Dynamic	Factor of Safety
Soil slope section (D1S2)	Dry	0.487	Dry	0.371
	Wet	0.284	Wet	0.240
Soil slope section (D1S4)	Dry	0.267	Dry	0.156
	Wet	0.122	Wet	0.096
Soil slope section (D2S1)	Dry	0.545	Dry	0.412
	Wet	0.284	Wet	0.252

5.5.2. Finite Element Method Slope Stability Analysis of Soil

The Finite Element Method of slope stability analysis was used on three critical soil slope sections and was evaluated using Phase 2D to determine the factor of safety under static and dynamic loading conditions under dry and wet conditions. For this study horizontal earthquake coefficient is taken from EBCS 1995 was utilized for the dynamic analysis of the slope sections. Then, the input parameter inserted as an input value for both slope section and mesh was generated under the Gaussian Elimination solver type and the Mohr-Coulomb model (MC) was used for analysis. Input parameters for the three soil slope sections used in this model are Unit weight, Cohesion (c), Friction angle (φ), Dilatancy angles (ψ), Young‘s modulus (E), Poisson‘s ratio (ν). These parameters such as strength and stiffness parameters are determined using data collected from fieldwork, laboratory tests, and literature.

5.5.4.1. Finite Element Slope Stability Analysis of Soil Slope

For this analysis to determine the factor of safety using Phase 2D software, the parameters that were used as input parameters are presented in table 5.18 below. The analysis of all the three soil slope sections was performed for static dry, static wet, dynamic dry, and dynamic wet conditions under Phase 2D software.

Table 5.16: Input parameters of phase 2D software used under numerical modeling of soil slope section. Slope angle and slope height were used from table (5.15).

Soil slope section	Unitweight (KN/M^3)		Cohesion In KN/M^2	Φ (⁰)	Ψ°	Poisson ratio (v)	E (kN/m2)
	γsat	γdry					
(D1S2) S1	19.66	18.7	8.54	17.22	0	0.163	15600
(D2S1) S2	12.9	12	0.6	20.52	0	0.15	12000
(D4S1) S3	19.66	18.7	8.54	17.22	0	O.163	15600
Where (φ) - Friction angle, (ψ) - Dilatancy angles, (E) - Young‘s modulus (E),							

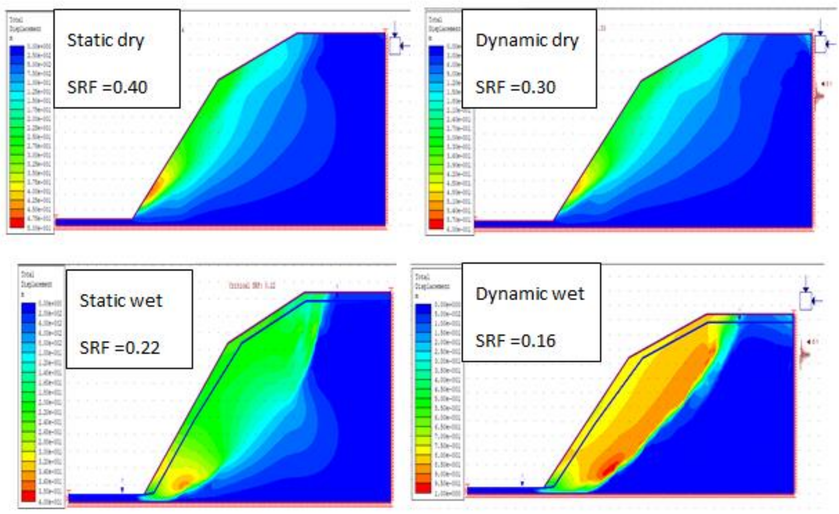

Fig 5.12: The model and value of factor of safety for soil slope section D1S2 determined using Phase 2D software.

The results of the analysis show that the safety factor of the slope section D1S2 is less than one or it is unstable at all anticipated conditions as it was under Slide 2D software. Additionally, the value of the factor of safety reduced from dry to wet conditions in both static and dynamic conditions. This reveals that there is a considerable effect of water as it is introduced to this unstable soil slope section. In addition to the effect of water, an earthquake or seismic effect is also considered in this slope section.

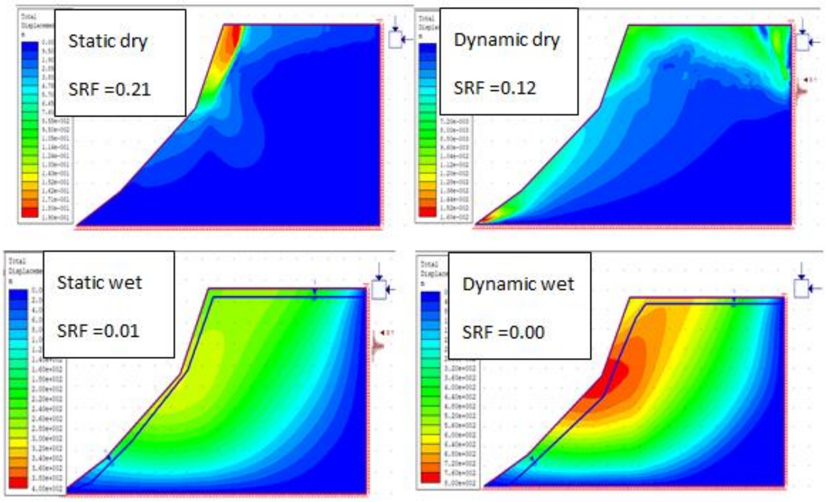

Fig 5.13 : The model and value of factor of safety for soil slope section D1S4 determined using Phase 2D software.

In these soil slope sections, the factor of safety is very small according to phase 2D analysis that reveals the slope section of soil is highly unstable and it is almost ready to fail. Additionally, the value of the factor of safety reduced from dry to wet and static to dynamic conditions reveals that the total effect of both groundwater and earthquake enhances the vulnerability of slope sections to failure.

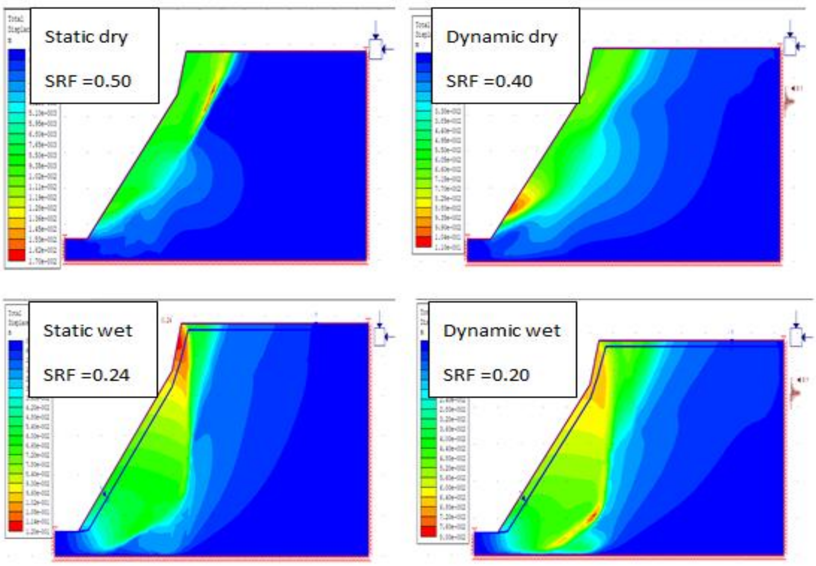

Fig 5.14: The model and value of factor of safety for soil slope section D2S1determined using Phase 2D software.

In soil slope section D2S1 the results of the analysis show that the safety factor of the slope section is less than one at all anticipated conditions as it was under Slide 2D software. In addition, the value of the factor of safety reduced from dry to wet conditions as well as static to dynamic conditions. This shows that additional external factors like the introduction of water and the earthquake loading process could exaggerate the instability of the slope section. In general, at all three unstable soil slope sections, the value of factor of safety calculated under Phase 2D software is closer to the value of factor of safety calculated under Slide 2D software. The detailed summary of the factor of safety calculated under Slide software using the spencer method is presented in (Table 5.17) below.

Table 5.17: Summary of strength reduction factor value determined under Finite Element Method.

slope sections	Loading conditions			
	Static	Strength Reduction Factor	Dynamic	Strength Reduction Factor
Soil slope section (D1S2)	Dry	0.40	Dry	0.30
	Wet	0.22	Wet	0.16
Soil slope section (D1S4)	Dry	0.21	Dry	0.12
	Wet	0.01	Wet	0.00
Soil slope section (D2S1)	Dry	0.50	Dry	0.40
	Wet	0.24	Wet	0.20

5.6 Comparing the results of the Limit Equilibrium Method (LEM) and Finite Element Method (FEM)

The result of factor of safety strength reduction factor for soil slope obtained from both slide 2D phase 2D software respectively are used to compare limit equilibrium finite element methods of slope stability analysis. When we compare the value of the factor of safety obtained using slide software is slightly higher than that of phase 2D of finite element methods. The result obtained from phase 2D gives more information about the stress, strain, deformation, and displacements at any point in the slope section than the result obtained from slide 2D. In addition to this, FEM can monitor progressive failure including overall shear failure. Due to this, the result obtained from phase 2D is more reliable than that of slide software. The limit equilibrium method under slide 2D software gives only a uniform factor of safety along the failure surface only.

5.7 Remedial measures

Among different slope stabilization methods, a geometrical method is easy and inexpensive; however, it requires enough space to apply it. The stability of the slope can be increased easily by converting the steeper slopes into gentler slopes. This method can be performed by cutting the slope to make the slope free from extra loading. Under this study to stabilize unstable soil slopes using slide 2D, benching and flattening of slope methods were considered. Hence, the effect of reducing slope angle and benching were investigated to determine the safest stability condition of the slope sections. To be economical benching method is a more preferable stabilizing method for this slope. Furthermore, other methods were also suggested accordingly.

5.7.1 Benching Technique Analysis Using slide 2D

Benching is one of the techniques for increasing the stability of the slope and this can be done by dividing the slope into multiple small slopes in order to minimize its failure probability. Among the three unstable soil slopes, the slope section (D1S4) was used to determine optimum slope design by using slide 2D under benching techniques of the stabilization method. In this slope static dry condition with the factor of safety 0.267 is selected for benching analysis of stability. In the analysis, the effect of bench width and bench number on the stability of slope cut was investigated using slide 2D software by varying the width of the bench at constant slope height for the same slope section and by increasing the number of benches in the same width. According to the analysis as shown below (fig 5.14) (fig 5.15), the factor of safety increased from 0.547 to 1.222 as the width of the bench increased from 1m to 5m the factor of safety increased from 0.794 to 1.219 as the number of benches increased from 1 bench to 3 benches at constant bench width of 3m. So, the slope became stable as the width of the bench reach 5m and the number of benches reaches 3 under another analysis. The analysis of bench width and bench number was presented below in the figure separately. In this slope sections benches were used on both top and bottom slopes. The factor of safety was calculated by the spencer method as the former analysis.

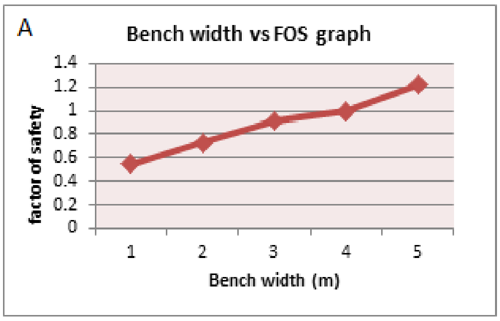

Bench width(m)	FOS from slide 2D
1	0.547
2	0.725
3	0.919
4	1.001
5	1.222

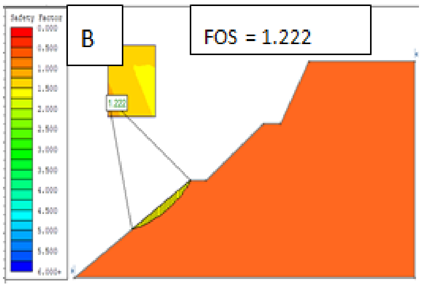

Fig 5.15: A) Effect of bench width on a factor of safety B) the value of factor of safety slope model with 5m wide benches under Slide 2D, of soil slope section (D1S4).

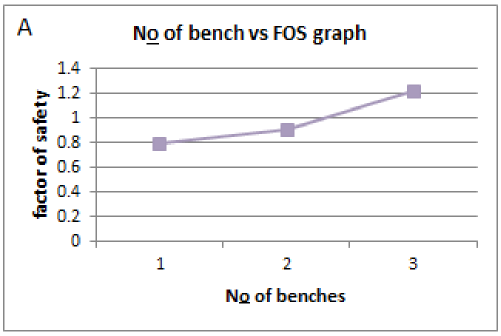

No of benches	FOS from slide 2D
1	0.794
2	0.902
3	1.219

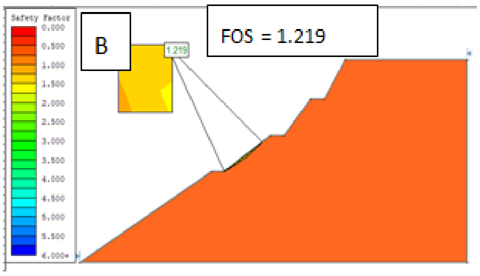

Fig 5.16: A) Effect of bench number on a factor of safety B) the value of factor of safety slope model of 3 benches of the same width under Slide 2D, of soil slope section (D1S4).

5.7.2 Flattening Slope Angle Using 2D Slide Software

The steep slope is highly susceptible to sliding due to the gravity effect when compared with the gentle slope section. The effect of slope angle was evaluated using the worst condition of dynamic saturated of soil slope section (D1S2) with the factor of safety 0.240

using Slide 2D. According to the analysis shown below (fig 5.16), the factor of safety which was initially 0.284 at slope angle 45˚ increased to 0.77 at 35˚ it increased again to 0.89 at 28˚, 1.022 at 25˚, lastly as an angle of the slope made 18˚it reaches 1.151 which in turn made the slope section stable. The increase in the (H/V) ratio due to the flattening of the slope is also shown below. Here flattening was conducted on the bottom slope of the section. The factor of safety was calculated by the spencer method as the former analysis.

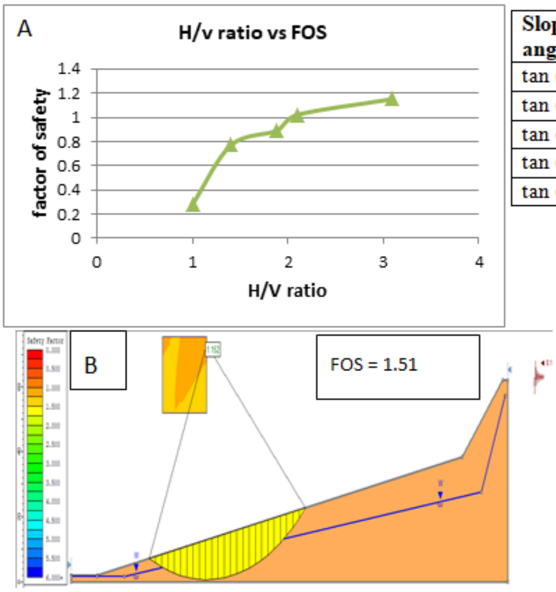

Slope angle	slope ratio	H/V Ratio	FOS in slide 2D
tan (45)	1H:1V	1	0.240
tan (35)	1.5H:1V	1.4	0.77
tan (28)	2H:1V	1.88	0.89
tan (25)	2.5H:1V	2.1	1.022
tan (18)	3H:1V	3.09	1.151

Fig 5.17: A) Effect of slope flattening on the factor of safety, B) the value of factor of safety and the slope model at slope angle 18˚of soil slope section (D1S2).

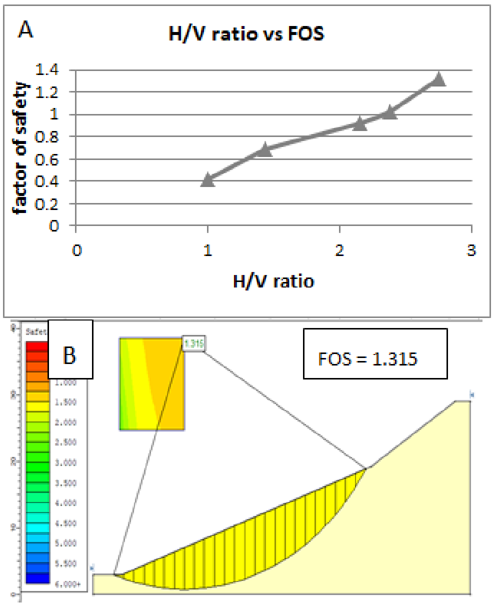

slope angle	slope ratio	H/V Ratio	FOS in slide 2D
tan (46)	1H:1V	1	0.545
tan (35)	1.5H:1V	1.43	0.684
tan (25)	2H:1V	2.15	0.92
tan (23)	2.5H:1V	2.38	1.02
tan (20)	3H:1V	2.747	1.315

Fig 5. 18: A) Effect of slope flattening on the factor of safety, B) the value of factor of safety and the slope model at slope angle 20˚of soil slope section (D2S1).

In the soil slope section (D2S1) the effect of slope angle was evaluated using Static dry conditions with the factor of safety 0.545 using Slide 2D. According to the analysis shown below (fig 5.17), the factor of safety which was initially 0.545 at slope angle 46˚ increased to 0.684 at 35˚ it increased again to 0.920 at 25˚, then 1.020 at 23˚, lastly as an angle of the slope made 20˚ the factor of safety reaches 1.315 which in turn made the slope section stable. The increase in the (H/V) ratio due to the flattening of the slope is also shown below. Here flattening was conducted on the bottom slope of the section. The factor of safety was calculated by the spencer method similar to the former analysis.

5.7.3 Vegetation cover

The existence of vegetation cover has decreasing effects on soil erosion susceptibility because it protects the soil from raindrop impact and splash, additionally; it reduces the erosive action of surface runoff and allows excess surface water to infiltrate. It is probably the best slope protection, particularly against the erosion of soil slopes. A grass mat covering of the slope will not only bind the surface material together but will also tend to inhibit the entry of water to the slope. A grass mat covering of the slope is a highly recommendable slope stabilization method which is also an economically feasible method.

5.7.4 Drainage systems

Saturation and pore water pressure building up in the subsoil is the factor that increases the slope failure. Providing a proper drainage system is a possible approach to stabilizing the slope by minimizing the pore water pressure and saturation of subsoil. This slope stabilization method requires the conditions where proper maintenance of surface and sub-surface drains is performed. Using the proper design of surface and subsurface drainage system, the pore water pressure build-up in the subsoil of a slope can be can minimized and the stability of a slope can be enhanced.

5.7.5 Increasing public awareness

Increasing public awareness comprises teaching people who live near or around the area of unstable slopes to keep themselves from the impact of slope failure as well as creating awareness to not do any day to day practices that can be considered as a cause for slope instability, like cutting of trees, overgrazing, making terrace for houses intensive agricultural practices, small path improper drainage need to be emphasized the locals to be educated about the seriousness of the slope failure its impacts on human life as well as properties.

CHAPTER SIX

6. CONCLUSION AND RECOMMENDATION.

6.1 Conclusion

The present study was conducted on the stability analysis of the selected critical slope section of Adama ridge (Dibibbisa) at Adama town east shewa. Under this study, the stability condition of the slope of the ridge was evaluated by integrating field and laboratory test data with different methods of slope stability analysis. At the field, Discontinuity surveying, in-situ strength test of intact rock using Schmidt hammer rebound test, and sampling of rock and soil for laboratory testing were done. At the laboratory, the direct shear test of soil and unit weight tests of soil and rock was done. The stability analysis of slope sections was carried out using kinematic, limit equilibrium, and finite element methods. Limit equilibrium and finite element methods of slope stability analysis were used to determine the factor of safety and the evaluation of this was made under dry and wet states of static and dynamic loading conditions. Finally, the following conclusion was made after evaluation.

1. Based on field manifestation such as; removal of slope toe, tilting of slope face, orientation of discontinuity three critical soil slopes two critical structural controlled rock slope sections were identified.
2. The two rock slope sections were kinematically admissible to failure under kinematic and limit equilibrium analysis.
3. The rest three soil slope sections were evaluated using finite element and limit equilibrium methods. The analysis results revealed that all three soil slope sections are unstable for all anticipated conditions in both methods.
4. According to the results of rock mass rating, the rocks in the study area range from fair to good quality, and their rock mass rating values range from 51 to 65 respectively.

Additionally, this study comprises the evaluation of some comparative studies for a suggestion of remedial measures and modification of slope geometry for unstable critical soil slope sections (D1S2), (D1S4), and (D2S1) under different anticipated conditions. These slope sections were examined by benching (D1S4) at the dry static condition and flattening of slope angle (D1S2 & D2S1) at Dynamic wet and Static dry conditions respectively under Slide 2D and the following conclusion was made.

- The factor of safety increases as the width of benches increases and according to the analysis the slope section of (D1S4) became stable with the factor of safety 1.222 as of 5m wide used under slide 2D which was initially unstable with the factor of safety 0.267 and as 3 benches of the same width used under slide 2D the factor of safety of the slope section reaches 1.219 which makes it stable.
- At the slope section (D1S2) reducing the slope angle or flattening from initial 45º to 35º, 28º, 25º, 18º increase the factor of safety of the slope from initial 0.240 to 0.77, 0.89, 1.022 1.151 respectively. Finally, at 18º the slope section became stable according to slide 2D analysis.
- The third slope section (D2S1) was flattened from an initial 46º to 35º, 25º, 23º, and 20º then the factor of safety, in turn, increased from initial 0.545 to 0.684, 0.920, 1.02, and 1.315 respectively. Finally, at 20º the slope section became stable according to slide 2D analysis.

6.2 Recommendation

The current study was carried out on the slope stability analysis of Dibibisa ridge near Adama town using mainly limit equilibrium and finite element methods. After the compilation of the study, some comparative analysis was made and some remedial measures such as benching and flattening of critical slopes were suggested. Based on the finding of this research the following recommendations were mentioned.

- According to the comparative analysis under slide 2D, to stabilize soil slope section D1S4 two 5m wide benches or three benches of 3m width is recommended.
- For rock slope sections using an adequate surface and subsurface drainage system is recommended.
- Stabilization of rock slope sections using softwares is also recommended for future study.
- In this study, structural controlled rock slope sections were examined by using only the limit equilibrium slope stability analysis method due to the unavailability of software to determine it under the finite element method. So, for comparison, it is recommendable to examine the rock slope by numerical modeling based on the availability of software.

REFERENCES

Abera, W., Brocca, L., & Rigon, R. (2016). Comparative evaluation of different satellite rainfall estimation products and bias correction in the Upper Blue Nile (UBN) basin. *Atmospheric research, 178,* 471-483.

Abramson, L. W., Lee, T. S., Sharma, S., & Boyce, G. M. (2001). *Slope stability and stabilization methods*. John Wiley & Sons.

Ahmadi, M., & Eslami, M. (2011). A new approach to plane failure of rock slope stability based on water flow velocity in discontinuities for the Latian dam reservoir landslide. *Journal of Mountain Science, 8*(2), 124-130.

Anbalagan, R. (1992). Landslide hazard evaluation and zonation mapping in mountainous terrain. *Engineering geology, 32*(4), 269-277.

Arora, V. K., Chiew, F. H., & Grayson, R. B. (1999). A river flow routing scheme for general circulation models. *Journal of Geophysical Research: Atmospheres, 104*(D12), 14347-14357.

Aryal, K. P. (2006). Slope stability evaluations by limit equilibrium and finite element methods.

ASTM (2001). Standard test method for determination of rock hardness by rebound hammer method. ASTM Stand. 04.09 (D 5873-00)

ASTM D 3080 (1998). Standard test method for direct shear test of soils under consolidated drained conditions. ASTM Stand. Conshohocken, PA, Vol. 04.08, pp.339-344.

Ayalew, L. (1999). The effect of seasonal rainfall on landslides in the highlands of Ethiopia. *Bulletin of Engineering Geology and the Environment*, *58*(1), 9-19.

Ayalew, L., Yamagishi, H., & Ugawa, N. (2004). Landslide susceptibility mapping using GIS-based weighted linear combination, the case in Tsugawa area of Agano River, Niigata Prefecture, Japan. *Landslides*, *1*(1), 73-81.

Ayele, A., Woldearegay, K., & Meten, M. (2021). A review on the multi-criteria seismic hazard analysis of Ethiopia: with implications of infrastructural development. *Geoenvironmental Disasters, 8*(1), 1-22.

Ayele, S., Raghuvanshi, T. K., & Kala, P. (2014). Application of Remote Sensing and GIS for Landslide Disaster Management: A Case from Abay Gorge, Gohatsion–Dejen Section, Ethiopia. In *Landscape Ecology and Water Management* (pp. 15-32). Springer.

Barton, N., & Bandis, S. (1990). Review of predictive capabilities of JRC-JCS model in engineering practice. In: Balkema, A.A, (Ed), *Proceedings of International*

Bandis, S. (1990). Mechanical properties of rock joints. *Rock joints*, 125-140.

Barton, N. (1973). Review of a new shear-strength criterion for rock joints. *Engineering geology*, *7*(4), 287-332.

Barton, N. (1976). The shear strength of rock and rock joints. International Journal of rock mechanics and mining sciences & Geomechanics abstracts,

Barton, N. (2014). Shear Strength of Rock, Rock Joints and Rock Masses-Problems and Some Solutions. ISRM Regional Symposium-EUROCK 2014, Barton, N. (2016). Non-linear shear strength for rock, rock joints, rockfill and interfaces. *Innovative Infrastructure Solutions*, *1*(1), 1-19.

Barton, N., & Choubey, V. (1977). The shear strength of rock joints in theory and practice. *Rock mechanics*, *10*(1), 1-54.

Bieniawski, Z., & Bernede, M. (1979). Suggested methods for determining the uniaxial compressive strength and deformability of rock materials: Part 1. Suggested method for determining deformability of rock materials in uniaxial compression. International journal of rock mechanics and mining sciences & geomechanics abstracts,

Bieniawski, Z. T. (1989). *Engineering rock mass classifications: a complete manual for engineers and geologists in mining, civil, and petroleum engineering*. John Wiley & Sons.

Boylan, N., Jennings, P., & Long, M. (2008). Peat slope failure in Ireland. *Quarterly Journal of Engineering Geology and Hydrogeology*, *41*(1), 93-108.

Broch, E., & Franklin, J. (1972). The point-load strength test. International Journal of Rock Mechanics and Mining Sciences & Geomechanics Abstracts,

Bushira, K. M., Gebregiorgis, Y. B., Verma, R. K., & Sheng, Z. (2018). Cut soil slope stability analysis along national Highway at wozeka–gidole road, Ethiopia. *Modeling Earth Systems and Environment*, *4*(2), 591-600.

Chala, E. T., & Rao, K. (2021). Evaluation of Weathered Rock Mass Strength and Deformation Using Weathering Indices. IOP Conference Series: Earth and Environmental Science,

Chemeda, Y. C. (2020). Engineering Geological Investigation of Adama Town: Implication to Engineering Practice. *Ethiopian Journal of Science and Sustainable Development*, *7*(2), 103-116.

Cravero, M., Iabichino, G., Lollino, G., & Piana, F. (2010). Geomechanical study for stability and land protection evaluation at a large quarry site. 44th US Rock Mechanics Symposium and 5th US-Canada Rock Mechanics Symposium,

Cruden, D. M., & Varnes, D. J. (1996). Landslides: investigation and mitigation. Chapter 3-Landslide types and processes. *Transportation research board special report*(247).

Dahal, R. K., Hasegawa, S., Nonomura, A., Yamanaka, M., Dhakal, S., & Paudyal, P. (2008). Predictive modelling of rainfall-induced landslide hazard in the Lesser Himalaya of Nepal based on weights-of-evidence. *Geomorphology*, *102*(3-4), 496-510.

Das, D., Das, N., & Mathew, L. (2010). Kinetics, equilibrium and thermodynamic studies on biosorption of Ag (I) from aqueous solution by macrofungus Pleurotus platypus. *Journal of Hazardous Materials*, *184*(1-3), 765-774.

Dawson, E., Roth, W., & Drescher, A. (1999). Slope stability analysis by strength reduction. *Geotechnique*, *49*(6), 835-840.

Deere, D. U., & Deere, D. W. (1989). *Rock Quality Designation (RQD) after Twenty Years*.

Duncan, J. M., & Bursey, A. (2013). Soil modulus correlations. In *Foundation Engineering in the Face of Uncertainty: Honoring Fred H. Kulhawy* (pp. 321-336).

Eberhardt, E., Stead, D., & Coggan, J. (2004). Numerical analysis of initiation and progressive failure in natural rock slopes—the 1991 Randa rockslide. *International Journal of Rock Mechanics and Mining Sciences*, *41*(1), 69-87.

Energy, Z. R. (2002). Geotech Data Report Kittitas Valley Wind Power Project.

Furi, W., Razack, M., Haile, T., Abiye, T. A., & Legesse, D. (2011). The hydrogeology of Adama-Wonji basin and assessment of groundwater level changes in Wonji wetland, Main Ethiopian Rift: results from 2D tomography and electrical sounding methods. *Environmental Earth Sciences*, *62*(6), 1323-1335.

Goodman, R. E., & Kieffer, D. S. (2000). Behavior of rock in slopes. *Journal of geotechnical and geoenvironmental engineering*, *126*(8), 675-684.

Griffiths, D., & Lane, P. (1999). Slope stability analysis by finite elements. *Geotechnique*, *49*(3), 387-403.

Hamza, T., & Raghuvanshi, T. K. (2017). GIS based landslide hazard evaluation and zonation–A case from Jeldu District, Central Ethiopia. *Journal of King Saud University-Science*, *29*(2), 151-165.

Harrison, J. P., Hudson, J. A., & Popescu, M. (2002). Engineering rock mechanics: Part 2. Illustrative worked examples. *Appl. Mech. Rev.*, *55*(2), B30-B31.

Hoek, E., & Bray, J. D. (1981). *Rock slope engineering*. CRC Press.

Hoek, E., & Karzulovic, A. (2000). Rock mass properties for surface mines. *Slope Stability in Surface Mining, WA Hustrulid, MK McCarter and DJA van Zyl, Eds, Society for Mining, Metallurgical and Exploration (SME), Littleton, CO*, 59-70.

Hoek, E., & Marinos, P. (2009). Tunnelling in overstressed rock. ISRM Regional Symposium-EUROCK 2009,

Hunt, T. L., & Lipo, C. P. (2009). Revisiting Rapa Nui (Easter Island)"Ecocide" 1. *Pacific Science*, *63*(4), 601-616.

ISRM, (1978). International Society of Rock Mechanics. Suggested methods for determining tensile strength of rock materials. *International Journal of Rock Mechanics and Mining.*

Kim, J., Jeong, S., Park, S., & Sharma, J. (2004). Influence of rainfall-induced wetting on the stability of slopes in weathered soils. *Engineering geology*, *75*(3-4), 251-262.

Kliche, C. A. (1999). Rock slope stability.

Kramer, R., Bochev, P., Siefert, C., & Voth, T. (2013). An extended finite element method with algebraic constraints (XFEM-AC) for problems with weak discontinuities. *Computer Methods in Applied Mechanics and Engineering*, *266*, 70-80.

Kroy, K., Sauermann, G., & Herrmann, H. J. (2002). Minimal model for sand dunes. *Physical Review Letters*, *88*(5), 054301.

Kulhawy, F. H., & Mayne, P. W. (1990). *Manual on estimating soil properties for foundation design*.

Kumar, R., & Anbalagan, R. (2016). Landslide susceptibility mapping using analytical hierarchy process (AHP) in Tehri reservoir rim region, Uttarakhand. *Journal of the Geological Society of India*, *87*(3), 271-286.

Kumar, V., Burman, A., Himanshu, N., & Gordan, B. (2021). Rock slope stability charts based on limit equilibrium method incorporating Generalized Hoek–Brown strength criterion for static and seismic conditions. *Environmental Earth Sciences*, *80*(6), 1-20.

Lamessa, G., & Meten, M. (2021). Stability analysis of rock slope along selected road sections from Gutane Migiru town to Fincha sugar factory, Oromiya, Ethiopia. *SN Applied Sciences*, *3*(2), 1-16.

Leulalem, S., Kifle, W., & Nata, T. (2016). Geological and geotechnical investigations of Axum dam site, Tigray, Northern Ethiopia. *International Journal of Scientific & Technology Research*, *5*, 84-111.

Mengesha Tefera, T. C., & Haro, W. (1996). Explanation of the geological map of Ethiopia. Ministry of Mines and Energy, EIGS. Bull, (3).

Merifield, R. S., Lyamin, A. V., & Sloan, S. (2006). Limit analysis solutions for the bearing capacity of rock masses using the generalised Hoek–Brown criterion. *International Journal of Rock Mechanics and Mining Sciences*, *43*(6), 920-937.

Mishra, A. K. (2016). *Analysis Of Double Curvature Arch Dam and Abutment Stability Using Three Dimensional Nonlinear Finite Element Numerical Modeling In MATLAB R2013a Of Budhigandaki Hydroelectric Project* Pulchowk Campus].

Mulatu, E., Raghuvanshi, T. K., & Abebe, B. (2010). Assessment of slope stability and remedial measures around Gilgel Gibe-II Hydroelectric Project, Southwest Ethiopia. *SINET: Ethiopian Journal of Science*, *33*(1), 1-20.

Muthu, K., & Petrou, M. (2007). Landslide-hazard mapping using an expert system and a GIS. *IEEE transactions on geoscience and remote sensing*, *45*(2), 522-531.

Nilsen, B. (2000). New trends in rock slope stability analyses. *Bulletin of Engineering Geology and the Environment*, *58*(3), 173-178.

Nurjanah, Q., Najib, N., & Santi, N. (2017). *Analisis Kestabilan Lereng dengan Metode Finite Element pada Pit North Tutupan PT. Adaro Indonesia, Kabupaten Balangan, Kalimantan Selatan* Faculty of Engineering].

Palmstrom, A. (2005). Measurements of and correlations between block size and rock quality designation (RQD). *Tunnelling and Underground Space Technology*, *20*(4), 362-377.

Pantelidis, L. (2009). Rock slope stability assessment through rock mass classification systems. *International Journal of Rock Mechanics and Mining Sciences*, *46*(2), 315-325.

Park, H., & West, T. (2001). Development of a probabilistic approach for rock wedge failure. *Engineering geology*, *59*(3-4), 233-251.

Patton, R. G., & Gardner, L. I. (1963). *Growth failure in maternal deprivation*. Thomas.

Raghuvanshi, T. K. (2019). Plane failure in rock slopes–A review on stability analysis techniques. *Journal of King Saud University-Science*, *31*(1), 101-109.

Raghuvanshi, T. K., Ibrahim, J., & Ayalew, D. (2014). Slope stability susceptibility evaluation parameter (SSEP) rating scheme–an approach for landslide hazard zonation. *Journal of African Earth Sciences*, *99*, 595-612.

Sharma, S., Raghuvanshi, T., & Sahai, A. (1999). An engineering geological appraisal of the Lakhwar dam, Garhwal Himalaya, India. *Engineering geology*, *53*(3-4), 381-398.

Shi, G. h., & Goodman, R. E. (1989). Generalization of two-dimensional discontinuous deformation analysis for forward modelling. *International Journal for Numerical and Analytical Methods in Geomechanics*, *13*(4), 359-380.

Shukla, S. K., & Hossain, M. M. (2011). Stability analysis of multi-directional anchored rock slope subjected to surcharge and seismic loads. *Soil Dynamics and Earthquake Engineering*, *31*(5-6), 841-844.

Somasundaram, K., Zhang, L., Sherman, D., Begeman, P., Lyu, D., & Cavanaugh, J. (2019). Evaluating thoracolumbar spine response during simulated underbody blast impact using a total human body finite element model. *Journal of the mechanical behavior of biomedical materials*, *100*, 103398.

Sorbi, A., & Farrokhnia, A. (2018). Landslide Hazard Evaluation and Zonation of Karaj-Chalus Road (North of Iran). *International Journal of Geography and Geology*, *7*(2), 35-44.

Stead, D., Eberhardt, E., & Coggan, J. (2006). Developments in the characterization of complex rock slope deformation and failure using numerical modelling techniques. *Engineering geology*, *83*(1-3), 217-235.

Swan, C. C., & Seo, Y. (1999). Slope stability analysis using finite element techniques. 13 th lowa ASCE Geotechnical Conference. Williamsburgh, lowa,

Tang, L., Zhao, Z., Luo, Z., & Sun, Y. (2019). What is the role of tensile cracks in cohesive slopes? *Journal of rock mechanics and geotechnical engineering*, *11*(2), 314-324.

Tsige, D., Quezon, E. T., & Woldearegay, K. (2017). Geotechnical conditions and stability analysis of landslide prone area: a case study in Bonga town, South-Western Ethiopia. *J Sci Eng Res*, *8*, 239-248.

Turrini, M. C., & Visintainer, P. (1998). Proposal of a method to define areas of landslide hazard and application to an area of the Dolomites, Italy. *Engineering geology*, *50*(3-4), 255-265.

Wang, X., & Niu, R. (2009). Spatial forecast of landslides in three gorges based on spatial data mining. *Sensors*, *9*(3), 2035-2061.

Wieland, M. (2014). Seismic hazard and seismic design and safety aspects of large dam projects. *Perspectives on European Earthquake engineering and seismology*, *1*, 627-650.

Woldearegay, K. (2013). Review of the occurrences and influencing factors of landslides in the highlands of Ethiopia: With implications for infrastructural development. *Momona Ethiopian Journal of Science*, *5*(1), 3-31.

Wolff, S., & Wang, M.-J. (1992). Filler—elastomer interactions. Part IV. The effect of the surface energies of fillers on elastomer reinforcement. *Rubber chemistry and technology*, *65*(2), 329-342.

Wright, S. G., & Duncan, J. M. (1991). Limit equilibrium stability analyses for reinforced slopes. *Transportation Research Record*(1330).

Wu, Q., & Kulatilake, P. (2012). REV and its properties on fracture system and mechanical properties, and an orthotropic constitutive model for a jointed rock mass in a dam site in China. *Computers and Geotechnics*, *43,* 124-142.

Wyllie, D. C., & Mah, C. (2004). *Rock slope engineering*. CRC Press.

ZainAlabideen, K., & Helal, M. (2016). Determination of the safe orientation and dip of a rock slope in an open pit mine in Syria using kinematic analysis. *Al-Nahrain Journal for Engineering Sciences*, *19*(1), 33-45.

APPENDICES

Appendix A Geological strength index (GSI) and disturbance factor (D)

The GSI was determined by considering the weathering conditions of discontinuity surface, rock mass structure, and interlocking of rock blocks (Hoek, 2002).

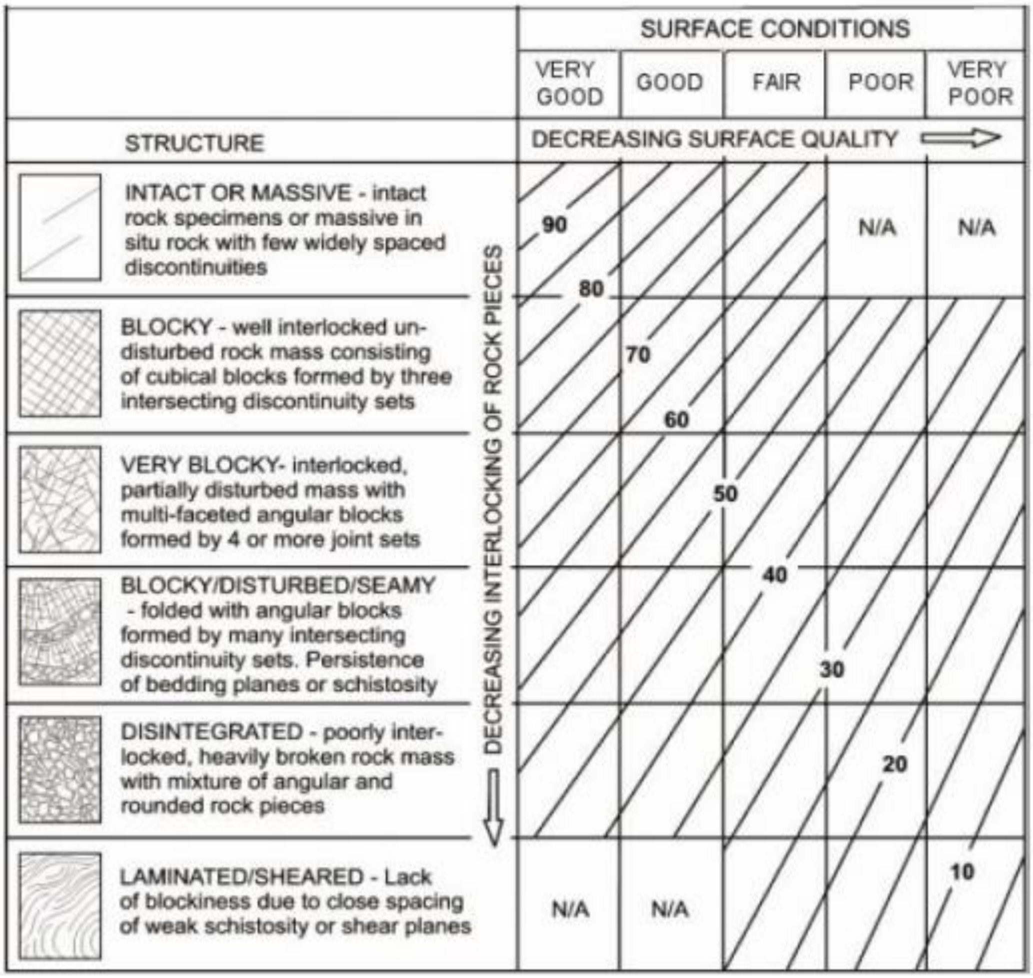

Fig 1: Characterization of blocky rock masses based on interlocking and joint conditions (Hoek, 2002).

Appendix B Rock mass classification system according to (Bieniawski, 1989)

Table 1: Rock Mass Rating System (After Bieniawski 1989).

1.	Strength of intact rock material	Point load strength index (MPa)	> 10	4 – 10	2 – 4	1 – 2			
		Uniaxial compressive strength (MPa)	> 250	100 – 250	50 – 100	25 – 50	5 – 25	1 – 5	< 1
	Rating		15	12	7	4	2	1	0

2.	RQD (%)	90 – 100	75 – 90	50 – 75	25 – 50	< 25
	Rating	20	17	13	8	3

3.	Joint spacing (m)	> 2	0.6 – 2	0.2 – 0.6	0.06 – 0.2	< 0.06
	Rating	20	15	10	8	5

4.	Condition of joints	not continuous, very rough surfaces, unweathered, no separation	slightly rough surfaces, slightly weathered, separation <1 mm	slightly rough surfaces, highly weathered, separation <1 mm	continuous, slickensided surfaces, or gouge <5 mm thick, or separation 1–5 mm	continuous joints, soft gouge >5 mm thick, or separation >5 mm
	Rating	30	25	20	10	0

5.	Ground-water	inflow per 10 m tunnel length (l /min), or	none	< 10	10 – 25	25 – 125	> 125
		joint water pressure/major in situ stress, or	0	0 – 0.1	0.1 – 0.2	0.2 – 0.5	> 0.5
		general conditions at excavation surface	complete ly dry	damp	wet	dripping	flowing
	Rating		15	10	7	4	0

Appendix C Direct shear test of soil.

Table 2: Data table for trial 1 of direct shear test of pumice (sandy soil). For D1S4

TR-1	Area=0.0036m2	Ms=103.2 g	
Normal stress = 50 kpa			
Shear force (N)	**Shear stress (KN/m2)**	**Displacement (m)**	**Displacement (mm)**
0	0	0	0
3	0.83	0.015	15
7	1.94	0.03	30
8	2.22	0.045	45
8.5	2.36	0.06	60
9	2.50	0.075	75
10.5	2.92	0.09	90
11.5	3.19	0.105	105
13	3.61	0.12	120
17	4.72	0.135	135
19	5.28	0.15	150
24.5	6.81	0.165	165
29	8.06	0.18	180
35.5	9.86	0.195	195
38	10.56	0.21	210
42	11.67	0.225	225
47	13.06	0.24	240
53.5	14.86	0.255	255
57	15.83	0.27	270
59.5	16.53	0.285	285
56	15.56	0.3	300
51.5	14.31	0.315	315
47	13.06	0.33	330
42.5	11.81	0.345	345

Table 3: Data table for trial 2 of direct shear test of pumice (sandy soil).

TR-2	Area=0.0036m2	Ms=102.4 g	
Normal stress = 100 kpa			
Shear force (N)	**Shear stress (KN/m2)**	**Displacement (m)**	**Displacement (mm)**
0	0.00	0	0
7	1.94	0.015	15
12	3.33	0.03	30
16	4.44	0.045	45
19.5	5.42	0.06	60
23	6.39	0.075	75
27.5	7.64	0.09	90
33	9.17	0.105	105
41	11.39	0.12	120
48.5	13.47	0.135	135
57	15.83	0.15	150
64.5	17.92	0.165	165
76	21.11	0.18	180
89.5	24.86	0.195	195
97	26.94	0.21	210
103	28.61	0.225	225
109.5	30.42	0.24	240
116	32.22	0.255	255
123	34.17	0.27	270
124.5	34.58	0.285	285
128	35.56	0.3	300
131.5	36.53	0.315	315
137	38.06	0.33	330
141.1	39.19	0.345	345
144	40.00	0.36	360
148	41.11	0.375	375
151.5	42.08	0.39	390
147	40.83	0.405	405
143.5	39.86	0.42	420
138	38.33	0.435	435

Table 4: Data table for trial 3 of direct shear test of pumice (sy soil).

TR-3	Area=0.0036m2	Ms=103.1 g	
Normal stress = 200kpa			
Shear force (N)	**Shear stress (KN/m2)**	**Displacement (m)**	**Displacement (mm)**
0	0	0	0
13	3.61	0.015	15
28	7.78	0.03	30
41	11.39	0.045	45
57.5	15.97	0.06	60
78	21.67	0.075	75
93.5	25.97	0.09	90
103	28.61	0.105	105
118	32.78	0.12	120
131	36.39	0.135	135
147.5	40.97	0.15	150
158	43.89	0.165	165
172	47.78	0.18	180
183	50.83	0.195	195
189	52.50	0.21	210
201	55.83	0.225	225
208	57.78	0.24	240
216	60.00	0.255	255
221.5	61.53	0.27	270
229	63.61	0.285	285
236	65.56	0.3	300
244.5	67.92	0.315	315
259	71.94	0.33	330
266.5	74.03	0.345	345
261	72.50	0.36	360
257	71.39	0.375	375
249	69.17	0.39	390
235	65.28	0.405	405

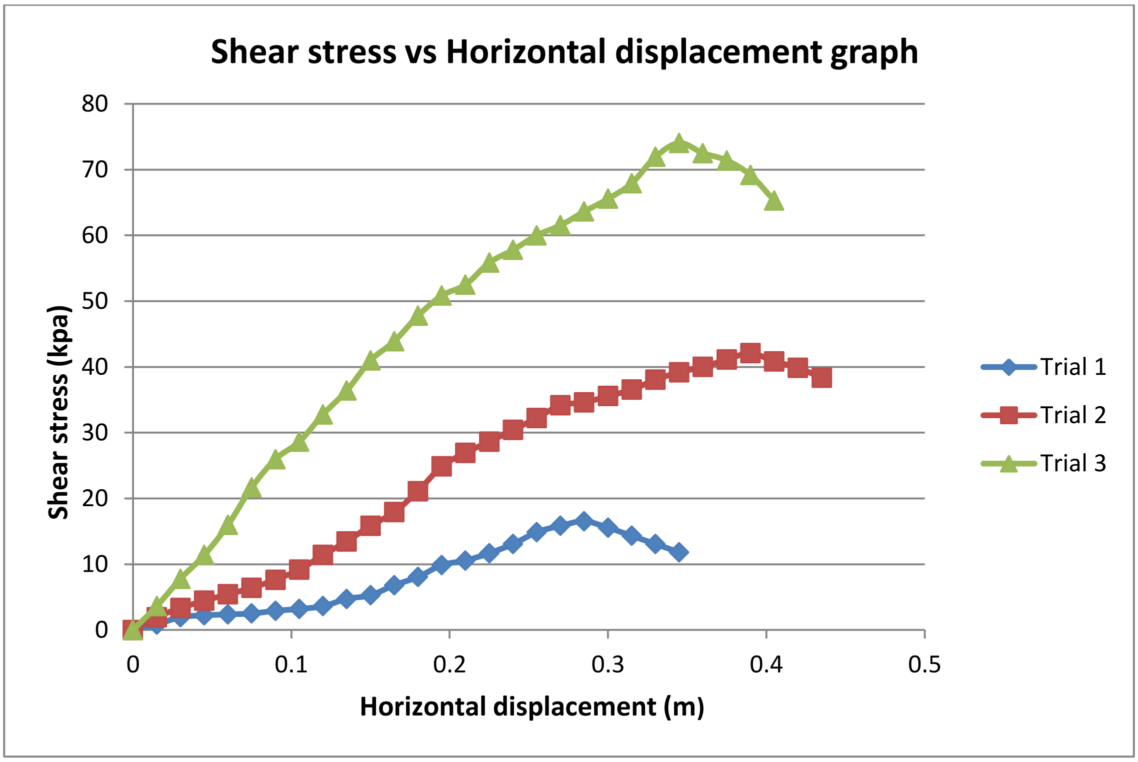

Fig 2: Shear stress (kpa) vs Horizontal displacement (m) graph of the three trials D1S4

For soil sample 1(sandy soil)

Table 5: Summary of shear stress and normal stress of three trials of the direct shear test.

Normal stress (kpa)	Shear stress (Kpa)
50	16.53
100	42.08
200	74.03

Then, the Normal vs Shear stress graph was plotted using excels to determine cohesion friction angle as follows see fig 5.6 5.7:

Table 6: the value of cohesion and Friction angle.

Cohesion c in kpa	0.6
slope (m)	0.374
phi (rad)	0.358
Friction angle (⁰)	20.516

Table 7: Data table for trial 1 of direct shear test of Residual soil.

TR-1	Area=0.0036m2	Ms=176 g	
Normal stress=50kpa			
Shear force (N)	**Shear stress (KN/m2)**	**Displacement (m)**	**Displacement (mm)**
0	0	0	0
14	3.89	0.075	75
17	4.72	0.09	90
23	6.39	0.105	105
25	6.94	0.12	120
29	8.06	0.135	135
31	8.61	0.15	150
38	10.56	0.18	180
39.5	10.97	0.195	195
44	12.22	0.21	210
48.5	13.47	0.225	225
53	14.72	0.24	240
57	15.83	0.255	255
62.5	17.36	0.27	270
68	18.89	0.285	285
71	19.72	0.3	300
75.5	20.97	0.315	315
72	20.00	0.33	330
67	18.61	0.345	345
61.5	17.08	0.36	360
57	15.83	0.375	375

Table 8: Data table for trial 2 of direct shear test of Residual soil.

TR-2	Area=0.0036m2	Ms=176.4	
Normal stress=100kpa			
Shear force (N)	**Shear stress (KN/m2)**	**Displacement (m)**	**Displacement (mm)**
0	0	0	0
13	3.61	0.015	15
19	5.28	0.03	30
26	7.22	0.045	45
31.5	8.75	0.06	60
34	9.44	0.075	75
43	11.94	0.09	90
47.5	13.19	0.105	105
52	14.44	0.12	120
56	15.56	0.135	135
62.5	17.36	0.15	150
65.5	18.19	0.165	165
67	18.61	0.18	180
79.5	22.08	0.195	195
96	26.67	0.21	210
107.5	29.86	0.225	225
116	32.22	0.24	240
122	33.89	0.255	255
128.5	35.69	0.27	270
143.5	39.86	0.285	285
151	41.94	0.3	300
157	43.61	0.315	315
159	44.17	0.33	330
154	42.78	0.345	345
143.5	39.86	0.36	360
136	37.78	0.375	375
129	35.83	0.39	390

Table 9: Data table for trial 3 of direct shear test of Residual soil.

TR-3	Area=0.0036m2	Ms=175.7 g	
Normal stress=200kpa			
Shear force (N)	**Shear stress (KN/m2)**	**Displacement (m)**	**Displacement (mm)**
0	0	0	0
11	3.06	0.015	15
19.5	5.42	0.03	30
31	8.61	0.045	45
48.5	13.47	0.06	60
63	17.50	0.075	75
71.5	19.86	0.09	90
88	24.44	0.105	105
109.5	30.42	0.12	120
125	34.72	0.135	135
137	38.06	0.15	150
153.5	42.64	0.165	165
166	46.11	0.18	180
179	49.72	0.195	195
198.5	55.14	0.21	210
213	59.17	0.225	225
221	61.39	0.24	240
227	63.06	0.255	255
239	66.39	0.27	270
246.5	68.47	0.285	285
248.5	69.03	0.3	300
245	68.06	0.315	315
234.5	65.14	0.33	330
228	63.33	0.345	345

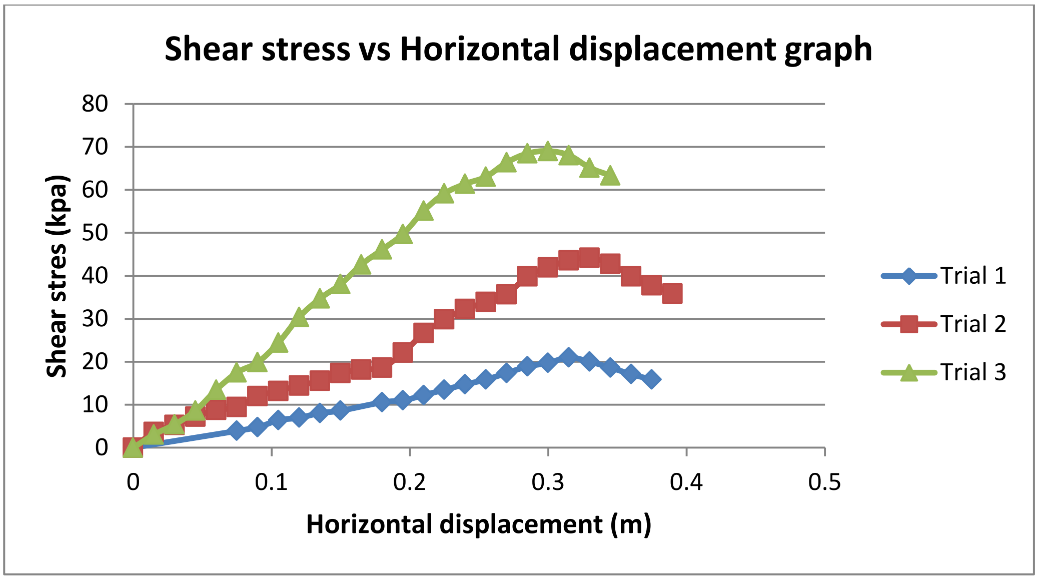

Fig 3: Shear stress (kpa) vs Horizontal displacement (m) graph of the three trials.

For soil sample 2 (residual soil) D1S2

Table 10: summary of shear stress and normal stress of three trials.

Normal stress (kpa)	Shear stress (Kpa)
50	20.97
100	44.17
200	69.03

Then, the Normal vs Shear stress graph was plotted using excels to determine cohesion and friction angle as follows:

Table 11: the value of cohesion and Friction angle.

Cohesion c in kpa	8.54
slope (m)	0.310
phi (rad)	0.301
Friction angle (^{0})	17.224

Sieve analysis and atterberg limit tests

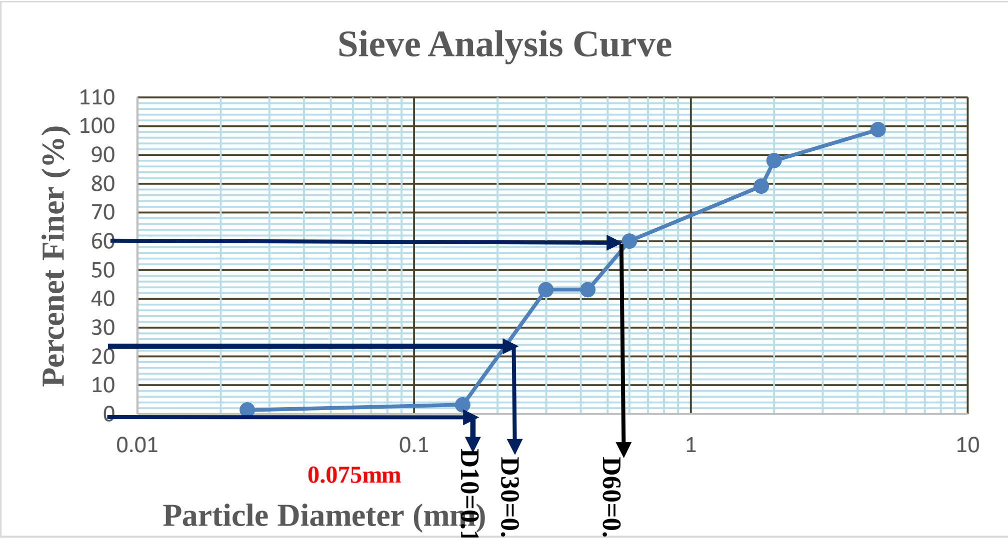

Fig 4: From grain size distribution Curve.

%gravel = 3.2%	D10 = 0.1755mm
%sand = 94.8%	D30 = 0.25mm
%fines = 2%	D60 = 0.598mm
Cu = 3.407	Cc = 0.596

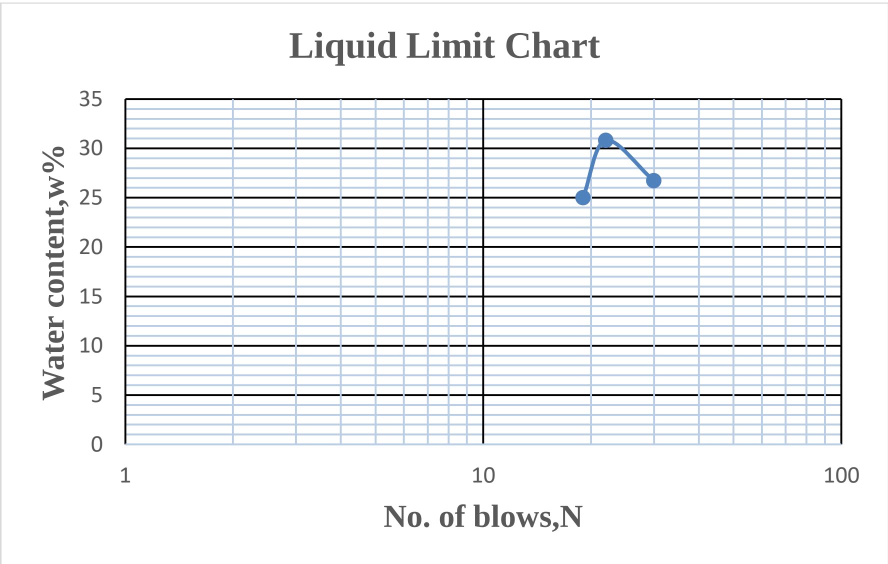

Fig 5: Liquid limit chart.

Final results

- ✓ Liquid Limit (LL) = 29.26%
- ✓ Plastic Limit (PL) = 27.75%
- ✓ Plasticity Index (PI) = LL- PL = 1.5%

Appendix D Software's analysis results

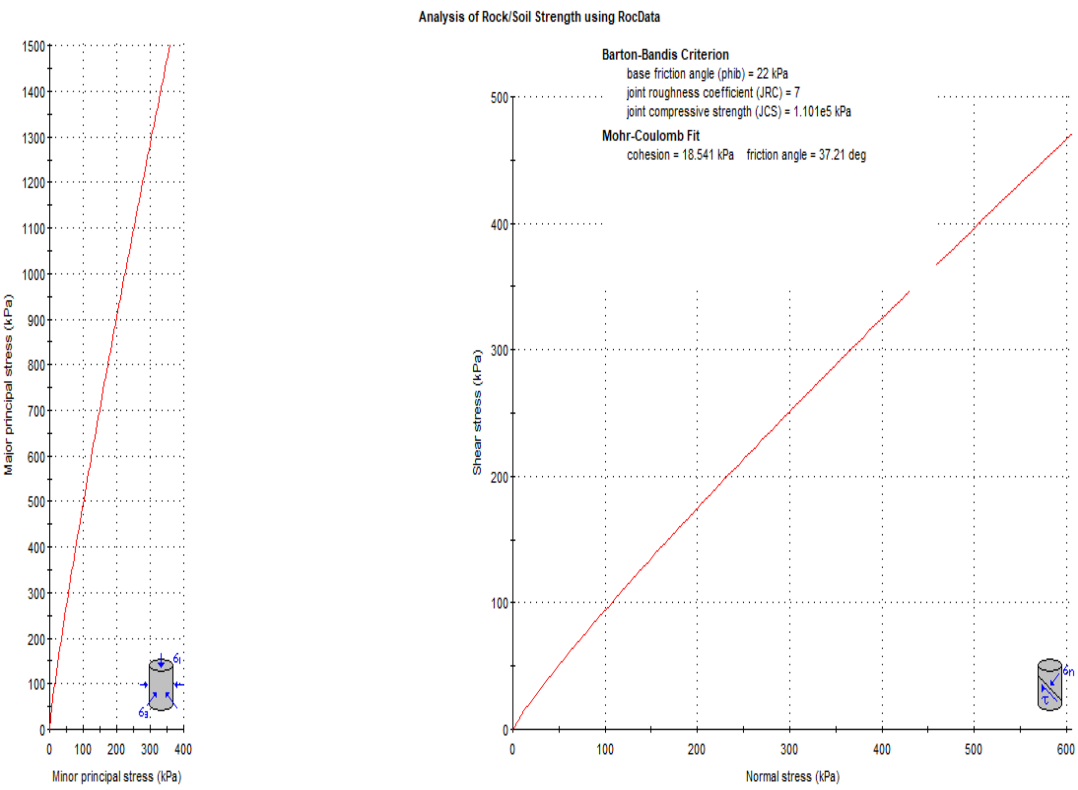

Fig 6: Cohesion and friction angle from rocdata software (D1S1).

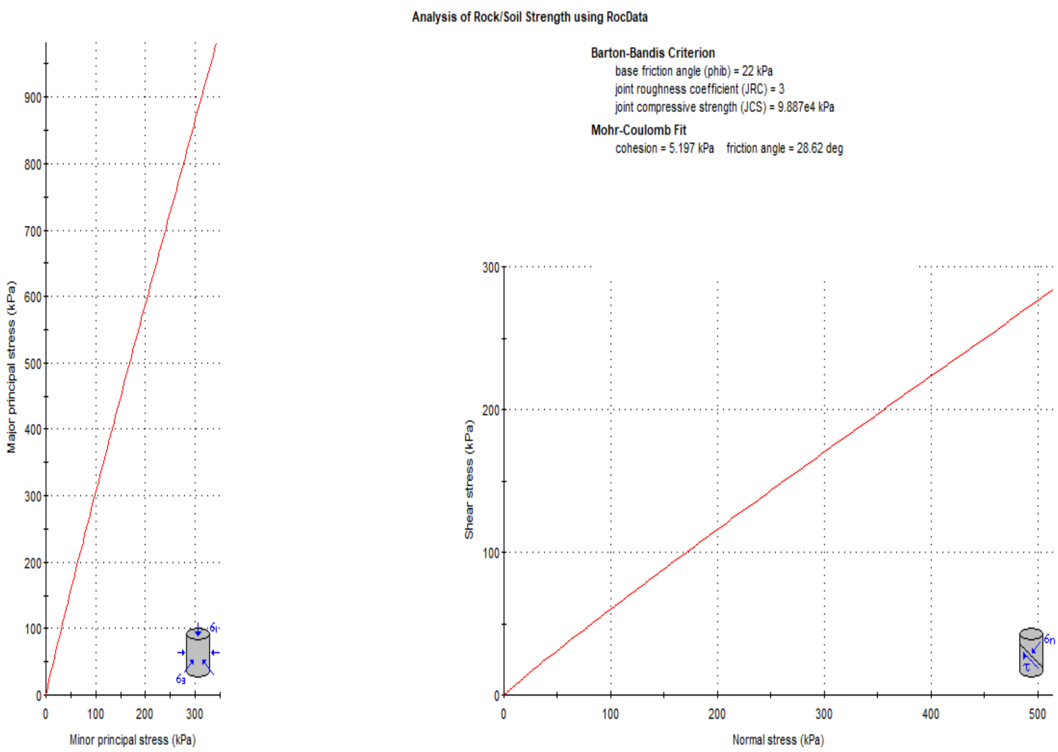

Fig 7: Cohesion and friction angle from rocdata software (D1S3).

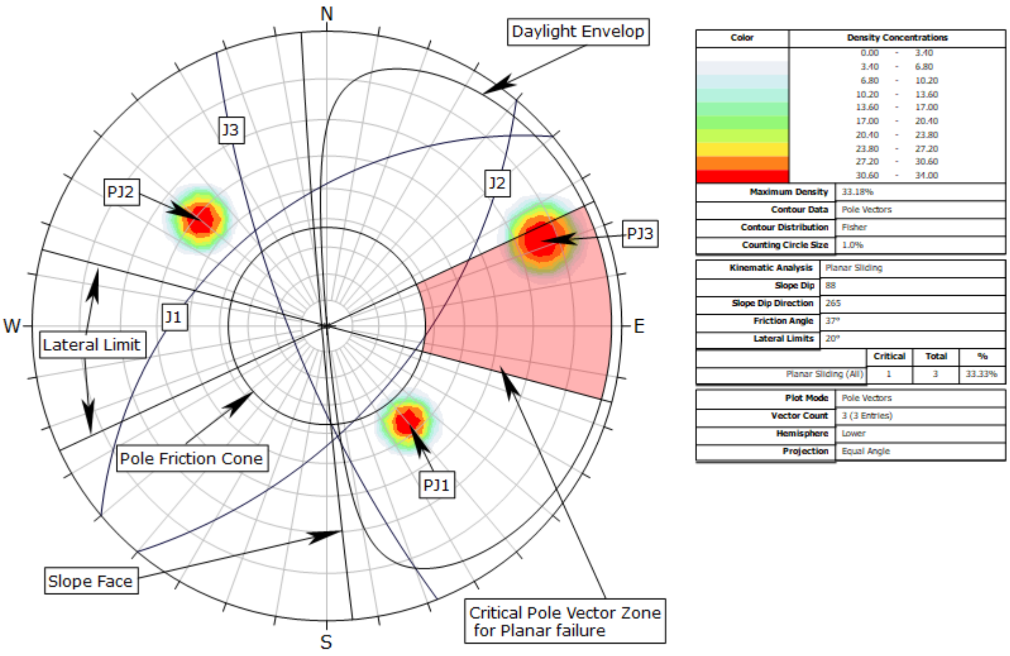

Fig 8: kinematic analysis result of rock section (D1S1).

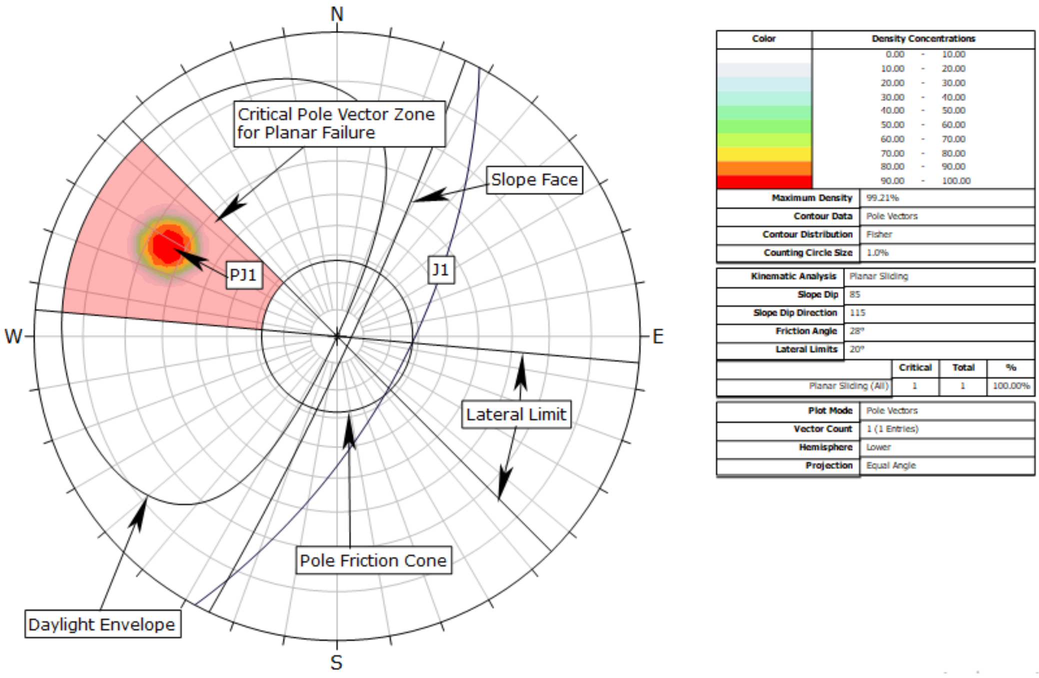

Fig 9: kinematic analysis result of rock section (D1S3).

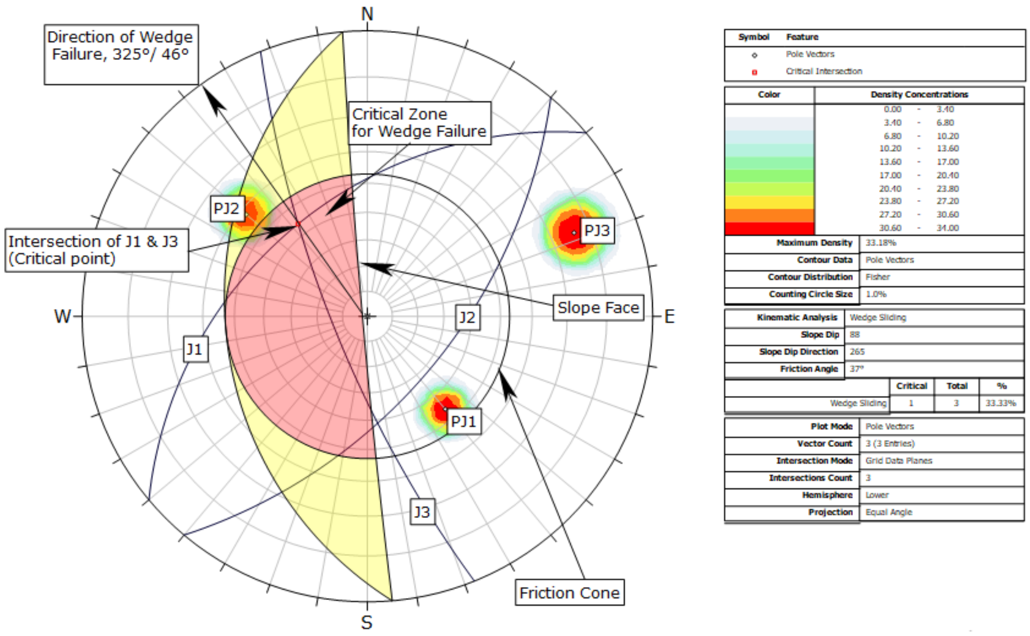

Fig 10: Results of Wedge failure analysis by dips software of (D1S1).

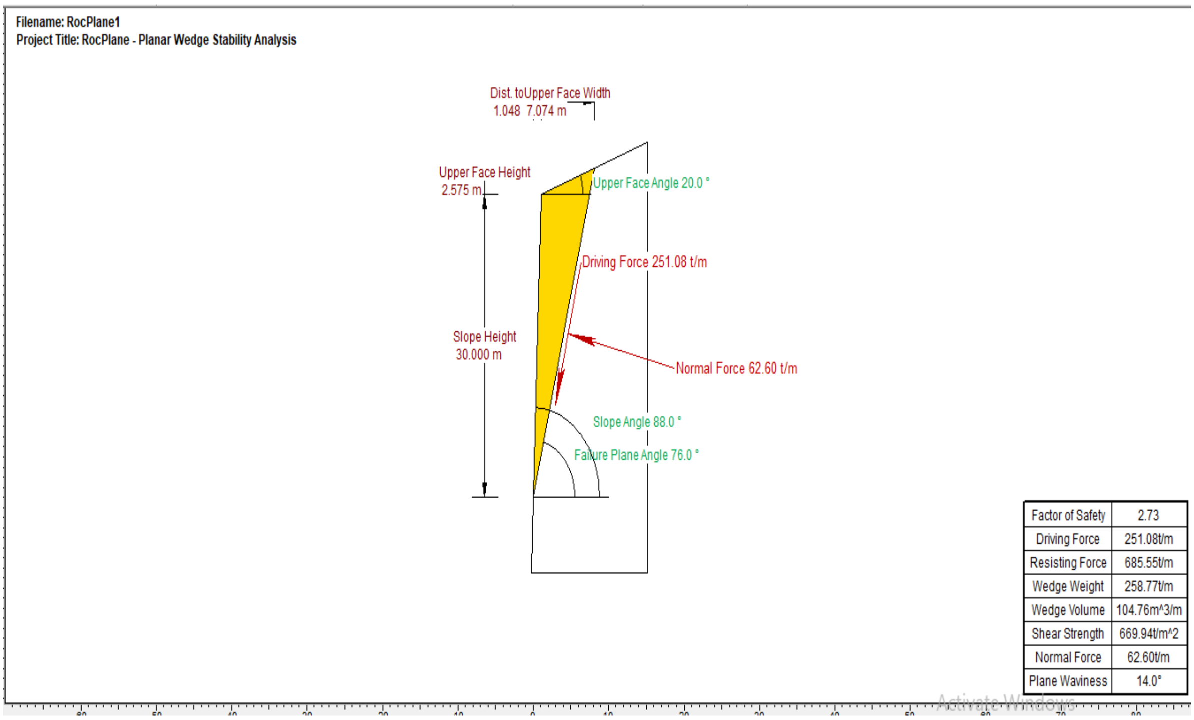

Fig 11: Result of limit equilibrium analysis of planar failure at D1S1 by Rocplane 2D software at dry condition.

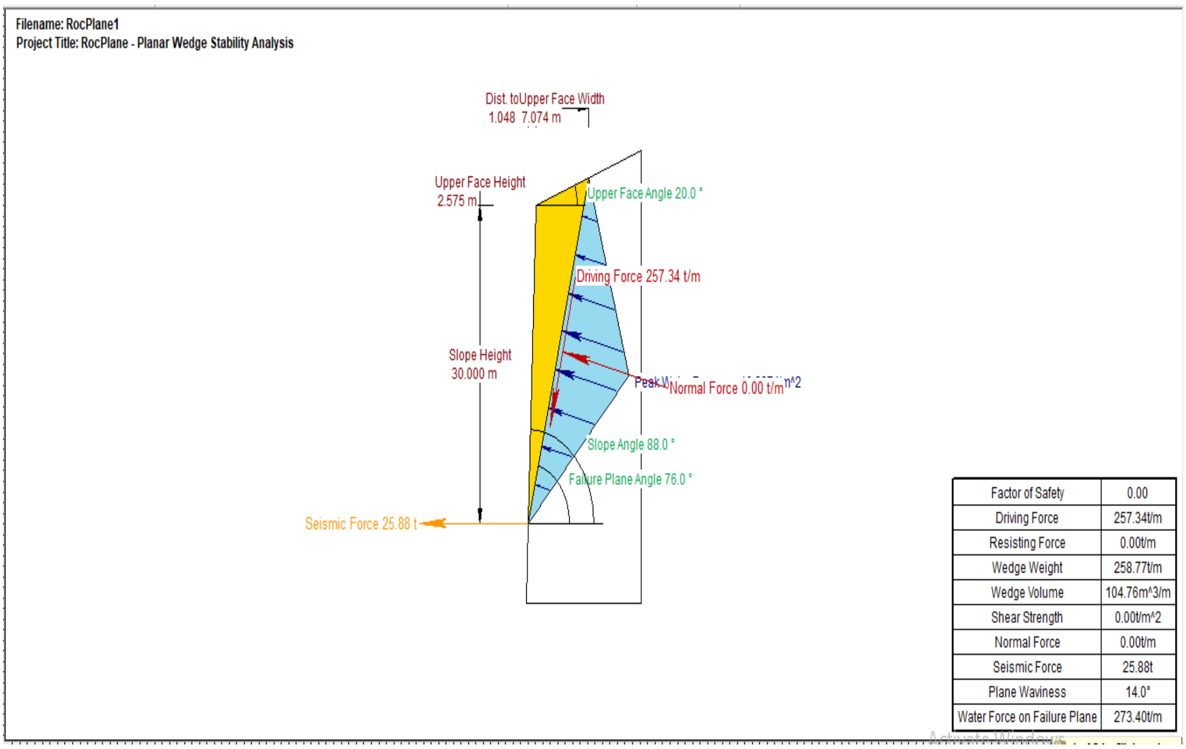

Fig 12: Result of limit equilibrium analysis of planar failure at D1S1 by Rocplane 2D software at saturated condition.

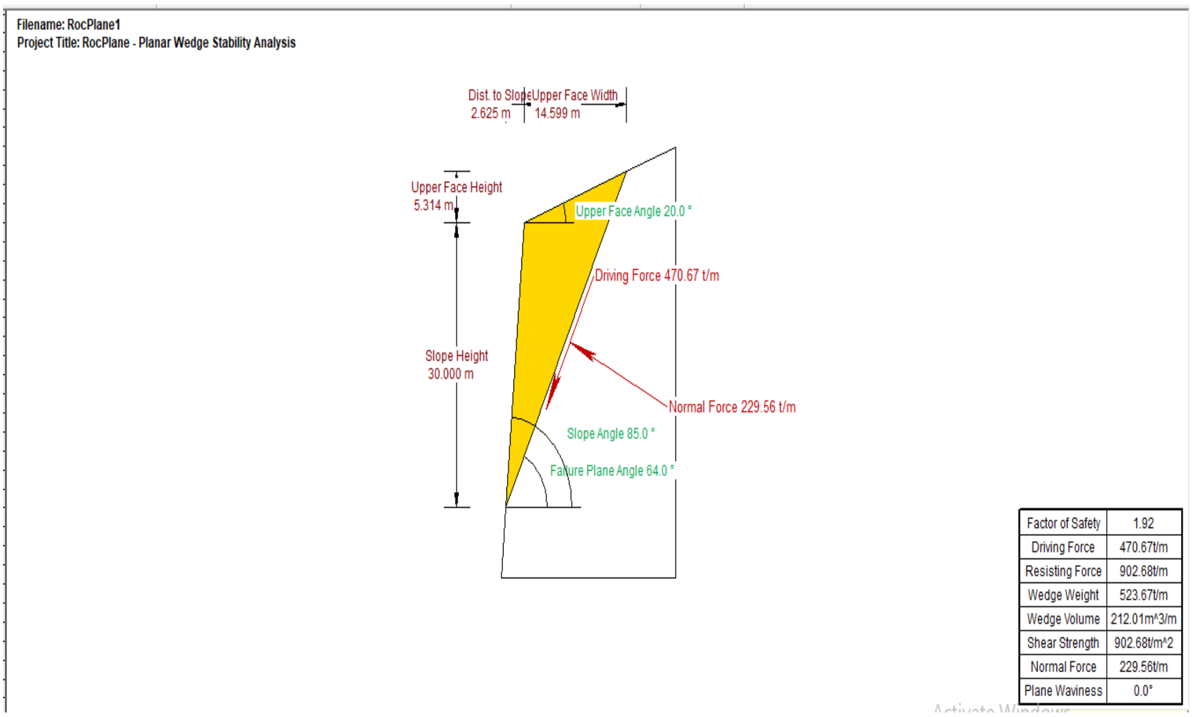

Fig 13: Result of limit equilibrium analysis of planar failure at D1S3 by Rocplane 2D software dry condition.

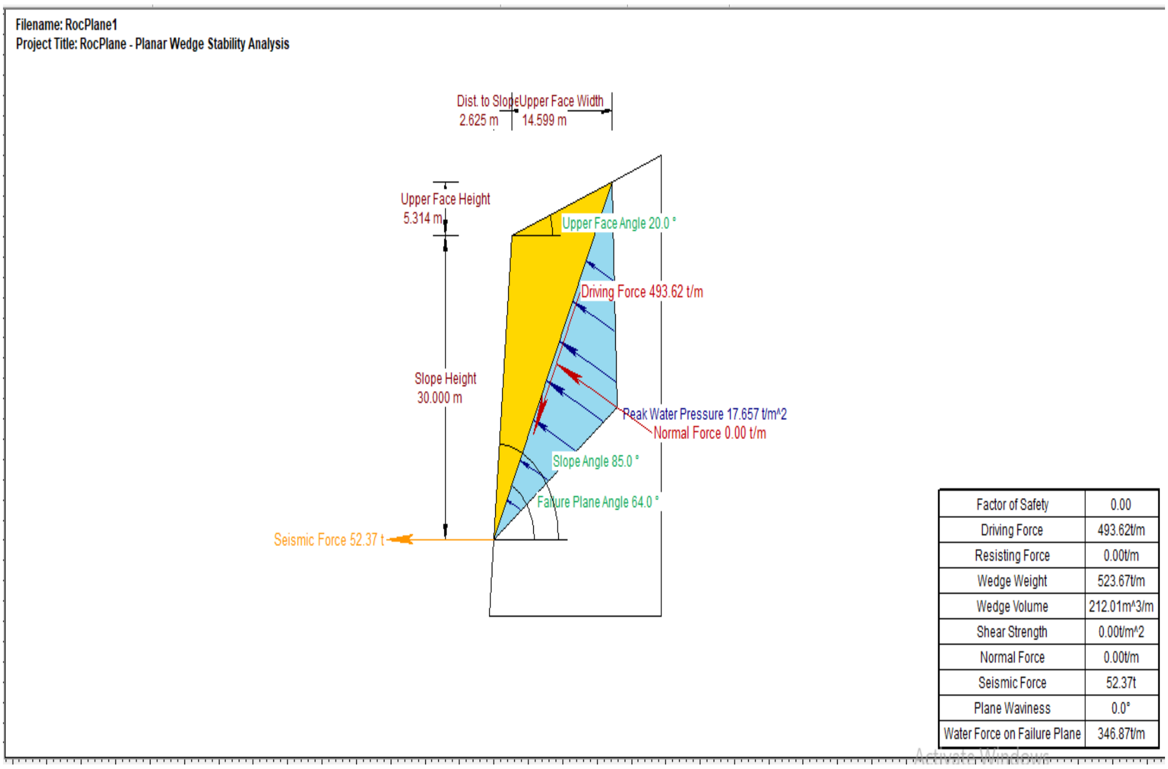

Fig 14: Result of limit equilibrium analysis of planar failure at D1S3 by Rocplane 2D software at saturated condition.